AGARDograph 23

BELGIQUE
CANADA
DANMARK
DEUTSCHLAND
ELLAS
FRANCE
ISLAND
ITALIA
LUXEMBOURG
NEDERLAND
NORGE
PORTUGAL
TURKIYE
UNITED KINGDOM
UNITED STATES

AGARDograph

OPTICAL METHODS FOR EXAMINING THE FLOW IN HIGH-SPEED WIND TUNNEL

PART I

Schlieren Methods

by

D. W. Holder and R. J. North

PART II

Interferometer Methods

by

G. P. Wood

NOVEMBER 1956

NORTH ATLANTIC TREATY ORGANIZATION

ADVISORY GROUP FOR AERONAUTICAL RESEARCH AND DEVELOPMENT

(ORGANISATION DU TRAITE DE L'ATLANTIQUE NORD)

OPTICAL METHODS FOR EXAMINING THE FLOW IN HIGH-SPEED WIND TUNNELS

PART ONE
SCHLIEREN METHODS

By

D. W. Holder

and

R. J. North

National Physical Laboratory
England

PART TWO
INTERFEROMETER METHODS

By

George P. Wood

National Advisory Committee for Aeronautics
U. S. A.

November 1956

This is one of a series of Wind Tunnel AGARDographs
concerned with wind tunnel design, operation, and test techniques.
Professor Wilbur C. Nelson of the University of Michigan is the editor.

ACKNOWLEDGEMENT

The authors wish to thank the following authorities or laboratories for providing information which was of value in the preparation of the AGARDograph.

The National Advisory Committee for Aeronautics	U.S.A.
The Office of Technical Services of the Department of Commerce	U.S.A.
The Boeing Airplane Company	U.S.A.
The Applied Physics Laboratory, Johns Hopkins University	U.S.A.
The Rand Corporation	U.S.A.
Flygtekniska Försoksanstalten	Sweden
Kungl Tekniska Högskolan	Sweden
Svenska Flygmotor A. B.	Sweden
Office National D'études et de Recherches Aéronautiques	France
Nationaal Luchtvaartlaboratorium	Netherlands
Ministero della Difesa-Aeronautica	Italy
Centre National D'études et de Recherches Aéronautiques	Belgium

This AGARDograph was prepared with the cooperation of the Air Force Office of Scientific Research of the Air Research and Development Command, United States Air Force.

TABLE OF CONTENTS

PART ONE
SCHLIEREN METHODS

TABLE OF CONTENTS
(Continued)

PART TWO
INTERFEROMETER METHODS (SECTION III)*

*For purposes of continuity, Part Two of this paper is also considered Section III.

SUMMARY

The paper reviews the present state of knowledge concerning the use of schlieren, direct-shadow, and interferometer techniques for visualizing and photographing the flow in high-speed wind tunnels. Emphasis is placed on the most widely used techniques, but brief details are also given of methods which are in an early stage of development, or which are useful only in a limited range of investigations. Information on suitable light sources and photographic materials is included.

SOMMAIRE

Cette étude passe en revue les emplois que nous connaissons, à l'heure actuelle, du schlieren, de l'ombre portée, et des techniques interférométriques, pour visualiser et photographier l'écoulement dans les souffleries à haute vitesse. L'accent est placé sur les techniques les plus communément employées, cependant, quelques détails sont aussi donnés sur des méthodes qui commencent seulement à se développer, ou qui ne s'appliquent qu'à un domaine limité d'investigations. Des renseignements sur les sources de lumière, et le matériel de photographie, à employer, complètent cette étude.

PART ONE
SCHLIEREN METHODS

I. INTRODUCTION

Numerous methods are available for visualizing the flow past the model under test in a wind tunnel. These include the use of tufts (Refs. 1 and 2), smoke (Ref. 2), an oil film placed on the surface of the model (Refs. 3 and 4), and the vapour-screen (Ref. 5) and tuft-grid (Ref. 6) techniques for observing the vortex pattern behind the model. Many methods for the visualization of boundary-layer transition are also available (Refs. 1 and 2) and frequently depend on the physical or chemical behaviour of a deposit placed on the surface of the model. For information on these techniques the reader is referred to the references cited and to their bibliographies.

The present paper is concerned with the use of optical methods for observing the changes of refractive index which accompany the changes of density that are present in the flow past the model at sufficiently high Mach number. These methods are of considerable value in a wide range of investigations. They enable a large field to be surveyed rapidly without introducing exploring instruments that may disturb the flow, and can be arranged to give almost instantaneous records thus avoiding difficulties that may arise, if the flow is unsteady, from the comparatively long response times of other methods of observation.

We are here concerned with the use of optical methods in routine wind tunnel experiments; although much of the material is applicable, we do not deal explicitly with the uses of the techniques in flight or in ballistic ranges or shock tubes. For details of these applications the reader is referred to Refs. 7 to 21. Also, no account is given of the uses of the techniques for the study of specialized problems (e.g. combustion problems and turbulence measurements) many of which are adequately covered in Ref. 22.

Most attention is given to the methods that have been found to be useful for a wide range of wind tunnel investigations; other methods, many of which require further development before their value can be properly assessed, are dealt with only briefly. Since a number of accounts of the theory of the methods have already been published, emphasis is placed on the physical nature of the methods and on the practical problems that may arise in using them. However, it was felt that a brief statement of the theory dealing with the effects on a light beam of the density of air in the working section of a wind tunnel would be appropriate.

The refractive index, n, of a gas is related with sufficient accuracy to its density, ρ, by the equation

$$n - 1 = k\rho \tag{1}$$

where k is a constant for a particular gas and a particular wavelength of light.

For air, it is convenient to write this equation in the form

$$n - 1 = K\frac{\rho}{\rho_0} \tag{2}$$

where ρ_0 is the density at normal temperature and pressure. The factor K is dimensionless and, for air, varies between 0.000290 and 0.000298 for the visible-light spectrum.

Thus the density changes which occur in the motion of a compressible fluid past a body are accompanied by changes of refractive index which may be observed by optical techniques. If the technique is such that the

refractive index can be measured quantitatively either absolutely or in relation to some datum value (e.g. that of the undisturbed stream), the corresponding absolute or relative density can be calculated. Knowing the local density, it is then possible in some cases to deduce the other local conditions from a knowledge of the conditions at the intake of the wind tunnel and that the flow is substantially homentropic, or by making supplementary local pressure measurements, or by allowing for the changes which take place through shock waves upstream of the measuring station.

Although the principal use of optical methods is for the visualization of flows at high Mach numbers where there are comparatively large density changes, some of them have been used with success to observe the small density changes that are present in the flow in atmospheric tunnels working at speeds as low as 100 ft./sec. The methods have also been used to observe artificial refractive-index changes produced by introducing into the flow filaments or small isolated volumes of a gas whose refractive index differs from that of the general stream. This may be done by injecting a gas such as carbon dioxide into the wind tunnel, by heating a filament (Refs. 23 and 24) or a small volume (Refs. 24, 25 and 26) of the airstream, or, in the case of a high-speed tunnel, by observing (Ref. 27) the wake of a wire placed across the flow ahead of the working section. It must be remembered, however, that although filament lines or particle paths may be observed by the use of artificial changes of refractive index, this is not the case when the method depends on the natural changes of refractive index.

Consider a beam of light which is passed across the working section through glass side windows and which eventually falls on a screen. If the density in the working section changes, the time of arrival at the screen of a particular point on a light wave will change because the velocity of light, c, is related to the refractive index, n, by the equation

$$c = \frac{1}{n} c^* \qquad (3)$$

where c^* is the velocity in vacuo. In the interferometer technique, due to Mach (Ref. 28), the refractive index in the working section is obtained by measuring this change in relation to the time of arrival of a point on a second light wave which does not pass through the flow field which is being studied.

If in the working section there is a gradient of refractive index normal to the light rays, the rays will be deflected because the light travels more slowly where the refractive index is larger (Eq. (3)). The deflection of the light rays is a measure of the first derivative of the density with respect to distance (i.e. the density gradient) and may be observed by one of a number of so-called schlieren techniques. The best known is that due to Toepler (Ref. 29).

Should the refractive index gradient normal to the light rays vary, the deflections of adjacent rays will differ so that they will converge or diverge, giving increased or decreased illumination on the screen. These changes of illumination are observed in a particularly simple schlieren system called the direct-shadow or shadowgraph and usually attributed (Ref. 30) to Dvorak. On certain assumptions it may be shown that the effects observed with the direct-shadow method are a function of the second derivative of the density.

Since the interferometer, the Toepler-schlieren, and the direct-shadow methods give observations which depend on the density and on different derivatives of the density, the three methods are complementary rather than alternative, each showing features of the flow which may not be clearly observed by

the others. Photographs of the flow at high subsonic speed past a two-dimensional aerofoil taken by the three methods are reproduced for comparison in Figs. I-1a, I-1b, and I-1c. For the interferometer, the apparatus was adjusted so that the fringes represent approximately lines of constant density in the flow. In each case the exposure time was approximately one microsecond.

Of the three methods, the only one which has been used extensively for quantitative density measurements is the interferometer. The main use of the Toepler-schlieren and direct-shadow methods is at present to show the positions and shapes of regions of density changes such as those occurring in shock and expansion waves, and boundary layers and wakes. Used in this fashion these two methods require only comparatively simple apparatus and have contributed largely to the knowledge of the physical nature of many phenomena of high-speed flow.

II. SCHLIEREN METHODS

The arrangement of a schlieren apparatus depends to some extent on the nature of the flow that is to be observed. Many features are, however, common to all types of schlieren systems and for simplicity it will be assumed in the following paragraphs that the flow is two-dimensional. Later (see II(o)) the modifications that are required if the apparatus is to be used to observe other types of flow will be considered briefly.

(a) The Deflection of a Light Beam by a Density Gradient

The schlieren methods depend on the deflection of a ray of light from its undisturbed path when it passes through a medium in which there is a component of the gradient of refractive index normal to the ray. It may be shown (Refs. 31, 32, and 33) that the curvature of the ray is proportional to the refractive-index gradient in the direction normal to the ray and that if the z-axis is taken in the direction of the undisturbed ray, the curvatures in the xz and yz planes respectively are given by

$$\frac{\partial^2 x}{\partial z^2} = \frac{1}{n}\frac{\partial n}{\partial x} \tag{4}$$

$$\frac{\partial^2 y}{\partial z^2} = \frac{1}{n}\frac{\partial n}{\partial y}. \tag{5}$$

If the total angular deflections in the xz and yz planes are denoted by ϵ'_x and ϵ'_y respectively, then

$$\epsilon'_x = \int \frac{1}{n}\frac{\partial n}{\partial x}\, dz \tag{6}$$

$$\epsilon'_y = \int \frac{1}{n}\frac{\partial n}{\partial y}\, dz. \tag{7}$$

If the optical disturbance is in the working section of a wind tunnel, the ray of light will be deflected on leaving the tunnel so that

$$n \sin \epsilon' = n_o \sin \epsilon \tag{8}$$

where n_o is the refractive index of the air surrounding the tunnel, and n the refractive index in the working section. Thus, the final angular deflections, ϵ , measured beyond the tunnel are

$$\epsilon_x = \frac{1}{n_o}\int \frac{\partial n}{\partial x}\, dz \tag{9}$$

$$\epsilon_y = \frac{1}{n_o}\int \frac{\partial n}{\partial y}\, dz \tag{10}$$

where the integrals are taken over the width of the working section.

In the case of two-dimensional flow in a tunnel of width L, these expressions become simply.

$$\epsilon_x = \frac{L}{n_o} \frac{\partial n}{\partial x} \qquad (11)$$

$$\epsilon_y = \frac{L}{n_o} \frac{\partial n}{\partial y} \qquad (12)$$

the deflection being in the direction of the refractive index gradient (i.e. towards the region of highest density).

(b) The General Arrangement of the Apparatus

A typical schlieren apparatus is sketched in Fig. II-1. Here the light source, S, is placed at the focus of the concave mirror, M_1, so that the working section is illuminated by a parallel beam of light. A second concave mirror, M_2, placed beyond the working section, produces an image of the source in its focal plane, K, beyond which a focussing lens, L, is used to give an image of the model in the working section on the screen or photographic plate, Q. Since the light is parallel between M_1 and M_2, that from each point in the xy plane may be considered to give an individual image of the source in the focal plane of M_2. If there is no gradient of refractive index (or if the gradient is uniform) over the working section, the individual images of the source will coincide, but if the gradient in a small area differs from that in the rest of the field, the angular deflection of the light, ϵ, will cause the corresponding image in the focal plane, K, to be moved by an amount given with sufficient accuracy by $f_2\epsilon$, where f_2 is the focal length of M_2. Irrespective of its direction, all light from a point in the object is brought to a focus at the corresponding point on the viewing screen. The image on the screen is accordingly not displaced by the deflection of the rays produced by the refractive index gradients in the object.

Several methods are available for detecting the displacement of the image of the light source.

(c) The Toepler Method

In the Toepler method (Refs. 29, 31, 32 and 33), the displacement of the image of the source corresponding to the deflection of the light passing through a particular point in the field results in a change of illumination of the image of this point on the screen, Q. A rectangular source is used and a knife edge is placed at the focal plane, K. The edge is adjusted so that in the absence of the optical disturbance, part of the light from the image of the source is cut off from the focussing lens, L, so that the illumination on the screen is reduced uniformly.

If, when the optical disturbance is introduced, part of the image of the source is displaced as shown in Fig. II-2, the illumination of the corresponding part of the image on the screen, Q, will decrease or increase by an amount proportional to $\epsilon_y f_2$ according to whether the deflection is towards or away from the opaque side of the knife edge. Displacement of the image of the source parallel to the knife edge produces no effect at the screen and the edge must therefore be set perpendicular to the direction in which the density gradients are to be observed. Thus for shock wave observations the edge is, for greatest sensitivity, set in a direction roughly parallel to the shock front, and for boundary layer observations it is set parallel to the surface of the body.

The operation of a Toepler apparatus is illustrated by Fig. II-3, which shows photographs of the flow round a 12.5 percent thick double wedge held in the working section of a wind tunnel running at a Mach number (M) of 1.6. In the first photograph, the knife edge* was perpendicular to the chord of the aerofoil so that the components of the density gradient parallel to the chord are visualized. The positive directions of these components are sketched in the diagram and the deflection of the light being in this direction (Eqs. (11) and (12)), the shock waves appear as regions of decreased illumination and the expansions as highlights. In the wake, the direction of the density gradient is almost perpendicular to the chord, so that this is not so clearly visible** as in the photograph described below.

In the second photograph the knife edge was parallel to the chord, and the positive directions of the components of the density gradients perpendicular to the chord are shown. In this case the images of the shock waves above the aerofoil are regions of increased illumination, and those of the shock waves below the model regions of decreased illumination; the converse is true for the images of the expansion waves. The density gradient changes sign in the middle of the wake,*** and one-half of its image is of high, and the other of low illumination. Except in the shock and expansion waves and in the wake, the density gradient is zero (although, of course, the density is not the same in the different regions of the flow) and the remainder of the photograph is accordingly evenly illuminated.

A further example is reproduced in Fig. II-4. This is of the flow past an aerofoil at high subsonic speed, and shows the separation of the boundary layer at the shock wave on the upper surface, and eddies formed in the wake. Since these eddies are moving in relation to the light beam at speeds approaching that of sound, this example illustrates the importance of short exposure times for the photography of such flows.

(1) The Sensitivity and Working Range

If light losses are neglected, it is easy to show that when the knife edge is absent the uniform illumination, I_0, of the screen, Q, (Fig. II-1) is given with sufficient accuracy by

$$I_0 = \frac{Bbh}{m^2 f_1^2} \qquad (13)$$

where B is the brightness, b the breadth, and h the height of the light source; m is the magnification of the image on the screen; and f_1 is the focal length of the first mirror.

The dimensions of the image of the source formed at the knife edge are $(f_2/f_1)h$ and $(f_2/f_1)b$, and if all but a height, a, of the image is cut off by a knife edge parallel to the breadth, b, of the source, the illumination

---

*In the photographs, the direction of the knife edge is indicated by the line dividing the black and white halves of a circle. The black part of the circle shows the position of the opaque side of the knife edge.

**The reason it is visible is discussed in section (II)(ℓ)(1) in connection with focussed direct-shadow systems.

***The static pressure being approximately constant through the wake, and the temperature highest at the middle.

of the screen falls uniformly to a value, I, given by

$$I = \frac{Bba}{m^2 f_1 f_2} \tag{14}$$

where f_2 is the focal length of the second mirror.

When the optical disturbance producing an angular deflection, $\delta\epsilon$, of the light rays is introduced, the corresponding image of the source is displaced relative to the knife edge by an amount, $f_2 \delta\epsilon$, so that the change of illumination of the corresponding part of the image on the screen is given by

$$\delta I = \frac{Bb\delta\epsilon}{m^2 f_1}. \tag{15}$$

The contrast, C, of this part of the image with respect to the background is, therefore, given by

$$C = \frac{\delta I}{I} = \frac{f_2 \delta\epsilon}{a} \tag{16}$$

and the contrast sensitivity, S, by

$$S = \frac{dC}{d\epsilon} = \frac{f_2}{a}. \tag{17}$$

Eq. 15 will cease to apply if the image of the source is displaced completely off or completely on to the opaque side of the knife edge. If this occurs, the image on the screen will either have an illumination I_0 given by Eq. (13), or be dark, and further displacement will have no effect.

The maximum range of displacement of the image of the source for retention of sensitivity is, therefore, equal to the height $(f_2/f_1)h$ of the image, and the corresponding range of angular deflection $\overline{\delta\epsilon}$ is given by

$$\overline{\delta\epsilon} = \frac{h}{f_1}. \tag{18}$$

If the range of displacement for deflections towards the opaque side of the knife edge is n times that for deflections away from the edge, the quantity a is given by

$$a = \frac{n}{n+1} f_2 \overline{\delta\epsilon} \tag{19}$$

and the corresponding illumination on the screen by

$$I = \frac{n}{n+1} I_0. \tag{20}$$

Under these conditions Eq. (17) may be written

$$S = \frac{n+1}{n} \frac{1}{\overline{\delta\epsilon}} \tag{21}$$

so that the maximum sensitivity that can be achieved in conjunction with a given range of deflection towards and away from the knife edge is (Ref. 34) inversely proportional to the total range of angular deflection, and independent of any property of the optical system or of the light source. In practice the system is frequently set up so that the range is the same for deflections towards and away from the knife edge (i.e., n = 1).

It is usually undesirable for the range to be exceeded in part of the image of the flow,* because if this occurs there may be little contrast between the images of regions of strong and weak density gradient. To give an extreme example, a strong shock wave would not be visible if it was embedded in a region of gradual compression where the density gradient was sufficient to exceed the range of the apparatus.

The range of the apparatus may be increased (Eq. (18)) either by replacing the first mirror by one of shorter focal length (which is usually inconvenient), or by increasing the height of the source. The height of the source may be increased physically (see section II(m)), or by means of an optical system consisting of a condenser lens as sketched in Fig. II-5. With the notation of this diagram, the magnification, m_c, of the source (i.e. the increase of the range of the apparatus) is given by

$$m_c = \frac{p}{q} \tag{22}$$

and the focal length, f_c, of the condenser by

$$f_c = \frac{m_c q}{m_c + 1} . \tag{23}$$

If the full field of the mirrors is to be used for visualization, the maximum illumination is obtained when the condenser is adjusted so that the light beam just fills the first mirror, i.e. when

$$\frac{f_1}{d} = \frac{p}{d_c} \tag{24}$$

where d is the diameter of the mirror, and d_c the diameter of the condenser.

If the transmission of the condenser system is perfect, the brightness of the image of the source is the same as that of the source. Thus, under the above circumstances, the illumination on the screen is increased in proportion to the increase of source area, that is, in proportion to m_c^2. In practice, this advantage cannot be fully realised, because it is usually necessary to stop down the image of the source produced by the condenser if the part of the image exposed to the first mirror is to be uniform. Also, if it is required to increase the range without increasing the breadth of the source a slit, of width equal to that of the source, must be introduced in the plane of the source image, and in this case the illumination is increased by a factor m_c. Since in practice the brightness of the source is reduced by using a condenser because of imperfect transmission, the use of a condenser is undesirable if a source can be obtained with dimensions which give the required range. Because of the reduction of illumination, it is also undesirable to use too large a source and a condenser to produce an image of reduced size.

The lens used for the condenser should be corrected for chromatic aberration, and free from internal or surface defects.

Although, for wind tunnel applications, the main problem is usually to obtain adequate range, there are sometimes applications where high sensitivity is the main consideration. The quantity, a, in Eq. (17) then needs

*Except perhaps in the image of a region of very strong density gradient where it can hardly be avoided if the apparatus is to be sufficiently sensitive to visualize the remainder of the flow.

to be small, and if the brightness is fixed, there is an advantage to using a large source breadth, b, in order to keep the illumination of the screen from becoming so low that visual observations or photography are difficult.

(2) Estimation of the Range and Sensitivity Required

The deflection of the light rays produced by various simple types of aerodynamic disturbances can be calculated. It depends on the direction at which the light enters the disturbance, and on the extent of the disturbance as well as the density distribution within it. For two-dimensional disturbances (i.e. disturbances extending across the working section from one glass window to the other) the light rays entering the disturbance remain within it, and are continuously deflected across the whole width of the tunnel if the disturbance is weak and of large extent.* The final deflection of the light rays is then proportional to the tunnel width as shown in Eqs. (11) and (12). If, however, the disturbance is strong and of small extent,** the light rays which enter it may be deflected so that they leave the disturbance before traversing the whole width of the working section. Under these circumstances, the final deflection is independent of the tunnel width.

The weakest density gradients which need to be detected are usually of the first type described above, and the strongest density gradients of the second. Thus, as the width of the tunnel is increased, the range of deflections which the schlieren apparatus has to detect becomes smaller, and difficulties associated with the achievement of a satisfactory compromise between range and sensitivity become less severe.

Formulae giving the deflections occurring in expansion waves and in plane and curved shocks have been derived in Refs. 35 and 36. These provide a useful method for estimating the range and sensitivity required in the preliminary design of a schlieren apparatus, but it is desirable to check these estimates by experiments with the apparatus before putting it into routine use. For this reason it is valuable to arrange the apparatus in such a way that the range and sensitivity are readily adjustable. This may be done, for example, by designing the source so that its height is adjustable (see section II(m)), or by having available a suitable set of graded filters (see section II(d)).

(3) The Effects of Diffraction

The discussion in section II(c)(1) of the effects of a displacement of the image of the source on the illumination at the viewing screen was based on geometrical optics. A more rigorous examination based on wave theory shows (Refs. 37 and 38), however, that the effects of diffraction may be important. It is found that, although the illumination on the viewing screen is usually approximately constant in the absence of the knife edge, this is no longer the case when a knife edge is present. The effects of diffraction then usually result in increased illumination on the viewing screen as the boundaries of the aperture are approached (e.g. near the images of the wind tunnel walls and the model under test). Also, the illumination does not fall sharply to zero at the boundaries, but dies away gradually. The magnitude and extent of these effects increase as the amount by which the image of the source is cut off by the knife edge increases; for the amount of cut off used in most practical systems the

---

*For example, a Prandtl-Meyer expansion far from its centre.

**For example a shock wave, or an expansion wave close to its centre.

effects are usually confined to regions very close to the images of the boundaries, and result in the formation of narrow bright bands running adjacent to them.

If a deflection is produced in the parallel light beam by the introduction of a density gradient, the effects of diffraction may result in a change of illumination on the viewing screen which differs appreciably in both extent and magnitude from that expected on the basis of geometrical optics. These effects are again usually small if the apparatus is used at low sensitivity with only a small amount of the source image cut off, but may become dominant if the sensitivity is high. The effects are not readily calculable, and thus affect the accuracy of the schlieren methods when used for quantitative density measurements.

(d) The Graded-Filter Methods

In wind tunnel work the range (see section II(c)(1)) of a schlieren apparatus frequently needs to be large, and it may be inconvenient to provide a uniform source which is large enough to give this, especially if the duration of the exposure has to be very short for high-speed photography. Moreover, if the range is adjusted by changing the dimensions of the source, the position of the knife edge in an off-axis system needs to be changed because of the effects of astigmatism (see section II(e)).

To overcome these drawbacks of the conventional Toepler method, a modified apparatus has been developed (Refs. 39, 40, and 41). Here, instead of a knife edge in the focal plane of the second mirror, a filter is used. This is graded in one direction so that the proportion of light that is transmitted changes as the image of the source is displaced. Since such a filter can be produced with any required dimensions there is no limit to the range that can be obtained; moreover, a "point" light source can be used thus minimizing the optical aberrations and increasing the depth of focus of the apparatus (see section II(o)(3)), as well as enabling direct-shadow photographs to be taken without having to change the source.

Filters have been made by using a photographic enlarger to print from a neutral glass wedge on to a photographic plate, different sensitivities and ranges being obtained by altering the enlargement in the printing process. Filters with any required characteristic could be produced by using a cam-driven shutter to control the photographic exposure. In particular, the use of a linearly-graded density in the filter would give an apparatus whose sensitivity was independent of the position of the source image relative to the filter, although of course the general level of illumination would change. This might be of value in a system subject to considerable vibration.

The use of a graded filter instead of a knife edge is also found to lead to an improvement in the sharpness of the schlieren photograph. The improvement obtained with the filter is associated with the different effects of a knife edge and a filter on the diffracted light (Ref. 42) from the fine details of the flow.* In the focal plane of the second mirror, this light is distributed round the image of the light source. If a knife edge is introduced, the sharpness of the final image deteriorates because the diffracted light near one extremity of the source image is uninterrupted, whereas that near the other extremity is entirely cut off, and that near the middle half cut off. For a graded filter, the diffracted light is nowhere completely cut off, but the intensity of its contribution

*Similar effects of gradation of the aperture are discussed in Ref. 43.

to the final image depends on the position where it falls on the filter. Since the field of diffracted light is usually comparatively small, this effect is not serious for filters of shallow gradient, and the sharpness of the final image is hardly affected.

In this connection it is of interest to compare the images of a pin hole placed in the object plane (e.g. the working section of the wind tunnel) obtained with schlieren systems using a knife edge and a graded filter, with the image when neither is present. Fig. II-6a shows the extension of the image in a direction perpendicular to the knife edge that would be expected (Ref. 42) because of the effects on the diffraction pattern of an aperture of this type. Fig. II-6b shows that the effect of the graded filter on the image is comparatively small.

The importance of the above considerations decreases as the required sensitivity is increased, and for very sensitive systems (e.g. those for which the maximum angular deflection is about 0.0005 radian) a graded filter is found to have little advantage over a knife edge as far as image sharpness is concerned. Also, the improvement achieved by using a graded filter will frequently not be significant if the image is unsharp for some reason other than the effects of diffraction (e.g., too long an exposure time).

(e) Aberrations Arising in Off-Axis Mirror Systems

Since the light source and knife edge must be placed so that they do not interrupt the parallel beam of light between the two concave mirrors, strictly the mirrors should be figured so that their foci lie off the axis of the parallel beam. Such mirrors would be expensive, however, and in practice axially-figured mirrors give satisfactory results if the ratio of the focal length to the diameter (the f number) is not too small, and the precautions described below are taken when arranging the optical system.

The diameter of the mirrors is usually determined by the size of the flow field to be examined. The focal lengths affect the illumination in the image, the range, and the sensitivity as discussed in section II(c)(1), as well as the space required to install the apparatus. The aberrations discussed here depend largely on the ratio of the focal length to the diameter and, in practice, this ratio usually lies between 6 and 12. The additional expense involved in purchasing parabolic mirrors is not usually justifiable unless the f number is small* since the mirror is to be used with the source off axis, and because, for mirrors of typical focal length and diameter, the maximum difference between the surface shapes of a sphere and a paraboloid is usually of the order of only about one-half wavelength. Spherical mirrors are, therefore, usually employed, and notes on the desirable accuracy of surface shape are given in section II(h).

The aberrations that arise (Refs. 38, 44, and 45) when a mirror system is used with the light source and knife edge offset from the axis affect the image of the light source formed by the second mirror, and, when the image is partially cut off by the knife edge, may result in uneven illumination on the viewing screen even when no optical disturbance is present.

An aberration termed "coma" occurs because the direction of the light reflected from the mirror depends on the position on the mirror of the point of reflection, and in practice results in uneven illumination on the

---

*For example, parabolic mirrors are used at the Ames Laboratory when the f number = 5.5, whereas spherical mirrors are used when the f number = 7.

viewing screen. Referring to Fig. II-7, light from the source, S, falling on O, the centre of the first mirror, is reflected along OO', but light reflected at A or B proceeds in a slightly different direction (the angular difference being given with sufficient accuracy by $d^2\theta/16f_1^2$). Similar effects occur when the rays are reflected at the second mirror, and if this mirror is tilted in the manner shown, these are of opposite sign to those arising at the first mirror. Thus, the effects of coma on the image of the source at K can be reduced by tilting the mirrors as in Fig. II-7, and if the focal lengths of the mirrors are equal the effects may be eliminated by using equal and opposite angles of tilt.

Although the effects of coma may be avoided or reduced by arranging the mirrors in the manner described above, the effects of another aberration, termed "astigmatism," are always present in an off-axis mirror system. If a point source is used at S, astigmatism will result in the image of the source consisting not of a point, but of two lines at different positions along O' K, one in the plane of the paper and perpendicular to O' K, and the other perpendicular to the plane of the paper.

In practice an extended source is used, but the effects of astigmatism may be considered by assuming that it consists of a number of point sources. If, as is usual, the source is of rectangular shape it should be arranged so that one side is perpendicular to the plane of the paper (Fig. II-7). In this case, it will be possible to adjust the positions of the source and knife edge so that the effects of astigmatism are largely confined to an extension of the dimension of the source image in a direction parallel to the knife edge, so that the illumination on the viewing screen is not affected. If the source and knife edge are then rotated through 90 degrees to alter the direction in which components of the density gradient are to be observed, it will be necessary to adjust slightly* the position of the source and knife edge along OS and O' K, so that the effects of astigmatism are again minimized. This may be done by successively altering the source and knife-edge position until the viewing screen darkens as uniformly as possible when the knife edge is traversed across the source image.

Methods for the correction of astigmatism by the insertion of a suitably shaped lens in the optical system are described in Refs. 44 and 46. Because of the aberrations (particularly astigmatism and spherical aberration), errors may arise with an off-axis system in the representation of angles in the image of the flow. These may be significant if the inclinations of shock waves are to be measured with a schlieren system in which the offset angles are large. The magnitude of these errors may be estimated by the examination of the image of a grid held in the working section. Also, because of astigmatism it is not possible for vertical and horizontal lines in the object to be simultaneously in focus.

Under most practical conditions, none of the effects discussed above are serious if the angular offset (2θ) of the source and knife edge does not exceed about 5 degrees. Larger angles are often used, however, where some deterioration of the image quality is acceptable.

---

*The movement is about one-sixteenth of an inch for 100-inch focal length mirrors of 10-inch diameter, with the source and knife edge offset so as to lie just outside the parallel light beam.

(f) Details of the Focussing Lens

On the basis of thin lens theory, the focal length, f_3, of the focussing lens is given by the equation

$$f_3 = \frac{m(f_2^2 - \ell g)}{f_2 - m\ell} \qquad (25)$$

where the notation is that shown in Fig. II-8(i), and m is the magnification of the inverted image on the viewing screen or photographic plate. The distance, ℓ, between the object (e.g. the optical disturbance in the working section) and the focal plane of the second lens or mirror, M_2, is to be taken as positive when (as sketched in Fig. II-8(i)) the object is outside the focus of M_2, and negative when it is inside the focus.

On the same basis, the distance, e, of the viewing screen from the focussing lens is given by

$$e = m\left[f_2 - \frac{\ell g}{f_2}\right] = \frac{f_3(f_2^2 - \ell g)}{f_2^2 - \ell g + f_3 \ell}. \qquad (26)$$

If, as is frequently the case, ℓ and g are small compared with f_2, both f_3 and e are approximately equal to mf_2.

For practical reasons it is sometimes necessary to place the viewing screen at a large distance from the knife edge without using a large image size which may result in insufficient illumination. This may be achieved by using a second lens, L', as shown in Fig. II-8(ii).

With the notation of this diagram, the focal length, f_4, of this lens is given approximately by the equation

$$f_4 = \frac{sm'}{(1 + m')^2} \qquad (27)$$

where m' is the magnification of the final erect image in relation to the size of the inverted image produced by the first focussing lens, L. The distance, u, between the lens, L', and the image plane of the lens, L, is given by

$$u = \frac{s}{1 + m'}. \qquad (28)$$

The diameters of the focussing lenses must be sufficiently large for them not to act as stops in the optical system. In order to keep the diameter of L as small as possible, it should be placed as close as possible to the knife edge. On the basis of geometrical optics, its size may then be determined from the expressions given in section II(c)(1) for the dimensions of the image of the light source and its range of deflection.

In order to achieve maximum image sharpness, the diameter should in practice be larger than that calculated on the above basis, so that the lens will receive the necessary part of the light diffracted at the object. However, since the effect of the presence of the knife edge on the image sharpness is usually much greater than the effect arising from the limited lens diameter, this allowance need not be large. It is suggested that the diameter should be approximately 0.01 f_2 greater than the value calculated on the basis of geometrical optics to allow for the diffracted light, and the possibilities of misalignment.

The nature of the focussing lens depends on its focal length and aperture. Single component lenses of the type used in spectacles are readily available in a wide range of focal lengths, and are satisfactory if the focal length is large (e.g., greater than 20 inches) and the required diameter small (e.g., less than one inch). For more exacting conditions, a superior type of lens is desirable, and it is usually simplest to make use of a camera lens, such as those available from war surplus stocks. As far as field coverage is concerned, the performance of such a lens will be unnecessarily good, but it is usually cheaper to buy one than to have a lens specially made to a less rigid specification.

(g) Techniques for Setting Up the Apparatus

The procedure which is adopted for setting up a schlieren system is simple and straightforward, but depends to some extent on the nature and arrangement of the apparatus (e.g., whether it is based on lenses or mirrors), and on the type of flow which is to be observed. The basic principles are, however, the same for most schlieren methods and will be illustrated here by describing the procedure for the most common type system, namely a Toepler system using two concave mirrors (see Figs. II-1 and II-2). There are several equally satisfactory ways of achieving some of the required settings, and alternatives to those described below may be preferred in certain applications or by other workers.

It is assumed that means are available for making the necessary adjustments, and that the supports for the components of the apparatus are arranged so that the aberrations are minimized. It is also assumed that the dimensions of the apparatus (especially those of the light source*) are such that the range and sensitivity are suitable for the flow which is to be observed.

The first adjustment is to locate the light source at the focus of the first mirror. The source is placed in approximately the correct position, and the first mirror is rotated until the light beam passes through the tunnel windows. If a screen is held perpendicular to OS (Fig. II-7) an image of the source will be found which results from the reflection of light from the first tunnel window** back into the first mirror. The position of the source along OS is then adjusted until this image is in focus in the plane of the source.

The next adjustment is usually to set the parallel light beam formed by the first mirror so that it passes through the tunnel in a direction perpendicular to the glass side windows. This can be done by adjusting the position of the first mirror until (with the light beam passing through the required part of the working section) the source and its image coincide. In the case of two-dimensional models, the span may not be exactly perpendicular to the glass side walls, so that the light beam when set up in the manner described above is not truly parallel to the span. If this is so, a screen held immediately behind the working section will reveal a bright band running parallel to one surface of the model, and resulting from reflection of the light from the surface. The

---

*For the purposes of this section, this may be the actual source or the image formed by a condenser system (see section II(c)(1)).

**If the light reflected back from the window does not give an image which is bright enough to be clearly visible, a small plane mirror may be held in contact with the window so that the reflecting surface is parallel to it.

position of the light source and the inclination of the first mirror are adjusted until this band disappears, leaving the approximately uniform bright band round the model which arises from the effects of diffraction. Examples of these phenomena are shown in Fig. II-9a.

The second mirror is next moved laterally or vertically until it is filled* by the parallel beam emerging from the working section, and is rotated until the light reflected from it passes through the focussing lens and forms an image of the model under test on the viewing screen. Although the focus will usually need to be readjusted when the tunnel is run, it is worthwhile at this stage to adjust the position of the screen so that the image on it is focussed on the middle of the working section. This can be done by focussing on the boundaries of the model, or on a wire grid held in the working section.

The knife edge is now inserted in the focal plane of the second mirror, and its position along O' K (Fig. II-7) is adjusted until the screen darkens as uniformly as possible when the edge is traversed across the image of the light source. The edge is then set so that the required fraction (usually half) of the image of the source is cut off; there are several methods for making this setting, but for qualitative work it is usually sufficient to estimate the amount of cut off by holding a white card immediately behind the knife edge so that the parts of the source which are cut off and unobscured can be observed.

It is found that the appearance of the images of shock waves and boundary layers, and the distortion of the boundaries of the model in the neighbourhood of large density gradients are more sensitive to the focussing of the apparatus than is the sharpness of the geometrical image of the model. Especially for an aerofoil spanning a wide wind tunnel, it is accordingly necessary to refocus the apparatus with the tunnel running so that the phenomena which are of greatest interest are shown as clearly as possible and with a minimum of distortion. Examples showing the effects of focussing on the image of the flow near the trailing edge of an aerofoil moving at high subsonic speed are reproduced in Fig. II-9b. In the upper photograph the focus was towards the tunnel wall farthest from the viewing screen, and in the lower photograph towards the wall nearest to the viewing screen. In both cases the exposure time was about one microsecond.

The procedure described above can be used with a light source that can be operated continuously, or flashed at a frequency that is high enough to give adequate persistence of vision. With some short-duration light sources this may not, however, be possible, and it is then usual to set up the apparatus with a continuous source such as a tungsten-filament lamp. If this is done, it is finally necessary to place the short-duration source in the position of the filament of the lamp. This can be done by placing the flash source roughly in position and adjusting its position until its image is in focus at the knife edge, and lies in the same position as that originally occupied** by the image of the tungsten filament.

It is, however, more convenient to design the apparatus so that the two sources are accurately spaced on a suitable base in

---

*Because of the finite source size, the light beam is slightly divergent, and in practice extends outside the second mirror by a small amount.

**With graded filters it is usual to make a small mark on the otherwise rather featureless surface to provide a datum for these adjustments.

relation to a rotatable or removable plane mirror used to pass light from either of them into the schlieren system. Alternatively, the flash source can be made in such a form that it is transparent, and an image of the continuous source can be formed at the discharge channel by a condenser lens The continuous source is then turned off or obscured when the short duration source is to be used. Another method is to illuminate the knife edge by means of a lamp with an opal bulb, and to place the flash source so that it coincides with the image of the edge* formed by light passing through the schlieren system in the direction opposite to that when the system is in normal use.

When the flash source is in position, the image on the viewing screen should be checked by visual observation, which is possible even with extremely short flash durations if the observer triggers the source, and thus knows when it is to operate. Since the appearance of the image of a region of unsteady flow (e.g., a wake) depends on the duration of the source, it may be necessary to adjust the focus slightly when the flash source is to be used. Fine focussing with a flash source is, in the authors' experience, difficult by visual observation, and it is desirable to take a series of trial photographs before the final focus setting is selected.

(h) The Quality Required for the Optical Components

The quality required for the optical components of a schlieren apparatus depends on its nature and arrangement, and on the sensitivity at which it is to be used. Accordingly it is difficult to suggest tolerances that are generally applicable; the following details, which apply to a conventional apparatus based on two concave mirrors, are given to indicate the factors that are important, and as a guide to the order of magnitude of the acceptable imperfections. Since most wind tunnel schlieren systems are required from time to time to work at high sensitivity, the values quoted are those which have been found to give satisfactory results under this condition. If the apparatus is always to be used at low sensitivity, or to visualize gradients of refractive index considerably larger than those which occur commonly in wind tunnels, the tolerances may be relaxed.

(l) Concave Mirrors

These are usually made from well-annealed selected plate glass, or specially manufactured glass blanks, whose thickness is usually between one-eighth and one-sixth the diameter of the mirror. Near the surface that is to be figured, the glass should not contain seed (gas bubbles), stone (solid inclusions) or ream (streaks or striations of glass whose refractive index differs from that of the surrounding glass).

After it has been figured, the surface of the mirror is coated with a highly reflecting film. The most common material is aluminium which has the practical advantage that, when necessary, it can be renewed easily and cheaply. A coating of rhodium is more robust, but is more expensive and difficult to replace. The surface of the reflecting film is sometimes protected by the application of a coating of silicon monoxide, lithium fluoride, or quartz.

The choice of coating and protective treatment depends mainly on the liability to contamination of the reflecting surface. Under ordinary laboratory conditions an aluminized surface usually remains satisfactory for several years without cleaning, if protected by a cover when not in use.

---

*Ibid.

When, however, the surface is liable to contamination by oil or by an exceptionally dust-laden or corrosive atmosphere, a more robust coating is desirable, especially as it may be necessary to clean* the surface periodically.

As indicated in section II(e), the surface of a concave mirror used in a schlieren apparatus is usually a segment of a sphere. In general, an error in the radius of curvature of the sphere is unimportant provided that it is not so large that it complicates the installation of the apparatus within the available space; a tolerance of ±2 percent or more is usually possible. The most important errors are those occurring in the surface slope, since these cause the local light rays to be reflected at an incorrect angle, and result in uneven illumination in the schlieren image. Such errors usually occur in concentric zones, the centre frequently coinciding with that of the mirror. They may be detected by several methods (Refs. 47, 48 and 49) of which the Foucault test (Refs. 47 and 50) (which involves using the mirror in what is, in effect, a coincidence schlieren apparatus as sketched in Fig. II-18a) is the best known. In the authors' experience, the errors of surface slope should be less than one-fourth wavelength of mercury light per inch, and the overall departure from a truly spherical shape should be less than one wavelength.

*Cleaning is seldom wholly satisfactory, but can be done by washing with distilled water containing a detergent (such as those supplied for photographic processing) which does not contain a reinforcing alkali. The surface should be blotted with clean white filter paper and allowed to dry, after which any water marks may be removed by very light polishing with lens tissue from the centre outwards.

Small defects in the surface finish, such as scratches or indentations, may not be readily detectable in a Foucault test but may, nevertheless, be apparent in schlieren photographs. They may usually be observed by placing a point light source in the focal plane of the mirror, and projecting the reflected beam of parallel light on to a viewing screen.

(2) Plane Mirrors

As sketched in Fig. II-10, it is sometimes desirable to insert a plane mirror in the light beam. The displacement of the image of the light source at the knife edge arising from a certain error of surface slope at such a mirror is roughly proportional to its distance from the knife edge.** Thus, the required quality of surface depends on the position of the plane mirror in the optical system, and for mirrors placed close to the knife edge an error of surface slope greater than that discussed above for the concave mirrors can usually be tolerated.

(3) Glass Windows

The glass used for the windows in the walls of the working section must be of high quality since internal refractive-index gradients, and errors of surface figure will appear in the schlieren image. The only satisfactory method for selecting suitable glass is to examine it in a schlieren system, and the surface must accordingly first be polished at least roughly.

The most objectionable type of internal imperfection is usually ream, and an example is shown in Fig. II-11 (other examples may

**Or from the source, if the mirror is placed between the source and first spherical mirror.

be found in Ref. 51). Seed (examples are visible in the direct-shadow photographs reproduced in Fig. II-9a) is usually less objectionable, and, unless the gas bubbles are very large or unfortunately located, they do not appear to have an appreciable effect on the strength of the glass.

Since the striations that constitute ream are often approximately straight, they may pass undetected if they happen to lie normal to the knife edge. When testing the window in a schlieren system it should, therefore, be rotated* about the optical axis in order to ensure that the striations are at some stage parallel to the knife edge, and are thus observed with maximum sensitivity.

The glass blank that is examined is sometimes thicker than that required for the finished window and it is, therefore, useful to know the depth of an internal imperfection below the surface, since it may be possible to remove it when machining the glass to its final thickness. Alternatively, it may be desirable to locate the depth of an air bubble to ensure that it does not break into the surface** when this is finally machined. The depths of the various internal defects may be found by rotating the window about on axes perpendicular to the optical axis of the schlieren apparatus, and observing the movements of their images relative to points marked*** on the surfaces.

The surfaces of the window need not be parallel since a lack of parallelism leads to a uniform deflection of the whole beam of parallel light, and this may be accommodated by a movement of the knife edge. Curvature of the surfaces cannot, however, be dealt with in this way, and it is desirable that each surface should be flat to within one-half wavelength per inch.

Optical or plate glass specially made to be as free as possible from ream is supplied by some manufacturers, but ordinary plate glass is sometimes suitable if it is selected by tests with a schlieren apparatus. Plate glass is, however, usually supplied with a "cloth" polish and the associated imperfections of surface finish are usually visible in the schlieren image as for the piece of glass marked A in Fig. II-11. This may be objectionable in many cases, and the surface should then be "pitch" polished to the stage where the errors are no longer visible in the schlieren image as for the piece of glass marked A1 in Fig. II-11.

It has been shown that phase-contrast systems (see section II(k)(3)) are particularly suitable for showing defects of surface polish because of their high sensitivity to small phase differences. Thus if a phase-contrast schlieren system is to be used, it is desirable to select the glass windows by using a system of this type.

For thicknesses larger than those available for plate glass it is necessary to use rolled or pressed optical glass, but again it is usually necessary to examine this with a schlieren apparatus before it is accepted. An

---

*If the surfaces are not parallel, rotation will result in a displacement of the image of the source, and the position of the knife edge will require adjustment to preserve approximately constant sensitivity.

**If this occurs the glass may break away at the edges of the bubble thus forming a relatively large crater; the particles of glass that result may lead to scratching of the surrounding surface during polishing.

***With a Chinagraph pencil or strips of adhesive tape.

alternative solution is to laminate thinner sheets of glass using a transparent cement as described, for example, in Ref. 52.

(i) Some Practical Details

The mount in which a schlieren mirror is housed should be designed to permit the necessary adjustments, to enable the mirror to be protected when not in use, and to be removed easily for cleaning or for the application of a new reflecting coating. An example is shown in Fig. II-12. Here the mirror is inserted into the rear of the housing on to thin rubber pads resting on a lip at the front. It is then fixed in position by means of three metal strips pressing on to rubber pads placed on the back of the mirror, after which the back of the housing is attached. When not in use, the front of the mirror is protected by closing the doors shown.

The mirror housing is mounted so that it can rotate about a vertical and a horizontal axis. Coarse adjustments are made by rotating the housing by hand, and fine adjustments by engaging radial arms which are then controlled by means of tangent screws. Small adjustments to the height of the mirror are made by means of the foot screws. If large adjustments to the height are required, they are made by altering the height of the stand on which the mirror mount is supported. An example of a stand providing continuous adjustment of height over a large range may be seen in Fig. II-13.

The other components of the schlieren system should be supported on optical benches with means for making the adjustments described in section II(g). Satisfactory equipment is available commercially, and examples can be seen in Fig. II-13, which shows the general arrangement of a schlieren system in which the light beams from the source and to the camera are folded by means of plane mirrors. The only fine adjustment that is usually essential is in the movement of the knife edge or graded filter across the image of the source, and for this purpose an adjusting screw with about twenty threads per inch is usually adequate provided that it is free from backlash.

An example is shown in Fig. II-14. The graded filter is held in a frame which can be moved vertically or horizontally by means of the adjusting screws shown. With the filter graded in a vertical direction (as shown) the vertical adjustment only is used; if the filter is turned in its frame through a right angle (so that the grading is in a horizontal direction) the horizontal adjustment is used. The filter is set in the focal plane of the second mirror by sliding the saddle on which it is supported along the optical bench. The focussing lens is usually attached to the graded filter but, for clarity, is not shown in the photograph.

Details of alternative designs for the mechanical arrangement of the optical components are given in Refs. 45, 53, 54, 55, 56, and 57.

Several techniques are available for mounting the glass windows in the metal side panels of the working section. One that is satisfactory for most purposes, and which has the advantage of not requiring the edges of the glass to be machined very accurately is illustrated in Fig. II-15. The glass window and metal frame have bevels cut at 45 degrees from their inner faces, and the overall dimensions of the glass are chosen so that there is a gap of about one-sixteenth of an inch between glass and frame. The frame is set up in a horizontal plane on a number of ground bars of circular cross section, which ensure that the frame and window are accurately aligned so that there is no discontinuity at the junction exposed to the airstream.

The inner edge of the frame is coated with a layer of plaster* mixed to a consistency which permits any surplus to be squeezed out when the window is pressed into its final position. The window is then lowered into the frame until it rests on the ground bars, and the plaster is allowed to set. Surplus plaster is then removed by scraping, and a clamping plate is attached to the back of the frame and presses on to the window through a gasket which is inserted to protect the surface of the glass. If the loading on the window is always inwards, this gasket is made of hard rubber, but when the loading is outwards (as in some pressurized tunnels) a harder packing material is used.

After long use the plaster frequently chips away from the metal-glass junction at the inner face of the assembly. To avoid this difficulty, the plaster may be removed for a depth of about one-eighth of an inch, and replaced by a metallic stopper of the type** supplied for preparing metal surfaces for cellulose spraying.

An alternative procedure (Ref. 56) is to use a low-melting point alloy such as Wood's metal instead of plaster. This may be inserted into the gap between the glass window and metal frame by heating the whole assembly in a water bath.

---

*The plaster should not contract when it dries. A suitable material is the LX2 plaster supplied by Messrs. G. W. Cafferata of Newark-on-Trent, England. If the frame is ferrous the plaster is mixed with a weak solution of potassium chromate to prevent rusting. To facilitate the subsequent removal of the glass, the edges of the glass and frame are lightly greased to within about one-quarter of an inch of the inner surface before assembly.

**For example, S4921 stopper supplied by Messrs. Cellon of Kingston-on-Thames, England.

Since the pressure in the working section generally differs considerably from that of the atmosphere, the thickness of the glass window is usually determined by the maximum stress that it can safely withstand. In the authors' experience, this should not exceed 1200 pounds per square inch for ordinary plate or optical glass, allowance being made for stress concentrations round any slots or holes that may be cut in the glass to support the model and, in such cases, for the contribution of the aerodynamic loads on the model. When the model is supported in a slot cut in the glass as shown*** in Fig. II-16 it is advisable to round or bevel the edges of the slot for a distance of about one thirty-second of an inch in order to prevent them from chipping. The interior of the slot should, if possible, be polished to avoid stress concentrations at local irregularities. Occasionally, the model is required to rotate or oscillate relative to the glass windows, and metal bearings may then be cemented into holes drilled in the windows.

(j) Other Schlieren Methods

So far, the discussion has been largely devoted to the most commonly used wind tunnel schlieren systems. In this section modified systems which may be useful in special cases are briefly described.

(1) The Use of a Circular Knife Edge

The conventional Toepler arrangement is sensitive to deflections of the source image in a direction perpendicular to the knife edge, and insensitive to deflections parallel to the

---

***In this example pressure leads from orifices located in the surface of the model are carried out of the tunnel through the tongues, and are finally connected to a monometer.

knife edge. This is usually advantageous since it enables the directions of the density gradients to be estimated, or the apparatus to be arranged so that only those features of the flow which are of greatest interest are observed with high sensitivity. If density gradients in all directions are of equal interest, however, it may be necessary with a Toepler apparatus to take two photographs with the knife edge in perpendicular positions to ensure that some of the gradients do not pass undetected.

An apparatus for taking these two photographs simultaneously is described in Ref. 58. Alternatively, the number of photographs may be reduced (at the expense of ambiguity in interpreting the results) by using a modified type of knife edge. A circular light source is used and the knife edge is constructed in the form of circular hole (Refs. 38, 59, and 60). The images of all regions of density gradient then appear darker than the background, since any displacement of the source image results in decreased illumination. The system may have advantages when the illumination is severely limited, because the undisplaced source image is not cut off at all. It may also be useful for showing the position and shape of small isolated regions of density gradient (e.g., eddies) since these appear as black dots in the image.

An alternative arrangement is to use an opaque circular stop which cuts off the circular image of the light source; displacements of the image then increase the illumination on the viewing screen. A system of this type using a square source and square stop is described in Ref. 61.

(2) Methods Giving Images in Colour

Simple modifications to either the Toepler apparatus or the graded filter apparatus enable a multicoloured image to be obtained in which each hue corresponds to a particular density gradient in the flow pattern. One method (Refs. 62 and 63) is to place a prism in front of a source of white light located at the focus of the first mirror, M_1, in Fig. II-1. A spectrum is thus produced at the focal plane of the second mirror, and the colour of the image on the screen can be adjusted by moving a slit (parallel to the bands of the spectrum) across the spectrum. When a density gradient is present part of the spectrum is displaced, and light of a different colour passes through the slit. The image of the region of density gradient is thus of a different colour to that of the surrounding image.

An alternative and somewhat simpler method (Ref. 64) analogous to that employed in the graded-filter apparatus is to use a point source, and to place a filter containing bands of different colours in the focal plane of the second mirror. The most satisfactory method for constructing the filter is, at present, to use strips of coloured gelatin film laid side by side and clamped between glass plates.

Since the eye is more sensitive to changes of hue than to changes of illumination, the colour methods are more sensitive than the conventional methods. However, because of the difficulties of processing and reproduction, colour methods are at present seldom used in routine work except when visual observations alone are required. Examples are reproduced in Refs. 63, 65, and 66.

(3) Anamorphic Systems

Occasionally, it may be desirable to arrange for the magnification of the image produced by a schlieren system to be different in mutually perpendicular directions. For example, the increase of boundary-layer thickness in the region of transition from laminar to turbulent flow may be detected more clearly if the magnification in a direction perpendicular to the surface on which the

boundary-layer is formed is greater than that parallel to the surface. The principles of an apparatus which enables this to be done by the use of cylindrical lenses are described in Ref. 67.

(4) Schlieren Systems Based on Lenses

A satisfactory schlieren system can be set up with lenses instead of concave mirrors, and the general arrangement is then as sketched in Fig. II-17a where it is assumed that the light beam passing through the working section needs to be parallel. The lenses must be corrected for spherical and chromatic aberration (the latter is never entirely eliminated unless monochromatic light is used, but is often less important for photography with panchromatic emulsions than for visual observations), and must be made of glass of high internal quality.

The construction of such a lens involves the accurate figuring of numerous surfaces, and is accordingly much more expensive than the construction of a mirror especially if the diameter is large. Except in special circumstances lens systems are, therefore, seldom used unless they employ a readily available type of lens* such as war surplus camera lenses. The majority of the discussion contained in the preceding sections of this paper applies to lens as well as to mirror systems, and (apart from obvious differences) the techniques for setting up the apparatus are similar.

*For example, a number of satisfactory systems (see, for example, Ref. 38) have been based on 36-inch focal length, 5.5-inch diameter, surplus telephoto lenses.

(5) Schlieren Systems Using Nonparallel Light Beams, or Double Passage of the Beam Across the Flow

Although it is usually desirable to arrange for the beam of light passing through the working section to be parallel, nonparallel beams are occasionally used and arrangements for producing these are sketched in Figs. II-17b, II-17c, and II-18. Only one mirror or lens is required (apart from the focussing lens), but this advantage is to some extent offset because its diameter must be larger in relation to the field to be examined than if a parallel beam is used.

In addition to employing a nonparallel light beam, the mirror system (Refs. 23, 59, 68, 69 and 70) shown in Fig. II-18a involves a double passage of the beam across the working section. The source is placed at the centre of curvature of the mirror, and part of the image of the source is reflected on to the viewing screen by a small plane mirror held near the source.** If the image of the source is deflected in a direction perpendicular to the edge of the plane mirror, the illumination on the viewing screen changes; the edge of the mirror thus plays the same part as the knife edge in a Toepler apparatus.

Since the source and its image are not truly coincident, the paths of the incident and reflected rays across the working section differ even in the absence of deflections produced by density gradients. This has an adverse effect on the image quality (in addition to any effect associated with the use of nonparallel light) since two slightly offset images are produced.

**Because the source and its image are very close to each other, the arrangement is often referred to as the "coincidence" system.

These images may be made to coincide at the expense of considerably reduced illumination by using the arrangement sketched in Fig. II-18b. Here a graded filter is placed at 45 degrees to the axis at the centre of curvature of the mirror. A condenser lens is used to produce an image of the source on the surface of the filter, and part of the light from this image is reflected into the mirror. The image of the source formed by reflection from the mirror is made to coincide with the original image on the surface of the filter, and the light transmitted by the filter is arranged to fall on the viewing screen in the usual way. The source and its image may thus be made exactly coincident so that, in the absence of density gradients, the incident and reflected beams coincide. This will no longer be the case when the rays are deflected by density gradients, and some loss of image sharpness, or difficulty in interpreting the observations, may then result.

A further difficulty arises because only one of the two images formed by the incident and reflected light can be in focus. It is usually best to focus the image associated with the reflected light since the incident rays are subject to further refraction during their second passage across the wind tunnel.

The principal advantage of the system is that the double passage of the light beam, and the fact that the source image is formed at the centre of curvature of the mirror instead of its focus, give increased sensitivity. For example, in a two-dimensional flow containing a region of density gradient of sufficient extent for the incident and reflected ray to remain within it, the angular deflection of the ray will be doubled by the use of such a system. Moreover, the displacement of the image of the source for a given angular deflection will be twice as large when the image is at the centre of curvature as when it is at the focus. Coincidence systems may thus be valuable where extreme sensitivity is required, (for example, tunnels working with very low density) although for ordinary use they are undesirable for the reasons mentioned above.

Part of the increased sensitivity associated with a double-passage system may be retained, without the difficulties associated with the use of nonparallel light by means of the arrangement sketched in Fig. II-19. Here a parallel beam of light is produced by a lens or mirror and after crossing the working section it is reflected back by means of a plane mirror.

(k) Schlieren Methods for Quantitative* Use

The use of schlieren systems to obtain direct measurements of the density gradients in the flow has been discussed frequently, but seldom attempted in aerodynamic research. High accuracy (better than about five percent on the measurement of density gradient) has not been claimed in any of the attempts that have been made, and the accuracy appears to be limited for fundamental reasons.

The conventional schlieren methods measure the total angular deflection experienced by a light ray in crossing the working section. Assuming for the present that this measurement can be made accurately, the problem remains of determining the density gradient from the measured deflection. This

---

*All schlieren and direct-shadow methods are quantitative in the sense that they enable the positions and shapes of shock waves and other phenomena to be determined. From the shape of the shock wave the drag can sometimes be calculated (Ref. 71). In this section, however, we restrict the term quantitative to the measurement of the density of the air flowing past the model under test.

would be simple (see, for example, section II(a)) if it were known that a ray of light entering the working section remained in a region of constant density gradient throughout its passage across the working section. Since, however, the ray is continuously refracted this condition may not be realized even in two-dimensional flow if the flow contains strong density gradients, and for three-dimensional flows the problem is further complicated by the variation of density across the working section. It is thus possible, for example, for two rays to suffer the same total deflection although they have followed different paths and traversed regions of different density gradient within the flow.

The magnitude of this difficulty depends, however, on the nature of the flow and the width of the working section; for flows that are two-dimensional or that possess axial symmetry (Refs. 32 and 72), the problem of relating the total deflection of a light ray to the density gradient is frequently soluble. Assuming that this is so, the measurement of the total angular deflection of the rays can be attempted in several ways.

(1) Methods Involving Photographic Densitometry

On the basis of geometrical optics the illumination in the image of the flow in a Toepler apparatus is simply related to the angular deflection of the light rays. Thus the deflections may be determined by, for example, examining a photographic negative of the image with a densitometer. Because of the effects of diffraction at the knife edge, however, the accuracy of such a method is low, especially if the sensitivity is required to be high. Moreover, difficulties also arise in deducing the illumination from measurements of the density of the negative.

An alternative approach which partially compensates for the effects of diffraction is to include in the field a number of "standard schliere" which may take the form of a series of glass wedges (Ref. 32), or bubbles (Ref. 54) of known size containing suitable gases, that produce known or calculable angular deflections. The images of these "standard schliere" on the photographic negative are then used as reference points when examining the negative with a densitometer. The effects of diffraction on the distribution of illumination in the image depend (Refs. 37 and 38), however, on the shape and position of the object observed in the schlieren field as well as on the angular deflection that it produces. The effects will, therefore, usually differ for the "standard schliere" and the region of the flow under consideration, and are thus not entirely eliminated.

In another method, described in Ref. 54, a series of photographs is taken with different knife-edge settings. A small source is used so that the general level of sensitivity is high, and there are rapid changes of photographic density across the photographic plate. It is found (Ref. 54) that the point in the negative where the change of photographic density is most rapid corresponds to the point at which the ray that meets the knife edge has passed through the object under examination. From the series of photographs, the displacements of the rays at the knife edge may be determined for a number of points in the image. Since a number of photographs are required, the method is unsuitable for the study of unsteady phenomena.

(2) Methods Using Grids

In view of the errors that may occur in photographic densitometry, methods that do not involve this process are of interest. The knife edge may be replaced by a grid (Refs. 73 and 38) of alternate transparent and opaque

strips of equal width, and spaced so that the maximum displacement of the image of the source is divided into several steps. The height of the image of the source is arranged to be less than the spacing of the strips of the grid so that, for deflections of the light rays that produce displacements less than this distance, the apparatus behaves as a conventional Toepler system. Suppose the displacement to be in such a direction that the final image initially darkens. For a larger displacement (i.e., a stronger density gradient of the same sign), the source image passes beyond the opaque strip of the grid, and the image lightens again. For gradually increasing density gradient across the object, the illumination across the image may be subject to several cycles of this process, and the image will thus contain bands or fringes each of which is a line of constant illumination, and corresponds to a certain displacement of the image of the source relative to the grid. To determine the displacements it is necessary to identify the particular grid element that gives rise to a particular band in the image. This can be done by taking additional photographs with some of the transparent strips covered up, or by using transparent bands of different colours in the grid and taking the photograph on colour film.

In the system described above, the grid is located in the focal plane of the second lens or mirror, so that in the absence of the disturbance the image is evenly illuminated. If however, the grid is moved along the optical axis away from the focal plane, the image contains a system of fringes running parallel to the strips of the grid, and increasing in number as the distance between the grid and the focal plane is increased. If a disturbance is introduced, the fringes are no longer straight and parallel, but move by an amount proportional to the deviation of the light rays produced by the disturbance. Referring to Fig. II-20, a point, P, in the working section is imaged by the second lens or mirror, M_2, and the focussing lens, L, (assumed for simplicity to lie in the focal plane of M_2) at the point P' on the viewing screen, Q. A grid is placed at distance, g, in front of the focal plane of M_2 so that the diameter of the light beam at the grid is $(g/f_2)d$, whereas the diameter of the final image is approximately $(f_3/f_2)d$.

If a ray passing through the point P' is parallel to the axis, it passes through the centre of the lens, L, before reaching P', but if the ray is deflected at P through an angle, ϵ, it follows a different path before arriving at P'. Thus, it strikes M_2 at a point separated from the undisturbed point of intersection by a distance $\ell\epsilon$, and the lens, L, at a distance $f_2\epsilon$ below the centre. The point on the grid through which the ray passes is thus separated by a distance

$$\epsilon\left[f_2 + \frac{g}{f_2}(\ell - f_2)\right]$$

from the corresponding point in the absence of the disturbance.

If the undisturbed ray passes through the edge of an opaque strip, and the disturbed ray passes through the centre of the strip, the fringe in the image resulting from the shadow of the strip will appear to have been displaced by one-half of its width in relation to the point P', which does not move. The number of fringes in the image depends on the number of strips in the grid illuminated by the light beam, and the spacing of the fringes depends on the spacing of the strips, and on the ratio f_3/g of the diameters of the light beam at the image and at the grid.

The apparent shift of the fringes is, therefore, equal to the displacement of the ray at the grid multiplied by the magnification of

this movement as viewed on the screen. That is, with the notation of Fig. II-20,

$$\text{Fringe shift} = \epsilon \frac{f_3}{g}\left[f_2 + \frac{g}{f_2}(\ell - f_2)\right] \qquad (29)$$

so that the angular deflection of the light ray, and hence the density gradient, can be determined by measuring the fringe shift.

The fringe shift does not depend on the spacing of the strips in the grid, and for detailed studies of the flow it is, therefore, desirable to use a large number of closely spaced strips in order to produce finely spaced fringes. Unfortunately, however, the grid acts as a coarse diffraction grating so that the sharpness of the image is seriously impaired if the spacing is too small. For example, Darby (Ref. 74) found that 100 lines per inch was the practical limit for his apparatus, and his photographs show that the definition was poor compared with that in a conventional schlieren apparatus. The difficulty discussed above for the other grid methods of identifying the fringes in regions of rapidly changing density gradient is present, and may be overcome in the way described.

(3) The Phase-Contrast and Field-Absorption Methods

Regions of the flow of different density have different optical thicknesses, so that light waves passing across the flow will emerge with differences of phase. Such differences cannot be detected visually unless they are are first converted to changes of illumination. This is, of course, done in the Mach-Zehnder interferometer (see section III) where the differences of phase between a light beam that has passed across the flow, and a reference beam, are observed by arranging for the two beams to interfere. The following methods, however, use a different principle for producing the interference, and are more conveniently described here than in section III. The arrangement of the apparatus is similar to that of a schlieren system, except that a certain portion of the light passing through the object plane undergoes special treatment in the plane of the image of the light source so that, in the final image, this light can interfere with the untreated light. Under certain conditions, the density in the flow can then be determined from the interference pattern.

In the phase-contrast (Ref. 75) method a point or line source of light is used in a conventional schlieren arrangement with the knife edge or graded filter omitted. The light that is diffracted by the boundaries and fine structure of the object under examination is scattered in various directions away from the optical axis, so that the images of the source formed by the diffracted light are displaced in the focal plane of the second lens or mirror relative to the central or direct image of the source. If the object is transparent, but contains regions of different optical thickness, the phase of the light waves is affected, but not their amplitude. When all the diffracted light passes undisturbed to the final image, the interference with the direct light is such that no visible effect is produced in the image, since phase differences between various points in the image and not intensity differences occur. If, however, the phases of all the diffracted light can be changed by 90 degrees with respect to the direct light, it may be shown (Ref. 75) that the interference of the diffracted light with the direct light results in intensity differences which correspond with the differences of optical thickness in the object.

The desired change of phase can be produced by putting a phase plate in the focal plane of the second lens or mirror. This plate is made of transparent material, and is

so constructed that its optical thickness in the region covered by the central image of the source differs from that of the remainder of the plate.

Although the phase-contrast method has been widely used in microscopes and for examining the polish of optical surfaces, very few results obtained by using it in wind tunnel work have been published. One difficulty arises because if the phase changes are large and occur as gradients (as is usual in a wind tunnel), appreciable deflections occur at the object with consequent displacements at the phase plate. The effects produced at the image are then more complex than discussed above. Also, the full sensitivity of the method is reached for optical path differences in the object of one wavelength, so that if large path differences are present, the intensity in the image varies through maxima and minima and fringes appear. Some aspects of these problems have been discussed in Ref. 76, where it is suggested that it would be advantageous to decrease the transmission of the outer part of the phase plate for the examination of aerodynamic fields. As far as the authors are aware, the only other paper dealing with the use of phase-contrast methods in aerodynamics is Ref. 77, which includes some photographs taken by the method for comparison with results obtained by the field-absorption method discussed below.

The field-absorption method which is similar in principle to the phase-contrast method has been described in Ref. 77. A narrow slit illuminated by a monochromator is used as the light source in an optical arrangement like a coincidence schlieren system (Fig. II-18a). Instead of a knife edge, however, an absorbing screen is used with a narrow central transparent region on which the source is imaged. In the work described in Ref. 77 this consisted of a partially aluminized glass plate on which a fine line was scratched, and it was found that the image of an aerodynamic field contained fringes depending on the orientation of the source and field-absorption plate. The fringe spacing corresponded approximately to integral intervals of optical thickness in the field. The theory of the method given in Ref. 77 is improved in Ref. 78, where the fringe spacings for simple types of object are calculated.

An analogous interference phenomenon is discussed in Ref. 79, where it is reported that if a line source is used and the central part of the diffraction spectrum formed in the image plane of the source is cut off by a thin wire, fringes appear in the final image. These fringes are found to represent lines of constant optical thickness in the object.

(4) A Method Using Polarized Light

The principle of the method (Refs. 80, 81 and 82) is given in the following description which has been abstracted from Ref. 80. Referring to Fig. II-21a, white light from a slit, S, is converted into a parallel beam by a condenser lens, L_1, and is then polarized by a polarizer, P. After passing through a semireflecting plate, G, a second lens, L_2, produces an image of the slit at the centre of curvature of the spherical mirror, M, placed behind the working section. The light is reflected back across the working section and passes through the lens, L_2, again, after which it is reflected at the semireflecting plate into a lens, L_3, which forms an image of the flow on the screen, Q.

If a suitably orientated Savart plate* is placed between G and L_3 so that the rays strike it normal to the surface, a ray, X,

---

*A Savart plate consists of two parallel-sided plates cut from quartz crystals at an angle of 45 degrees to the optical axis, and superimposed at right angles.

(Fig. II-21b) will be split into two rays, x and x', which are parallel, of the same intensity, polarized at right angles, and separated by a distance, d, which is known for a given Savart plate. One of these rays, x' for example, will coincide with a ray, y, resulting from a ray, Y, separated from X by a distance, d. If an analyser, A, is placed behind the Savart plate, the resultant of the rays x' and y will produce a colour on the viewing screen which is a function of the difference between the lengths of the optical paths followed by the rays X and Y. Thus by knowing the colour in the final image, it is possible to determine the difference between the optical path lengths in the flow of two rays separated by the small known distance, d. The local density gradient in the flow may thus be found.

In practice it is preferable (Ref. 81) to place the Savart plate between G and L_2 in Fig. II-21a, since a large light source may then be used, which increases the illumination in the image. This form of the apparatus has been used to study the flow past a half-aerofoil attached as a bump to the wall of a wind tunnel.

(b) The Direct-Shadow Method

If the density gradient normal to the light beam is nonuniform, adjacent rays will be deflected by different amounts, and will converge or diverge on leaving the working section. An image will then be formed directly as a shadow on a screen or photographic plate held behind the working section as sketched in Fig. II-22a. To obtain a sharp image the dimensions of the light source should be small.*

Referring to Fig. II-22b and, as usual, assuming that the displacement within the optical disturbance of a ray from its undisturbed path (parallel to Oz) may be neglected, the light which originally illuminated an area on the screen, dx dy, now illuminates an area increased by an amount given approximately by

$$l\,dx\,dy\left(\frac{\partial\epsilon}{\partial x}x + \frac{\partial\epsilon}{\partial y}y\right),$$

so that the change of illumination on the screen in terms of the initial illumination is

$$\frac{\Delta I}{I} = -l\left(\frac{\partial\epsilon}{\partial x}x + \frac{\partial\epsilon}{\partial y}y\right) \qquad (30)$$

where l is the distance of the screen from the optical disturbance.

Thus by Eqs. (9) and (10)

$$\frac{\Delta I}{I} = -\frac{l}{n_0}\int\left(\frac{\partial^2 n}{\partial x^2} + \frac{\partial^2 n}{\partial y^2}\right)dz \qquad (31)$$

where the integral is taken over the breadth of the two-dimensional disturbance. On this basis, therefore, the change of illumination is roughly proportional to the rate of change of density gradient. For this reason the method is sometimes superior to the Toepler method (in which the change of illumination is roughly proportional to the density gradient) for observing certain flow phenomena.

---

*The lack of image sharpness due to the finite source size in Fig. II-22a is given approximately by ld/f_1 where d is the source diameter, f_1 is the focal length of the mirror, and l is the distance between the optical disturbance and the viewing screen. As the source size is reduced, however, a limit is reached when the lack of sharpness is due to the effects of diffraction (see Refs. 32 and 114). The magnitude of the lack of sharpness due to diffraction is of the order of $\sqrt{2l\lambda}$, where λ is the wavelength of light, which is the distance between the edge of the geometrical shadow and the centre of the first dark diffraction fringe.

The process leading to the formation of the direct-shadow image of a two-dimensional shock wave is sketched in Fig. II-23. The left hand diagram illustrates the variation of density through the wave, and the second diagram the variation of density gradient. Because of this distribution of density gradient, the light rays are refracted as shown (see section II(a)) and, as a result, the illumination on the viewing screen is of the form sketched. The image contains a region of low illumination on the low-pressure side of the shock, and this is followed by a region of high illumination. Analogous considerations apply to the images of axially-symmetrical shocks, and an example illustrating the dark and light bands in the image is reproduced in Fig. II-24.

In certain circumstances the strength of the shock wave may be determined by measuring the width of the dark band in the image; details are given in Refs. 83, 84, and 85.

The exact nature of the illumination in the image clearly depends on the position of the screen relative to the working section, and on whether the rays are refracted out of the region of density gradient before completing their passage across the working section. Quantitative results can usually be obtained from the direct-shadow method only if, in addition to the usual assumption that the deviation of a ray from its undisturbed path is negligible within the working section, it is assumed that this is also true between the working section and the viewing screen. These assumptions are not usually valid in the regions of sharp change of density gradient commonly observed by the direct-shadow method. Accordingly it has seldom been used for quantitative measurements except in special cases.

It has been found (Ref. 86) that the direct-shadow method can frequently be used to determine whether the flow in the boundary-layer is laminar or turbulent, and to indicate the position along the surface at which transition from laminar to turbulent flow takes place. Fig. II-25 shows direct-shadow photographs of the rear of an aerofoil at zero incidence. In the upper photograph observations by a technique depending on the evaporation of a volatile oil from the surface showed that transition was at 0.73 of the chord behind the leading edge. The direct-shadow image of the laminar boundary layer ahead of this region is seen to include a white line running parallel to, but separated from, the surface of the aerofoil. This line bends towards the surface close to the transition region. The boundary layer was made turbulent from close to the leading edge before the lower photograph was taken, and the image of the boundary layer then contains a white line touching the surface.

The reason for this difference between the images of laminar and turbulent boundary layers may be explained by reference to Fig. II-26. The density profile* for a laminar layer sketched at the left hand side of the upper diagram is seen to contain two sharp changes of slope. At a small distance from the surface, the density gradient increases rapidly thus causing adjacent light rays to diverge as sketched in the centre of the diagram, and producing a region of low illumination, I, close to the shadow of the aerofoil surface as shown on the right hand side. Near the outer edge of the boundary layer the density gradient falls, thus causing the rays of light to converge, and producing a region of illumination (the white line in the photograph), greater than that, I_0, in the image of the undisturbed flow, at some distance

*In the diagram the ratio of the local air density, ρ, to the density, ρ_0, in the undisturbed stream is plotted against the ratio of the distance, y, from the surface of the aerofoil to the thickness, δ, of the boundary layer.

from the shadow of the aerofoil. The density profile for a turbulent boundary layer shown in Fig. II-26b contains only a single region in which the density gradient changes rapidly. Thus at a small distance from the surface the density gradient falls very sharply; this causes the light rays to converge, and produces a region of high illumination much closer to the surface than for a laminar layer.

It is clear from Fig. II-26 that the presence of the boundary layer leads to a region of low illumination close to the surface, that is, to an extension of the direct-shadow image of the surface in a direction roughly perpendicular to the surface. If the boundary layer should separate from the surface, this effect is reduced, so that the image of the apparent surface is displaced away from the flow after separation has taken place. This displacement of the boundary of the dark image may take place quite suddenly, and in such cases gives a useful indication of the position of separation.

According to Eq. (31), the screen should be held at a large distance, ℓ, from the optical disturbance if the greatest sensitivity is required. As the distance is increased, however, not only does the lack of sharpness due to diffraction and the finite source size increase, but the displacements of the boundaries of the dark shadow of the model under test increase. These displacements vary around the periphery of the model according to the local density gradient, so that the image may be markedly distorted if too large a value of ℓ is used. Moreover, as in the example illustrated in Fig. II-26, certain aerodynamic phenomena will not be visualized most clearly if the value of ℓ is too large. The practical result is that the photographic plate must usually be held quite close to the working section, the optimum position being found by a preliminary experiment.

(l) The Focussed Direct-Shadow Method

In the direct-shadow system described above the magnification of the image is unity, and the photographic plate must be held close to the working section. These features are sometimes inconvenient because it may be physically impossible to place the photographic plate close to the working section, or for example, because it may be necessary to darken the whole tunnel room during photography to avoid fogging. In such cases the so-called focussed direct-shadow system is sometimes used. The layout of this system is the same as in a conventional schlieren apparatus (Fig. II-1), except that there is no knife edge in the focal plane of the second mirror, and the focus is altered with the object of producing on the viewing screen an image of the spatial distribution of illumination in the plane occupied by the photographic plate during photography with the system shown in Fig. II-22a. Because of the finite depth of focus, the illumination in the final image does not in practice correspond to that in a plane, but is the integrated result of the distributions in planes spread along the parallel light beam. Also, the apertures of the second mirror and the focussing lens are seldom large enough to collect all of the light refracted and diffracted in the working section, and thus act as stops in the system and affect the illumination in the final image. The aberrations in the mirror system also have some effect. As a result, the image obtained in a focussed direct-shadow system is not identical to that formed by a conventional direct-shadow apparatus, and is usually less sharp.

(m) Light Sources for Schlieren and Direct-Shadow Observations

The most important properties of a light source for use in a schlieren or direct-shadow apparatus are its dimensions, its

brightness and, in the case of flash sources, its duration. The spectral properties of the light may also be important.

The dimensions required for a schlieren source are determined by the considerations discussed in section II(c)(1). A direct-shadow source must be small in order to give a sharp image (see section II(ℓ)).

The length of the exposure time required for a schlieren or direct-shadow photograph depends on several factors. Even if the flow is basically steady, it will usually be subject to small variations which, although of little aerodynamic significance, may nevertheless lead to a slight blurring of the schlieren image if long exposure times are used. Moreover, the flow will usually contain regions of unsteady motion, for example wakes, in which the eddies and fine structure may move in relation to the light beam at speeds of the order of the speed of sound. In this case, if the magnification of the image of the flow is about one-half, an exposure time of the order of one-fifth microsecond is required if the motion is not to be detectable in a photograph. For these reasons it is frequently desirable to use very short exposure times in routine schlieren photography.

There are, however, occasions when a longer exposure time is preferable on the grounds that a single instantaneous photograph may not indicate the time average of a slightly unsteady phenomenon. For example, if it is required to observe the shape of a region of separated flow between a separated turbulent boundary layer and a wall, it may frequently be preferable to use a long exposure time, since in an instantaneous photograph the images of the boundaries of the region may be confused by transient phenomena such as eddies.

If unsteadiness of the flow is to be studied, some information (for example, the amplitude of shock wave oscillations) may be obtained from a photograph taken with a long exposure time, particularly if it is compared with an instantaneous photograph which gives a sharp picture of the motion at some instant, and thus enables the various phenomena present to be identified. In general, however, a series of photographs gives more valuable information, and this may be obtained with a high-speed camera. Such a camera may either use a continuous light source and some type of shutter, or a short duration light source operating at regular intervals (Refs. 87, 88, and 70) or when triggered (Refs. 89 and 90) by the object under examination. In cases where the required frequency of flashes is too large for a single light source, an array of light sources triggered in sequence may be used (Refs. 91 and 92) with, in the case of a schlieren apparatus, a corresponding array of knife edges in the focal plane of the second lens or mirror.

If extremely short exposures or high repetition rates are required, it may be necessary to use a Kerr cell (Refs. 93, 94, and 95), a magneto-optic shutter (Ref. 96), or an image converter (Refs. 97, 98, and 99) of some kind.

(1) Light Sources for Visual Observation or Photography with Mechanical Shutters

For visual observations in subdued room lighting, the illumination (Ref. 100) on the viewing screen should be of the order of 50 metre candles (lumens per square metre). Assuming that the image of the light source is, typically, half cut off by the knife edge it follows that the value of the quantity $(Bbh)/(m^2 f_1^2)$ in Eq. (13) should be about 100 metre candles, where b and h are measured in centimetres, f_1 in metres, and B in stilb (candles per square cm). If the image magnification, m, is not large (about one-third, for

example) this requirement can usually be satisfied inexpensively and conveniently by using a tungsten-filament projector lamp as the light source. Lamps with a wide range of filament shapes and sizes are available, and it is usually possible to select one that is suitable for a particular schlieren system without the use of a condenser and slit. Examples are listed in Table I(a).

If a larger image is required without changing the source size (by using, for example, a condenser lens as discussed in section II(c)(1)), it is necessary to use a brighter source. Various types of discharge lamp may then be used, and examples are given in Table I(b). These lamps require special starting equipment and ballast resistors or shunts, and some of them have restricted burning positions.

High pressure mercury vapour lamps are often used since they are at least ten times as bright as a tungsten filament. A particularly high-powered and compact design, the Mazda BH-6 or B.T.H. MD/H which has been used in several laboratories because it can also be used as a flash source, requires water or forced air cooling. The light emitted is deficient in the red end of the spectrum, and is sometimes considered (Refs. 100 and 105) objectionable for visual observations. This difficulty has been partially overcome (Ref. 105) by the inclusion of other metal vapours in the envelope, and lamps of this type are available commercially with somewhat lower brightness than the unmodified types.

A new type of source, the zirconium arc lamp, has features which make it suitable for use in schlieren systems. The brightness is less than that of a high pressure mercury vapour lamp, but the spectral output is a continuum rising towards the red end of the spectrum with zirconium and argon lines superimposed.

A small xenon discharge lamp, the B.T.H. FA5, has recently been marketed. It has a comparatively low brightness when operated continuously, but can also be operated as a flash tube by changing the external circuit. As a source for visual observation it is inferior to a tungsten filament, because it is less bright, and requires special starting and control equipment.

The high intensity carbon-arc lamp is occasionally used when extreme brightness is required, but by comparison with the other sources mentioned above it is bulky and inconvenient.

The sources described above are suitable for photography as well as visual observation, if the required exposure time can be obtained by means of a mechanical shutter. Since the photographic negative can be enlarged, the image size can usually be smaller than for visual observation, and there is usually little difficulty in obtaining adequate illumination. Because of the very small image size, a bright source is not usually required for ciné photography even with a high-speed camera. For example, successful photographs have been taken with the fastest available 16 mm and 8 mm ciné cameras, such as the Fastax, using a 48-watt tungsten filament lamp as the light source in a conventional schlieren apparatus.

Unless long exposure times are to be used, it is desirable to use a direct current supply to a discharge lamp for still or ciné photography in order to avoid difficulties associated with the fluctuations of brightness of a source driven by alternating current.

(2) Short-Duration Light Sources for Flash Photography

If exposure times less than those obtainable with mechanical shutters are required, they are most simply achieved (Refs. 109,

110, 111, and 112) by discharging a capacitor through a flash tube or spark gap used as the light source in the schlieren apparatus. In the simplest case, the light source is connected across a capacitor (capacity C) which is charged from a source of high voltage. When the voltage has risen to a sufficiently high value, V_0 , the flash tube or spark gap breaks down, and an arc discharge begins. The resistance of the arc path rapidly falls to a low value, and a large oscillatory current flows in the circuit, decreasing in amplitude as the energy originally stored in the capacitor is dissipated. The gas in the arc channel is heated to a high temperature (Refs. 109, 113, and 114) (10,000 to 50,000°K) by the passage of the very heavy current, and acts as a light source of high colour temperature.

For negligible arc-channel resistance, the peak amplitude (Ref. 115) of the current in $V_0\sqrt{C/L}$, and the period of the current oscillation is $2\pi\sqrt{LC}$, where L is the inductance of the complete discharge circuit. It has been shown (Refs. 113 and 115) that, for a given flash tube or spark gap, the intensity of the emitted light increases with peak current and also with the rate of rise of current, which is inversely proportional to the period of the oscillation.

The duration of the light emission decreases with decrease of the period of oscillation. For a given light source, the aims of achieving simultaneously maximum intensity and minimum duration are, therefore, furthered by using a high voltage, V_0, a large value of the ratio, C/L, and a small value of LC. Assuming that the capacitor is used at the maximum voltage that it can withstand, the total light output can be increased by increasing C, as is illustrated in Fig. II-27. However, the period of the oscillation is thereby increased not only by the increase of capacity, but by the associated increase of inductance which usually arises from the increased size of the capacitor. The practical result is that the shortest duration of light output is usually obtained when the capacity, and hence the total light output of the source, is small.

The light emission lags (Refs. 109, 113, and 115) somewhat behind the development of the current through the light source. When the current decreases, the light emission decays more slowly, and does not fall to zero when the current ceases to flow. The duration of this afterglow may be several microseconds, and depends on the nature and pressure of the gas in the flash source (Refs. 92, 109, 113, and 116), and on the material of the electrodes (Refs. 113, 115, and 117). This effect results in a lengthening of the duration of the light emission as compared with the current duration, and this is most significant when the duration of the source is very short.

The intensity of the light is greatest (Refs. 92, 109, 112, 113 and 118) when gases such as mercury vapour, neon, argon, krypton and xenon are used in the flash source, but the duration of the afterglow is unfortunately longer than with air. Thus, when the duration of light emission is required to be very short, these gases are not used. When, however, a much greater light output is required, and the capacity, C, has to be large (with the associated increase of inductance), the period of the oscillation and the duration of the light emission are increased. The afterglow of the rare gases then becomes relatively less important, and advantage can be taken of the improvement of light emission which they give, without appreciably lengthening the duration.

The pressure of the gas and the length of the arc channel also affect the light output. For a given peak current, the intensity of the light is increased by increasing the length of the arc channel or the pressure of the

surrounding gas (Refs. 112 and 113). The maximum length of the arc channel is limited by the voltage available, and for a given voltage, is reduced when the pressure of the surrounding gas is increased.

Details of flash tubes and spark light sources that are suitable for use in schlieren systems are given in the following sections. It is not always convenient to connect the source directly across the capacitor, and to increase the voltage until the discharge gap breaks down, because the length of the gap is then fixed in terms of the voltage and, moreover, the discharge cannot be precisely triggered at any required instant. Methods that may be used to overcome these difficulties are discussed in section II(m)(1)c.

a. Flash Tubes. Two similar tubes, the Mullard LSD.2 and the Siemens SF.7, have sometimes been used as a source for schlieren photography. They suffer from the disadvantage that the arc position may vary considerably from flash to flash, but the effects of this movement may be minimized by setting the knife edge perpendicular to the axis of the electrodes. If operated at the highest possible voltage and with the minimum capacity, the duration can be reduced to between 2 and 5 microseconds.

A xenon discharge lamp, the B.T.H. FA5, is of different geometry to the tubes described above, the electrode spacing being only about one-half cm. As a result, the position of the arc channel is more nearly constant. The flash durations quoted for this source in the literature are rather long, but if a small amount of energy is used (e.g., 0.1 watt-second), the duration can be reduced to between 1 and 2 microseconds. As discussed above, this source can be operated continuously by changing the external circuit, and this can also be done with the Mazda BH-6 or B.T.H. MD/H sources. The latter are flashed at a voltage of from 2 to 3 kv, and, with a discharged energy of 4 watt-seconds, give a duration of between 3 and 6 microseconds. Any of these sources can be operated at a higher voltage by using a series gap or thyratron to hold off the excess voltage until the discharge is required to take place. By this means the duration can be reduced by reducing the capacity and inductance of the circuit.

Brief details of these and other flash tubes that have been used for schlieren photography are given in Table II. Further details may be obtained from the references cited.

b. Spark Light Sources. A number of successful spark light sources for schlieren photography have been described. The simplest form consists of two electrodes separated by an air gap. Such a gap has the disadvantage, however, that the path of the spark may be different for successive discharges so that the position of the effective light source is not constant.

The necessity for fixing the position of the source has resulted in a number of sources designed so that the spark channel is constrained. In the arrangement (Refs. 34, 40, 41, 114, 120, 121, 122, and 123) shown in Fig. II-28a, the spark is discharged up a tube of insulating material set up along the optical axis so that the diameter of the effective light source is approximately the same as that of the bore of the tube, and of the hole drilled in the front electrode. The separation of the electrodes depends on the voltage that is to be used,* and within limits (from about 0.01 inch to about 0.08 inch) the bore of the tube may be chosen to give the required source diameter.

---

*For the type of gap shown, the voltage is about 20 kv per centimetre of electrode separation.

The material from which the tube is made should be a good insulator which does not char due to heating, and should be strong enough for the tube not to crack or shatter when the discharge takes place. Unfired soapstone has been used, but some samples of this material tested at the N.P.L. have been found to have comparatively low resistance. An alternative material may, therefore, be preferable, and glass-bonded mica has given satisfactory results. It is available in the form of rods which can be drilled to provide a bore of the required diameter. Other materials which have given satisfactory results are fluorocarbons (e.g., Teflon) and glass capillary tubing. The electrodes may be made of mild steel or, if longer life is required, of stainless steel, tungsten, or tantalum. Magnesium or cadmium electrodes give (Ref. 115) a larger light output, but longer exposure times.

A widely used type of spark gap which is similar in principle to that discussed above is shown in Fig. II-28b, and usually ascribed (Refs. 112, 114, 120, 124, and 125) to Libessart. The main features are the small-diameter constraining bore, which assists in fixing the position of the light source, and its short length which improves the insulation of the rear electrode by surrounding it with an air gap. The fact that the spark channel is only confined for part of its length may also reduce the duration of the light emission, since some workers have found (Refs. 115, 117, 120, 122, 124, and 125) that the duration is increased by confining the spark.

The small circular light source provided by the spark gaps described above is suitable for use in a direct-shadow apparatus, or in a schlieren apparatus using a graded filter. Unless the range required is small it is not, however, suitable for direct use in a conventional knife-edge system. Spark gaps for this purpose are sketched in Fig. II-28c and d. In one example (Fig. II-28c) the discharge takes place between two electrodes in a glass capillary tube (Ref. 121) set up perpendicular to the optical axis, so that the source shape is a long thin rectangle. With this arrangement, difficulties may be experienced with shattering of the glass, and because the bore of the tube becomes partially opaque after long usage. An alternative scheme (Refs. 120, 121, 34, 41, and 40), which avoids these difficulties, is to form the spark between flat electrodes constrained as a sandwich between glass plates as shown in Fig. II-28d.

With a source of this type, the range and sensitivity can be adjusted (Refs. 34 and 41) by rotating the source about the optical axis so as to change its effective height (i.e., the dimension perpendicular to the knife edge). If this is done, however, it may be necessary to adjust the position of the knife edge along the optical axis because of the effects of astigmatism (see section II(e)).

c. Details of the Electrical Circuit. In order to minimize the inductance of the discharge circuit, it is necessary to use short, thick, closely-spaced connections between the capacitor and spark gap, or a concentric arrangement. The best arrangement depends on the form of the capacitor, and examples are shown in Fig. II-29. Further details of these and other arrangements may be found in Refs. 40, 41, 114, 115, 122, 123, 124, 125 and 126.

A number of suitable capacitors are commercially available; they should have small internal inductance and internal connections which are strong enough to withstand the loading that arises from the passage of the heavy discharge current. Designs using the squashed-foil type of construction (see, for example, Ref. 125) in a cylindrical case with a terminal at each end appear to be the most satisfactory at present available in the United Kingdom for use at high voltages (above 10 kv).

In an effort to improve the performance obtained with paper dielectric capacitors, tests have been made with a tubular capacitor with a barium titanate dielectric which, because of its high dielectric constant (1500 to 3000 as compared with 2.5 to 4 for paper), results in a very compact arrangement. The object of the work done (Ref. 123) in the U.S.A. was to use a barium titanate tube as a transmission line (Ref. 114) of such a low surge impedance that it matches the resistance of the spark gap. If this can be done, the current pulse through the gap should have constant amplitude, and a duration equal to the time required for a voltage wave to pass up and down the transmission line. Although a short duration of the light emission (2×10^{-7} second) was obtained, however, the duration was over ten times as long as the time calculated for the wave to pass up and down the transmission line.

In some similar tests (Ref. 40) in the United Kingdom, a tube of barium-strontium titanate was used as the dielectric of a capacitor arranged as in Fig. II-29b. The results were similar to those reported in Ref. 123, but since similar performance was subsequently obtained from a good condenser with a paper dielectric, it was felt that the exploitation of the novel type of capacitor could await its commercial development.

As remarked above, the total light output increases as the capacity or the voltage is increased. An example is reproduced in Fig. II-27 where the spark was formed across a 2 mm gap between stainless steel spheres in air, and commercial paper-dielectric capacitors were used. Here the energy stored in the capacitor was increased by increasing the capacity at constant voltage, but similar results were obtained if the voltage was raised with constant capacity. No systematic measurements of the brightness of spark sources are known to the authors, but the values appear to lie between 2×10^6 and 400×10^6 stilb.

Values of the duration of the light from various spark sources are included in Table III. Further details of the gaps used, and of the waveforms of the light emitted may be found in the references cited.

The power required for the high-voltage supply may be estimated from the energy discharged in each spark and the required frequency of sparks, allowing for half of the power to be lost in the charging resistor. If intermittent sparks only are required, cathode-ray tube power supplies of the type used in television receivers are suitable, but more powerful sources of high voltage are needed if frequent sparks are required for ciné photography or for setting up the apparatus (see section II(g)). Metal rectifiers may be used in a voltage-multiplying circuit as shown in Fig. II-30, or the schemes described in, for example, Refs. 21, 53, 87, 88, 89, 107, 114, 119, 128, 130, 131, and 132 may be used.

The arrangement used to control or trigger the spark depends on the required performance, and on the details of the circuit. The high-voltage supply can be connected to the capacitor as sketched in Fig. II-31 through a mechanical high-voltage relay which is closed when a spark is required. This scheme is, however, unsuitable for the controlled production of a rapid succession of single sparks, since the charging time must be long compared with the operating time of the relay. Other applications of high-voltage contactors and thyratron switches are described in Refs. 70 and 88.

An alternative scheme which may be used to produce single sparks at frequencies up to about two per second is to use (see Fig. II-32 and Ref. 121) an induction coil whose primary winding is pulsed from a DC supply by means of a contactor. The voltage generated on the break of the contactor is greater than on the make, and the length of the spark gap is adjusted so that it fires only on the break.

This system has the merit of simplicity and reliability, and is very safe because the high voltage occurs only when the contactor is made and broken.

In the majority of other systems that have been described, the capacitor is charged to the the steady level of the high-voltage supply, and the spark gap is fired by triggering a third electrode in the gap (see Figs. II-29c and II-29d and Refs. 14, 92, 112, 114, 124, 125, 127, 128, and 130), by triggering a three-electrode gap or thyratron connected in series with the main gap (Refs. 89, 92, 104, 107, 112, 114, 125, 132, and 133), or by triggering a three-electrode gap or thyratron which disturbs the potential across the main gap and causes it to break down (Refs. 90, 112, 120, 122, 131, and 134). Examples of these arrangements are sketched in Fig. II-33; they enable the spark to be fired at any chosen instant, or at instants synchronized with the event that is to be photographed.

The time that elapses between the arrival of a trigger pulse and the firing of the light source may sometimes be important, and depends on the details of the circuit and of the components used. The delay between the application of the high voltage to the light source or trigger gap can be made very short (0.02 to 0.1 microsecond)(Ref. 109), if the voltage applied to the electrodes is sufficiently (say, 20 percent) in excess of the minimum value required to break down the gap. The delay between the arrival of the trigger pulse at the thyratron control grid and the output pulse from the thyratron depends on the amplitude and rate of rise of the voltage pulse on the grid, on the circuit values, and on the type of thyratron used. It is usual to employ xenon or hydrogen thyratrons because of their shorter ionization (and deionization) times compared with mercury-vapour types. It is found (Refs. 120, 128) that the delay in the firing of such thyratron circuits is one microsecond or less.

The rise times associated with automobile spark coils are stated (Ref. 122) to be between 10 and 150 microseconds, and the delays with circuits employing them are therefore relatively long (e.g., 10 microseconds)(Refs. 90, 122, and 128). If a specially designed pulse transformer is used, the delay can be reduced (Refs. 122 and 125) to a fraction of a microsecond. An alternative approach is to omit (Ref. 128) the pulse transformer or spark coil as shown in Fig. II-33a, but this leads to a rather short life for the thyratron.

It is sometimes more important for the delay to remain the same on each operation than for it to be very short. Variability in the delay (termed "jitter") may arise from various causes such as varying supply voltage, circuit hum and noise, microphony, low rates of rise of trigger pulses, interference from external sources, and variable triggering due to the effects of varying ambient illumination on the thyratron. By taking suitable precautions, the jitter can be reduced to less than 0.1 microsecond (Ref. 128).

In some applications it is necessary to introduce a known delay between the trigger pulse and the firing of the light source. Many methods are available for doing this, and details are given in, for example, Refs. 14, 89, 125, 128, 132, 133 and 135.

(n) Photography of the Schlieren Image

The main factors leading to differences between schlieren photography and ordinary pictorial photography are the relatively low contrast of the schlieren image, and the frequent need in schlieren photography for very short exposure times.

If the schlieren image is formed on a photographic plate or film, the different illuminations, I, in the image will result, after development, in different densities, D, in the negative, D being defined by the equation

$$D = \log_{10} \frac{T_o}{T}$$

where T_o is the intensity of light incident (e.g., in the printing process) on the negative, and T the intensity of transmitted light for the point under consideration.

When the negative is printed, these differences of transmission density will appear as differences of reflection density, D_R, of the print, defined by

$$D_R = \log_{10} \frac{R_o}{R}$$

where R_o is the intensity of light incident on the print (e.g., when it is studied visually), and R is the intensity of the light reflected from the print.

The relationship between the appearance of the print and of the schlieren image depends on the photographic characteristics of the negative and positive materials, and these are conveniently discussed in terms of their characteristic curves. In these curves the negative and reflection densities respectively are plotted against the logarithm (to the base 10) of the exposure, which is the product of the exposure time and the intensity of the illumination falling on the photographic material. Such curves (see, for example, Figs. II-34 and II-39) usually contain portions which are approximately linear, and the slopes of these portions will be denoted by γ_N and γ_P for the negative and positive materials respectively.

If the contrasts C_I, C_N, and C_P of the schlieren image, the negative, and the print are defined by the expressions

$$C_I = \log_{10} \frac{I_{max}}{I_{min}}$$

$$C_N = \log_{10} \frac{T_{max}}{T_{min}}$$

$$C_P = \log_{10} \frac{R_{max}}{R_{min}} ,$$

it is clear that they are related by the equations

$$C_P = \gamma_P C_N = \gamma_P \gamma_N C_I .$$

It is usually possible to arrange for the product $\gamma_P \gamma_N$ to exceed unity, and the contrast* in the photographic print then exceeds that in the schlieren image. For this reason it may be possible to observe details in the print which are not visible by direct inspection of the schlieren image, although in practice the situation is complicated by the use of the nonlinear parts of the characteristic curves.

Fig. II-34 shows typical characteristic curves for a series of grades of printing paper. The exposure can be arranged to lie at any point along the abscissa by adjusting the printing time, but the difference between the logarithms of the maximum and minimum exposures is independent of printing time, and equal to the contrast, C_N, of the negative. It is clear from Fig. II-34 that the full range of tones of the printing paper from black to white cannot be used to show differences of illumination in the image if C_N is too small. For the range of printing papers available in the

*The maximum value of C_P is limited by the characteristics of the printing paper to a value between 1.5 and 1.9 (see Ref. 136).

United Kingdom, the experience with schlieren photography at the N.P.L. suggests that, if possible, the negative contrast should be about 0.5, although values down to 0.25 can be tolerated if a deterioration of print quality is acceptable. Thus, referring to Fig. II-35, which shows part of a typical characteristic curve for a negative emulsion, it is desirable that a negative contrast of at least the value given above should result from the contrast, C_I, of the schlieren image.

There is little published information on the contrasts of typical schlieren images, but an examination of a large number of examples suggests that it seldom exceeds unity (i.e., that the ratio of the maximum to the minimum illumination is less than ten). This value is lower than that calculated (Refs. 37 and 38) for simple types of objects on the basis of wave theory, the low value being due in part to the effects (Ref. 136) of stray reflections and flare in the optical system.

Accepting this value of the image contrast as typical, it follows that over the region used, the average slope of the characteristic curve for the negative material (Fig. II-36) should if possible be at least 0.5. There is usually no difficulty in satisfying this requirement if the exposure level is large enough to lie under the linear part of the curve, and this can generally be achieved in cases where short exposure time is not required. One of a wide range of different emulsions may then be used since, although each will give a different contrast, similar prints will be obtained on the correct grade of printing paper.

Equally satisfactory results have been obtained with panchromatic and non-panchromatic emulsions, but the fact that the latter can be handled in comparatively bright safe lighting is usually a practical advantage. According to Eqs. (13) and (20), the exposure in a typical system is approximately $1/2\left[(Bbh)/(m^2 f_1^2)\right] t$ where t is the exposure time, and the required values of the quantities that appear in this equation can thus be estimated in terms of the exposure required by the negative material. Approximate values are given for guidance in Table IV.

Although the emulsion speeds quoted by manufacturers are a useful guide, it is desirable to take a series of trial negatives before selecting the conditions for routine photography, because the contrast of the schlieren image is low compared with that usual in pictorial photography for which the manufacturer's speed ratings are given.

(1) Photography with Flash Light Sources

If a very short exposure time is required, it is necessary (see section II(m)(2)) to minimize the light output of the flash source. Under these circumstances it is desirable to use the minimum exposure of the negative that is compatible with obtaining a satisfactory print. The nonlinear portion at the toe of the characteristic curve may then be used in order to give an increase of speed, provided that adequate negative contrast is obtained. A useful guide to the speed of the emulsion when used in this way is the reciprocal of the exposure, E_I, (Fig. II-36) which gives a certain average slope (e.g., 0.5 or 0.25) of characteristic curve for an image contrast of unity.

Under normal conditions, the density of a given emulsion developed in a given way depends only on the exposure, It, and not on the individual values of the illumination, I, and the exposure time, t. Thus, for a given density, the illumination and exposure time are related (Ref. 136) by the "reciprocity" law, $It = \text{constant}$. For some emulsions this may no longer be true (Ref. 136) if t is very small, and the value of I correspondingly large. However, as far as schlieren photography is concerned, this failure of the

reciprocity law is not usually important, partly because the effects are small (Refs. 110, 137, and 138) with suitable emulsions and development, and partly because the exposure cannot in any case be accurately predicted for a spark source, because of inadequate data on the brightness and duration.

Since the sensitivity of a photographic emulsion depends (Ref. 136) on the wavelength of the incident light, the spectral properties (Refs. 109, 114, and 115) of the light emitted by the source may have some effect. As illustrated in Fig. II-37,* the light from a spark is usually deficient in the longer wavelengths as compared, for example, with that from a tungsten filament. The result is that any advantage of a panchromatic emulsion for photography with a tungsten source is somewhat reduced for spark photography.

Moreover, the spectral distribution of the light from a spark source or a flash tube varies with time, being richest in ultra-violet and blue in the early stages of the discharge, when the peak current is flowing and the temperature in the arc channel is highest. As the current decays and the channel expands and cools, the light output decreases and becomes redder. The duration of the light emission is thus shortest for the blue end of the spectrum so long as line spectra from, for example, the electrode materials, do not affect the latter stages of the emission. Accordingly, it has often been suggested that in order to reduce the effective duration of a spark light source, the photographic emulsion should be sensitive to blue light only.

The possibility of failure of the reciprocity law does not appear (Refs. 136 and 137) to depend on the wavelength of the light, but there is evidence (Ref. 136) that the slope of the characteristic curve of the emulsion is less for a spark than for a tungsten source. This effect may be important if the exposure is marginal, because it reduces the speed and contrast.

The characteristic curve for a particular emulsion depends on the type of developer used and on the development time, an example being shown in Fig. II-38. In general, the speed of the material and the slope of the characteristic curve increase with development time up to a certain limit. For ordinary photography, development times are often limited to values below these giving maximum speed in order to restrict the contrast and grain size of the negative. For schlieren photography this is not usually desirable, unless very small images** are used for which the grain size may be important, and it is preferable to use long development times and energetic developers in order to produce (Ref. 110) the maximum contrast and speed.

Because of the conditions of operation on many wind tunnels, it is sometimes difficult to avoid fogging the negative to some extent, especially when taking direct-shadow photographs. The curves of Fig. II-41 illustrate the effect of fogging on the characteristic curves, the photographic plates being exposed close to a safelight for some seconds in addition to a normal exposure with a spark light source. In addition to increasing the fog

*Curves for the reflectivity of aluminium and the transmittance of typical glass samples are included in Fig. II-39, and show that these quantities are insensitive to the wavelength of the light over a wide range.

**As discussed above, the permissible image size is related to the speed of the emulsion; for schlieren photography better resolution is in general obtained in the photograph when a fairly large image is used with a fast emulsion than when the alternative possibility of using a small image and a slow emulsion is adopted.

level, the slope of the characteristic curve is reduced and hence, also, the speed and contrast.

As a rough guide for the selection of an emulsion, the relative speeds for various conditions of several emulsions available in the U.S.A. (Ref. 137) and in the United Kingdom are shown in Tables V and VI respectively. In Table V values are given for two negative densities; the density of 0.1 above fog is representative of the conditions when the exposure is very small and, although the phenomena present in the schlieren image would be detectable in the negative, the print quality would be poor. The density of unity, on the other hand, is high by comparison with the values usually achieved in schlieren photography at short exposure times, and is more typical of the conditions that can be achieved with long exposure times. In each column the speed of the fastest emulsion is denoted by 100, and the speeds of the other emulsions are given relative to this speed. The numerical values in different columns cannot, in general, be compared.

In Table VI the relative speeds are given in the same way for a density 0.1 above the fog level, and for average slopes of the characteristic curves (see Fig. II-36) of 0.25 and 0.5.

Because of the desirability of using fairly bright safelights on the wind tunnel and in processing, and because of possible lengthening of the effective duration of the flash source, fast panchromatic emulsions are frequently not used for schlieren, and, especially, for direct-shadow photography. The practice at the N.P.L. is to use either Ilford Fast Blue Sensitive Type LN plates or Kodak Experimental Plates No. V1015, and it is found that under the conditions of spark photography these require an exposure of the order of 0.01 metre candle seconds for satisfactory results.

(2) The Photography of Colour-Schlieren Images

Although the same general principles apply to the photography of coloured schlieren images as to the photograph of monochromatic images, certain differences of detail arise. The colour material is normally designed to represent correctly the colours of an object illuminated by daylight or tungsten light of a certain colour temperature. If the best possible colour rendering is required, the colour temperature of the light source may, therefore, need to be considered, and filters used to correct it if necessary. It is not possible to assess the effect on the emulsion by visual observation of the image, because of the different spectral responses of the eye and the emulsion. Moreover, if a short exposure time is to be used, the colour rendering of the material may be altered by effects due to reciprocity law failure.

True colour rendering may not, however, be important for qualitative work since there are no natural standards of comparison for a colour-schlieren image, and all that is required is that the colour range and gradation should be satisfactory. If some distortion of colour rendering can be tolerated, the use of the toe of the characteristic curve and prolonged development can give increases of effective speed as with monochrome materials. Colour-schlieren images appear to have the same order of contrast as their monochrome counterparts, and are thus easily recorded on colour materials which, at present, have limited latitude and cannot accommodate satisfactorily high-contrast images.

For ciné photography the use of colour film is usually as simple as monochrome film, since it is often the practice for the processing to be done by a specialist firm in both cases. For single-exposure photography the extra

time required for processing colour materials is a disadvantage in routine work, but this is to some extent overcome by the newer types of film which enable a monochrome image to be examined before the colour development is carried out.

(o) Schlieren and Direct-Shadow Methods for Visualizing Three-Dimensional Flows

Many of the features described above apply no matter what type of flow is to be observed, and we now consider the special arrangements which may be necessary if three-dimensional flows are to be visualized. If a three-dimensional flow is examined with a parallel beam of light, the image lacks depth and it is difficult to determine the positions along the beam of the flow phenomena which are present. The strongest deflections of the light occur when the rays are tangential, or nearly so, to the shock and expansion waves. Thus the image resulting from a system using parallel light will give the impression of superimposed cross sections of the flow, the cross sections being taken normal to the beam at the points where the rays are tangential to the shock and expansion waves. It follows, for example, that for the visualization of the flow past swept wings it is frequently necessary (Refs. 139 and 140) to pass the light beam obliquely across the working section. Moreover, in a complicated flow the light rays may follow tortuous paths, and the deflections at exit from the working section may not be a true indication of the strengths of the disturbances.

These are only incidental difficulties, however, and in simple cases the use of a conventional schlieren system to observe a three-dimensional flow is satisfactory. For example, no difficulty usually arises for flows possessing axial symmetry since the image is essentially a cross section of the flow at the median plane from which (together with the traces of the interaction of the shock waves with the glass walls of the tunnel as shown, for example, in Fig. II-24) the complete flow pattern can be deduced. In many cases useful results can be obtained (Refs. 139, 141, and 142) by rotating the model about the longitudinal wind axis so that, in effect, a series of photographs is obtained from a number of directions perpendicular to this axis. Alternatively, valuable information often results from projecting (Ref. 143) the direct-shadow image of the flow on to one wall of the wind tunnel by means of a light beam entering the tunnel through the opposite wall.

In many cases, however, the conditions are more complicated, and it is then desirable to assign positions along the beam of light to the various flow phenomena. Several techniques have been devised to enable this to be done, and these are described briefly below. It should be emphasized that some of these techniques are in an early stage of development, and that more work is necessary before their value can be assessed.

(1) The Stereoscopic Method

The stereoscopic method was developed (Ref. 144) by Lyot and Françon for examining discs of glass, and has been used subsequently in France (Ref. 145) and America (Ref. 146) for observing combustion and aerodynamic phenomena. The apparatus (Fig. II-40) consists of either a single parallel beam of light used to photograph the flow in the working section from two different directions,* or two inclined beams used to

*In Fig. II-40a the setup is for the examination of a glass disc. It is then simpler to rotate the disc (from position I to position II) relative to the beam of light than it is to move the beam itself.

take photographs from two directions simultaneously. The photographs are viewed with a stereoscope. An example (Ref. 144) of a stereoscopic pair of photographs showing faults in a glass disc is reproduced in Fig. II-41.

(2) The Rangefinder Method

The rangefinder method was developed (Ref. 7) by Lamplough who used it for photographing the shock waves close to the wing of an aeroplane flying at high speed. The apparatus is sketched in Fig. II-42 and consists of a conventional parallel-beam arrangement with the addition of a glass wedge close to the collimating lens. The light beam is set up along the span of the wing, and the position of a shock wave along the beam is estimated by observing the relative displacement of the part of the image associated with light which has passed through the wedge. The type of record obtained is shown in the example reproduced in Fig. II-43. The displacement of the image is proportional to the distance from the shock wave to the plane in the object space conjugate to the viewing screen or photographic film, and is in opposite directions for shock waves lying on opposite sides of the conjugate plane.

In the apparatus used by Lamplough, no knife edge was used in the focal plane of the second lens. This arrangement appears to be satisfactory for observing shock waves, but if it is required to visualize the boundary layer as well, it may be desirable to use a knife edge as sketched in Fig. II-42. If a knife edge is used it must be set parallel to the displacement produced by the rangefinder wedge. Although phenomena producing deflections perpendicular to the edge may thus be visualized, it will be impossible to determine their position along the light beam.

If the shock waves are highly curved, it may be necessary to incline the light beam in the manner described in section II(o)(4) until it is approximately tangential to the element of the shock which is to be visualized. By taking photographs for a range of inclinations of the beam it may then be possible to obtain the position (and possibly also the slope) of a number of elements of the shock, and hence to deduce its shape.

(3) The Sharp-Focus Method

The sharp-focus method was developed (Ref. 147) on a small scale by Kantrowitz and has been the subject of considerable interest; in its present form it suffers from a number of disadvantages which have been discussed (Ref. 148) by Fish and Parnham. The method (Fig. II-44) depends on the fact that any point in the object is illuminated by rays of light within a solid angle, α, equal to that subtended at the first lens or mirror by the extended source. The depth of focus depends on the angle, β, and the diameter of the acceptable circle of confusion in the image; the angle, β, is determined by the angle, α, and the image size. Thus, for a given ratio of the diameter of the circle of confusion to the image size, the depth of focus is approximately inversely proportional to the angle, α. Hence a short depth of focus may be obtained by using a large source of light. The objection that the sensitivity as a schlieren system of the apparatus will be low when the source is large, is overcome by using an array of small slit sources and a corresponding array of knife edges as a cut off.

When the sensitivity is moderately high, the image quality suffers from the effects of diffraction at the multiple knife edges, and the situation is aggravated by the fact that the object plane in sharp focus is shown on a background of the out-of-focus object planes.

(4) Shock Wave Plotting Methods

The shock wave plotting method was developed (Ref. 7) by Lamplough and has been used to record shock wave patterns in flight and in the wind tunnel. The apparatus used in the wind tunnel observations is sketched in Fig. II-45; the apparatus used in flight operates on the same principle. It involves the use of a parallel beam of light which may be rotated about an axis normal to the plane of the wing, which will be taken as horizontal in the following discussion. The light passing through a horizontal slice of the working section is received on a film through a narrow horizontal slit. As the beam is rotated about the vertical axis the film is moved in a vertical direction, the slit remaining at rest. At any point in the rotation of the beam where the light rays are tangential to the shock front in the narrow slice of the flow field under observation, a dark band is recorded on the film. From this record it is possible to deduce the shape of the shock front in the part of the flow examined.

An example (Ref. 149) showing the result obtained when the shock contour is reconstructed from the original record by means of a specially designed "reduction box" is reproduced in Fig. II-46. This shows the shock contour a little above the surface of a wing with 50 degrees sweepback.

By moving the slit in front of the film to successive positions across the field of flow the entire field can be scanned, a frame of film being obtained for each slice explored.

The criticism has been made that when the method is used on a wind tunnel, the windows in the side walls need to be very long in order to allow the beam of light to be passed obliquely across the flow. The objection is not, however, confined to this particular method of visualization since most optical methods require that the light beam can be rotated until it is approximately parallel to the shock front which is to be observed.

(5) A Method for Conical Flows

For the visualization of conical or nearly conical flows, the technique described in Ref. 150 may be used. Here a conical beam of light whose vertex approximately coincides with that of the conical flow is used to produce a direct-shadow image on a screen held in the working section downstream of the model. In order to reduce the blockage caused by the screen, this takes the form of a propeller with flat white blades rotating at high speed. The arrangement of the apparatus for visualizing the flow past a half-span model supported from the tunnel wall is sketched in Fig. II-47. For complete models a point light source is mounted either directly in the nose of the model or in an extension of the nose.

(6) Techniques for Half-Span Models

If the wall or reflection plate from which a half-model is supported is transparent, a beam of light can be passed across the tunnel and any of the schlieren methods described above can be used. Alternatively, limited observations can be made through a small window located in the reflection plate; for example, the flow near the tip of a highly swept wing has been observed through a window located at the rear of the reflection plate.

In most cases, however, the wall or reflection plate is opaque, as the apparatus behind it will obstruct the beam of light. It may then be possible to use the reflection plate as an optical mirror and, using the schlieren methods described above, visualize the flow by reflecting the light back across the tunnel.

A simpler method for obtaining less detailed information is to project the image of shock waves and other flow phenomena on to the prepared surface of the reflection plate in the manner sketched in Fig. II-48, and

shown in the example reproduced in Fig. II-49. This technique is, of course, equally applicable to wing-body combinations (the image of the flow near the wing being projected on to the surface of the body) where the size of the body would prevent observations of the flow near the wing surface by the usual schlieren methods.

An alternative method (Ref. 151) which may be useful in special cases is to project the image of the shock wave on to the surface of the wing as shown in Fig. II-48. A similar method has been used (Ref. 8) in flight, the direct-shadow image of the shock wave being formed on the surface of the wing by light from the sun.

REFERENCES

1. Howarth, L., Editor, "Modern Developments in Fluid Dynamics - High Speed Flow," Vol. 2 Chapter XI, Oxford University Press, 1953.

2. Pankhurst, R. C., and Holder, D.W., "Wind Tunnel Technique," Pitman, 1952.

3. Hills, R., "Use of Wind Tunnel Model Data in Aerodynamic Design," J.R.Ae.S., p. 1, January 1951.

4. Black, J., "A Note on the Vortex Patterns in the Boundary Layer Flow of a Swept-Back Wing," J.R.Ae.S., Vol. 56, p.279, 1952.

5. Allen, H. J., and Perkins, E. W., "A Study of Effects of Viscosity on Flow over Slender Inclined Bodies of Revolution," NACA Report 1048, 1951.

6. Bird, J. D., and Riley, D. R., "Some Experiments on Visualization of Flow Fields Behind Low Aspect Ratio Wings by Means of a Tuft Grid," NACA TN 2674.

7. Lamplough, F. E., "Shock-Wave Shadow Photography in Tunnel and in Flight," Aircraft Engineering, April 1951.

8. Cooper, G.E., and Rothert, G. A. Jr., "Visual Observations of the Shock Wave," NACA RM A.8.C.25, 1948.

9. Cooper, G. E., and Bray, R. S., "Schlieren Investigation of the Wing Shock-Wave Boundary-Layer Interaction in Flight," NACA RM A.51.G.09, 1951.

10. Charters, A. C., "Ballistic Spark Photography," NAVORD Report 74-46, 1946.

11. Charters, A. C., "The Spark Photography Range," Paper read at the 6th International Congress of App. Mech., Paris, 1946.

12. Charters, A. C., and Thomas, R. N., "The Aerodynamic Performance of Small Spheres from Subsonic to High Supersonic Velocities," J.Ae.S., Vol. 12, p. 468, 1945.

13. Hankins, G. A., and Cope, W. F., "The Flow of Gases at Sonic and Supersonic Speeds," Proc.I.Mech.E., Vol. 155, p. 401, 1946.

14. Soule, H. V., and Sabol, A. P., "Development and Preliminary Investigation of a Method of Obtaining Hypersonic Aerodynamic Data by Firing Models through Highly Cooled Gases," NACA TN 2120, 1950.

15. Stephens, V. I., "Hypersonic Research Facilities at the Ames Aeronautical Laboratory," J.App.Phys., Vol. 21, p. 1150, 1950.

16. Becker, J. V., "Results of Recent Hypersonic and Unsteady Flow Research at the Langley Aeronautical Laboratory," J.App.Phys., Vol. 21, p.619, 1950.

17. Lobb, R. K., "A Study of Supersonic Flows in a Shock Tube," University of Toronto, U.T.I.A. Report No. 8, 1950.

18. Bleakney, W., Weimer, D. K., and Fletcher, C. H., "The Shock Tube. A Facility for Investigation in Fluid Dynamics," Rev.Sc.Inst., Vol. 20, p. 807, 1949.

19. Geiger, F., and Mantz, C. W., "The Shock Tube as an Instrument for the Investigation of Transonic and Supersonic Flow Patterns," Contract N6-ONR-232, Project M720-4, Eng. Res.Inst., University of Michigan. See also Phys.Rev., Vol. 79, p. 230, 1950.

20. Bleakney, W., and Taub, A. H., "Interaction of Shock Waves," Rev.Mod.Phys., Vol. 21, p. 584, 1949.

21. "The Manchester University Shock Tube," British A.R.C. No. 17,238, 1955.

22. Ladenburg, R. W., Lewis, B., Pease, R. N., and Taylor, H. S., Editors, "Physical Measurements in Gas Dynamics and Combustion," Vol. 9 of High-Speed Aerodynamics and Jet Propulsion, Princeton University Press, 1950.

23. Townend, H. C. H., "On Rendering Airflow Visible by Means of Hot Wires," British A.R.C. R.&M. 1349, 1931.

24. Townend, H. C. H., "Abstract of a Film Illustrating the Theory of Flight," R.&M.1767, 1937.

25. Townend, H. C. H., "Hot Wire and Spark Shadowgraphs of the Airflow through an Airscrew," R.&M. 1434, 1932.

26. Townend, H. C. H., "Visual and Photographic Methods of Studying Boundary Layer Flow," British A.R.C. R.&M. 1803, 1937.

27. Valensi, J., and Pruden, F. W., "Observations on Sharp-Pointed Profiles at Supersonic Speed," R.&M. 2482, 1947.

28. Mach, L., "Uber ein Interferenzrefraktometer," S. B. Wien. Akad., Vol. 98, p. 1318, 1889. Also Z. Instrumentenk, Vol. 11, p. 275, 1891 and Vol. 14, p. 279, 1894.

29. Toepler, A., "Beobachtungen nach einer neuen optischen Methode," Poggendorf's Ann. d. Phys. u. Chem., Vol. 127, p. 556, 1866. See also Vol. 128, p. 126, 1866 and Vol. 131, p. 33 and 180, 1867, and Vol. 134, p. 194, 1868.

30. Dvorak, V., "Uber eine neue einfache art der Schlierenbeobachtung," Wiedemann's Ann. d. Phys. u. Chem., Vol. 9, p. 502, 1880.

31. Schardin, H., "Das Toeplersche Schlieren Verfahren," V.D.I. Forschungsheft No. 367, Vol. 5, 1934.

32. Schardin, H., "Die Schlierenverfahren und ihre anwendungen," Ergebnisse der exakten Naturwissenschaften, Vol. 10, 1941.

33. Weyl, F. J., "Analytical Methods in Optical Examination of Supersonic Flow," NAVORD Rep. 211-45, 1945.

34. Holder, D. W., and North, R. J., "The Toepler Schlieren Apparatus," British A.R.C. R.&M. 2780, 1950.

35. Mair, W. A., "The Sensitivity and Range Required in a Toepler Schlieren Apparatus for Photography of Supersonic Flow," The Aeronautical Quarterly, Vol. 4., August 1952.

36. Gorges, H. A., and Johnson, E. R., "The Specification of Schlieren Optics for Wind-Tunnel Use," Australian Tech. Note No. H.S.A. TN/3, 1952.

37. Schafer, H. J., "Physical Optic Analysis of Image Quality in Schlieren Photography," J.Soc. Motion Picture Engineers, Vol. 53, p. 524, 1949.

38. Speak, C. S., and Walters, D. J., "Optical Considerations and Limitations of the Schlieren Process," British A.R.C. No. 13066, 1950.

39. North, R. J., "Schlieren Systems Using Graded Filters," British A.R.C. No. 15099, 1952.

40. Holder, D. W., and North, R. J., "Schlieren Methods for Photographing High-Speed Air Flows," Proc.Roy.Phot.Soc. Centenary Conference, p. 371, 1953.

41. Holder, D. W., and North, R. J., "Schlieren Methods for Observing High-Speed Flows," British A.R.C. C.P. 167, 1953.

42. Meyer, C. E., "The Diffraction of Light, X-rays and Material Particles," University of Chicago Press, 1934.

43. Jacquinot, P., "Quelques recherches sur les raies faibles dans les spectres optiques," Proc.Phys.Soc. 372B, Vol. 63, Part 12, 1950.

44. Aulin, E., "Geometry of Wind Tunnel Optics," Report of the Laboratory of Optics, No. 13, Royal Institute of Technology, Stockholm, 1951.

45. Barnes, N. F., and Bellinger, S. F., "Schlieren and Shadowgraph Equipment for Air Flow Analysis," J.Opt.Soc.Am., Vol. 35, p. 497, 1945.

46. Prescott, R., and Gayhart, E. L., "A Method of Correction of Astigmatism in Schlieren Systems," J.Ae.S., Vol. 18, p. 69, 1951.

47. Ingalls, A. G., Editor, "Amateur Telescope Making - Advanced," Munn & Company, 1946.

48. Anderson, J. A., and Porter, R. W., "Ronchi's Method of Optical Testing," The Astrophysical Journal, Vol. 70, p. 175, 1929.

49. Saunders, J. B., "An Improved Optical Test for Spherical Aberration," J.Opt.Soc.Am., Vol. 44, p. 664, 1954.

50. Gaviola, E., "On Quantitative Use of the Foucault Knife-Edge Test," J.Opt.Soc.Am., Vol. 26, p. 163, 1936.

51. Pearcey, H. H., and North, R. J., "Faults in Plate Glass, from the Wind Tunnel Point of View," National Physical Laboratory, Aero/178, 1949.

52. Djurle, E., Inglestam, E., and Johansson, L., "Cementing Optical Glasses to Obtain strong Joints Free from Striae," J.Sc.Inst., Vol. 31, p. 86, 1954.

53. Holliday, C. T., "Instrumentation for the 5 in. Hypersonic Wind Tunnel at Forest Grove station," A.P.L. Johns Hopkins University, CM-576, 1949.

54. Keagy, W. R., Ellis, H. H., and Reid, W. T., "Schlieren Techniques for the Quantitative Study of Gas Mixing," Rand Corporation, Report R-164, 1949.

55. Todd, K. W., "Some Developments in Instrumentation for Air Flow Analysis," Proc.I. Mech.E., Vol. 161, p. 213, 1949.

56. Ruptash, J., "Boundary Layer Measurements in the U.T.I.A. 5 by 7 inch Supersonic Wind Tunnel," University of Toronto, Institute of Aerophysics, U.T.I.A. Report No. 16, 1952.

57. Fallis, W. B., Johnston, G. W., Lee, J. D., Tucker, N. B., and Wade, J. H., "Design and Calibration of the Institute of Aerophysics 16 in. x 16 in. Supersonic Wind Tunnel," University of Toronto, Institute of Aerophysics, U.T.I.A. Report No. 15, 1953.

58. Barry, F. W., and Edelman, G. M., "An Improved Schlieren Apparatus," J.Ae.Sc., Vol. 15, p. 364, 1948.

59. Taylor, H. G., and Waldrum, J. M., "Improvements in the Schlieren Method," J.Sc.Inst., Vol. 10, p. 378, 1933.

60. Howarth, L., Editor, "Modern Developments in Fluid Dynamics - High Speed Flow," Vol. 2, p. 592, Oxford University Press, 1953.

61. Edmonson, R. B., Gayhart, E. L., and Olsen, H. L., "Radial Symmetry in a Schlieren Image," J.Opt.Soc.Am., Vol. 42, p. 984, 1952.

62. Holder, D.W., and North, R. J., "A Schlieren Apparatus Giving an Image in Colour," Nature, Vol. 169, p. 466, 1952.

63. Holder, D. W., and North, R. J., "Schlieren Methods for Observing High-Speed Airflow," The Aeroplane, Vol. 82, p. 16, 1952.

64. North, R. J., "A Colour Schlieren System Using Multicolour Filters of Simple Construction," National Physical Laboratory, Aero Note 266, 1954.

65. Dryden, H. L., "Fact Finding for Tomorrow's Planes," National Geographic Magazine, Vol. 54, p. 757, 1953.

66. Rogers, E. W. E., "Shock Waves in Air," Endeavor, Vol. 15, p. 34, 1956.

67. Buchele, D. R., and Goosens, H. R., "Lens System Producing Unequal Magnification in Two Mutually Perpendicular Directions," Rev.Sci.Inst., Vol 25, p. 262, 1954.

68. McLellan, C. H., Williams, T. W., and Bertram, M. H., "Investigation of a Two-Step Nozzle in the Langley 11 inch Hypersonic Tunnel, NACA TN 2171, 1950.

69. Ackeret, J., Feldmann, F., and Rott, N., "Investigations of Compression Shocks and Boundary Layers in High-Speed Gas Flows," Institut für Aerodynamik, E.T.H., Zurich, Report No. 10, 1946. Translated as British A.R.C. 10,044.

70. Bradfield, W. S., and Fish, W. Y., "A High-Speed Schlieren Technique for Investigation of Aerodynamic Transients," J.Ae.S., Vol. 19, p. 418, 1952.

71. Ferri, A., "Method for Evaluating from Shadow or Schlieren Photographs the Pressure Drag in Two-Dimensional or Axially Symmetrical Flow Phenomena with Detached Shock," NACA TN 1808, 1949.

Ohman, L., "An Experimental Method of Determining the Drag of a Shock Wave with Application to a Ducted Body," Swedish FFA Report 51, 1954.

72. Ferri, A., "Elements of Aerodynamics of Supersonic Flows," p. 107, The Macmillan Company, 1949.

73. Ronchi, V., "La Prova dei Sistema Ottici," Nicola Zanichelli Bologna, 1925. See also Revue d'Optique, Vol. 5, p. 436, 1926.

74. Darby, P. F., "The Ronchi Method of Evaluating Schlieren Photographs," NAVORD Rep. 74-46, p. 31, 1946.

75. Zernike, F., "Phase Contrast, A New Method for the Microscopic Observation of Transparent Objects," Achievements in Optics, p. 116. Monographs on the progress of research in Holland during the war, Elsevier Publishing Company, Inc., New York and Amsterdam, 1946.

76. Ingelstam, E., "Application des dispositifs à contraste variable à l'étude des champs aérodynamiques," Contraste de Phase et Contraste par Interférences, 15-21 May 1951. Editions de la Revue d'Optique Théorique et Instrumentale, p. 223, Paris, 1952.

77. Erdmann, S. F., "Ein Neues, Sehr Einfaches Interferometer Zum Erhalt Quantitativ Auswertbarer Strömungs-bilder," App.Sc.Res., Vol. B.2, p. 1, 1951. (Translated as NACA TM 1363.)

78. Van de Vooren, A. I., "Theory of the Erdmann Interferometer for Investigation of Compressible Flows," App.Sc.Res., Vol. B.3, p. 18, 1952.

79. Gayhart, E. L., and Prescott, R., "Interference Phenomenon in the Schlieren System," J.Opt.Soc.Am., Vol. 39, p. 546, 1949.

80. Renet, C., "La Strioscopie Quantitative," O.N.E.R.A., Réunion Technique du 18 juin, 1953.

81. Renet, C., "Strioscopie Quantitative en Soufflerie," O.N.E.R.A., Study No. 1, 695P, Technical Note No. 2, 1953. See also La Recherche Aeronautique No. 38, p. 63, 1954.

82. Francon, M., "Interférences par double réfraction en lumière blanche," Revue d'Optique, Vol. 31, No. 2, 1952.

83. Lewy, H., "On the Relation Between the Velocity of a Shock Wave and the Width of the Light Gap it Leaves on the Photographic Plate," APG. BRL. Report No. 373, 1943.

84. Keenan, P. C., "Shadowgraph Determination of Shock-Wave Strength," Bu Ord. Explosives Research Report, No. 11, 1943.

85. Hilton, W. F., "The Photography of Airscrew Sound Waves," Proc.Roy.Soc.A., Vol. 169, p. 174, 1938.

86. Pearcey, H. H., "The Indication of Boundary-Layer Transition on Aerofoils in the N.P.L. 20 in. by 8 in. High-Speed Tunnel," British ARC C.P.10, 1950.

87. Lindsey, W. F., and Burlock, J., "A Variable-Frequency Light Synchronized with a High-Speed Motion-Picture Camera to Provide Very Short Exposure Times," NACA TN 2949, 1953.

88. Holder, D. W., North, R. J., Standring, W. G., and Looms, J. S. T., "A High-Speed Camera for the Photography of Shock-Wave Oscillations in a Wind Tunnel," British ARC. R.&M. 2901, 1949.

89. Lawrence, L. F., Schmidt, S. F., and Looschen, F. W., "Self-Synchronizing Stroboscopic Schlieren System for the Study of Unsteady Airflows," NACA TN 2509.

90. Chinneck, A., Holder, D. W., and Berry, C. J., "Observations of the Flow Round a Two-Dimensional Aerofoil Oscillating in a High-Speed Air Stream," British ARC. R.&M. 2931, 1952.

91. Cranz, C., and Schardin, H., "Kinematographie auf ruhendem Film und mit extrem hoher Bildfrequenz," Z. Physik, Vol. 56, p. 147, 1929.

92. Devaux, P., Fayolle, P., and Naslin, P., "Electronic High-Speed Kinematograph and Associated Chronograph," Proc. Royal Photographic Society Centenary Conference, p. 377, 1953.

93. Froome, K. D., "An Electronically Operated Kerr Cell Shutter," The Photographic Journal, Vol. 92B, p. 158, 1952.

94. Sultanoff, M., "A 0.1 Microsecond Kerr-Cell Shutter," Photographic Engineering, Vol. 5, p. 80, 1954.

95. Ellis, A. T., "Techniques for Pressure Pulse Measurements and High-Speed Photography in Ultrasonic Cavitation," Proceedings of the Symposium on Cavitation in Hydrodynamics, National Physical Laboratory, 1955.

96. Edgerton, H. E., and Wyckoff, C. W., "A Rapid-Action Shutter with No Moving Parts," J.Soc. Motion Picture and Television Engineers, Vol. 56, p. 398, 1951.

97. Courtney-Pratt, J. S., "Image Converter Tubes and Their Application to High-Speed Photography," The Photographic Journal, Vol. 92B, p. 137, 1952.

98. Meek, J. M., and Turnock, R. C., "Electro-Optical Shutters as Applied to the Study of Electrical Discharges," The Photographic Journal, Vol. 92B, p. 161, 1952.

99. Chippendale, R. A., "Image Converter Techniques Applied to High-Speed Photography," The Photographic Journal, Vol. 92B, p. 149, 1952.

100. Hardy, A. C., and Perrin, F. H., "The Principles of Optics," McGraw Hill, 1932.

101. Aldington, J. N., "Bright Light Sources, (Part 1)," Trans. Illuminating Engineering Soc., Vol. 10, p. 1, 1945.

102. Barnes, N. F., "Optical Techniques for Fluid Flow," J.Soc. Motion Picture and Television Engineers, Vol. 61, p. 487, 1953.

103. Noel, E. B., and Farnham, R. E., "A Water Cooled Quartz Mercury Arc," J.Soc. Motion Picture Engineers, Vol. 31, p. 221, 1938.

104. Bergdolt, V. E., and Shear, D. D., "A Tube Light Source for Interferometry," Photographic Engineering, Vol. 4, p. 240, 1953.

105. Aldington, J. N., "Bright Light Sources, (Part 2)," Trans. Illuminating Engineering Soc., Vol. 11, p. 11, 1946.

106. Cotton, H., "Electric Discharge Lamps," Chapman and Hall, 1946.

107. Brown, R. H. J., "Flash Cinematography," The Photographic Journal, Vol. 92B, p. 130, 1952.

108. Buckingham, W. D., and Diebert, C. R., "Characteristics and Applications of Concentrated Arc Lamps," J.Soc. Motion Picture Engineers, Vol. 47, p. 376, 1946.

109. Schardin, H., and Fünfer, E., "Principles of Flash Cinematography," Z. Angew. Phys., Vol. 4, p. 185, and p. 224, 1952. Translated as British MOS TIB/T.4113.

110. Jones, G. A., "High-Speed Photography," Chapman and Hall, 1952.

111. Chesterman, W. D., "The Photographic Study of Rapid Events," Oxford University Press, 1951.

112. Fayolle, P., and Naslin, P., "Photographie instantanée et cinématographie ultra-rapide," Memorial de l'artillerie Francaise, Vol. 22, p. 657, 1948. See also Editions de la Revue d'Optique, 1950.

113. Craggs, J. D., and Meek, J. M., "Emission of Light from Flash Discharges," Proc. Roy.Soc.A., Vol. 186, p. 241, 1946.

114. Melton, B. S., Prescott, R., and Gayhart, E. L., "A Working Manual for Spark Shadowgraph Photography," Bumblebee Series Report No. 90, 1948.

115. Standring, W. G., and Looms, J. S. T., "The Electrical and Luminous Characteristics of Short Air Sparks Suitable for High-Speed Photography," Proc.Phys.Soc.B., Vol. 65, p. 108, 1952.

116. Chesterman, W. D., Coghlan, R. P., Glegg, D. R., and Stamp, W. R., "After-Glow in the Xenon Discharge," British Admiralty Research Laboratory Report, ARL/RI/96-05/D, 1949.

117. Standring, W. G., and Looms, J. S. T., "Light Output from a Spark 'Point Source,'" Nature, Vol. 165, p. 358, 1950.

118. Hoyt, G. D., and McCormick, W. W., "Study of Short-Duration High-Intensity Arc as a Source of Visible Light," J.Opt.Soc.Am., Vol. 40, p. 658, 1950.

119. "Micro-Second Flash Tube LSD2," Mullard Technical Report No. 3/1948, 1948.

120. Young, A. E., McCullough, S., and Smith, R. L., "Power Unit for High-Intensity Light source," NACA RM E50K27, 1951.

121. North, R. J., and Holder, D. W., "A Spark Light Source for Schlieren and Direct-Shadow Photography," National Physical Laboratory, Aero Note No. 187, 1950.

122. Whelan, W. T., and Allmand D. E., "A Spark Light Source and Trigger," Naval Ordnance Laboratory, Memorandum No. 10622, 1949.

123. Fitzpatrick, J. A., Hubbard, J. C., and Thaler, W. J., "A High Intensity Short Duration Spark Light Source," J.App.Phys., Vol. 21, No. 12, 1950.

124. Kovasznay, L. S. G., "High Power Short Duration Spark Discharge," Rev.Sc.Inst., Vol. 20, p. 696, 1949.

125. Goodfellow, H., "Single and Repetitive Light Sources," British A.W.R.E. Report No. 0-11/53.

126. Miller, F. N., "A Short Duration Collimated Light Source," NAVORD Report 3350, 1954.

127. Beams, J. W., Kuhlthan, A. R., Lapsley, A. C., McQueen, J. H., Snoddy, L. B., and Whitehead, W. D., Jr., "Spark Light Source of Short Duration," J.Opt.Soc.Am., Vol. 37, p. 868, 1947.

128. Naslin, P., "Electronics in Short-Time Measurement and High-Speed Photography and Kinematography," Trans. Instruments and Measurements Conference, Stockholm, 1949.

129. Looms, J. S. T., "Report on the Duration of Light from Flash Sources Tested for Aerodynamics Division," Electricity Division, National Physical Laboratory, Internal Report, 1954.

130. Fayolle, P., and Naslin, P., "Simple Electronic Devices for High-Speed Photography and Cinematography," J.Soc. Motion Picture and Television Engineers, Vol. 60, p. 603, 1953.

131. Quinn, H. F., and Bourque, O. J., "A New Flash Illumination Unit for Ballistic Photography," Rev.Sci.Inst., Vol. 22, p. 101, 1951.

132. Adams, G. K., "A Repetitive Spark Source for Shadow and Schlieren Photography," J.Sc.Inst., Vol. 28, p. 379, 1951.

133. Edgerton, H. E., "Double Flash Microsecond Silhouette Photographs," Rev.Sc.Inst., Vol. 23, No. 10, 1952.

134. Bardocz, A., and Klatsmanyi, A., "New Flash Illumination Unit," Rev.Sc.Inst., Vol. 26, No. 10, p. 945, 1955.

135. Edmonson, R. B., Gayhart, E. L., and Olsen, H. L., "Chronophotography of a Reproducible Phenomenon," Phot. Engineering, Vol. 3, p. 135, 1952.

136. Mees, C. E. K., "The Theory of the Photographic Process," Macmillan, 1942.

137. Castle, J., and Webb, J. H., "Results of Very Short Duration Exposure For Several Fast Photographic Emulsions," Phot. Engineering, Vol. 4, p. 51, 1953.

138. Castle, J., "The Photographic Response of Several High-Speed Emulsions at Very Short Exposure Times," Phot. Engineering, Vol. 5, p. 189, 1954.

139. Rogers, E. W. E., and Berry, C. J., "Experiments at M = 1.41 on Elliptic Cones with Subsonic Leading Edges," British ARC No. 17929, 1955.

140. Jacobs, W., "Transonic Flow Past Swept and Unswept Wings between Parallel Walls," F.F.A. Report No. 55, Stockholm, 1954.

141. Picard, C., "Analyse strioscopique d'écoulements supersoniques à trois dimensions," La Recherche Aéronautique No. 32, p. 15, 1953.

142. Hall, I. M., "Experiments on Supersonic Flow over Flat-Nosed Circular Cylinders at Yaw," Phil.Mag., Vol. 45, p. 333, 1954.

143. "Spark Shadowgraph System," Boeing Airplane Company, BAC Jet Lab. D-12276.

144. Lyot, B., and Francon, M., "Observation des défauts de poli et homogénéité au stéréoscope par la méthode du contraste de phase," Revue d'Optique, Vol. 27, p. 397, 1948.

145. Veret, C., "La strioscopie stéréoscopique," La Recherche Aéronautique, No. 29, 1952.

146. Hett, J. H., "A High-Speed Stereoscopic Schlieren System," J.Soc. Motion Picture Engineers, Vol. 56, p. 214, 1951.

147. Kantrowitz, A., and Trimpi, R. L., "A Sharp-Focusing Schlieren System," J.Ae.S., Vol. 17, p. 311, 1950.

148. Fish, R. W., and Parnham, K., "Focussing Schlieren Systems," British A.R.C. C.P.54, 1950.

149. Ormerod, A. O., "Note on the Use of the Three-Dimensional Shock-Wave Recorder for Studying Interference in a Supersonic Tunnel," British A.R.C. No. 13,940, 1950.

150. Love, E. S., and Grigsby, C. E., "A New Shadowgraph Technique for the Observation of Conical Flow Phenomena in Supersonic Flow and Preliminary Results Obtained for a Triangular Wing," NACA TN 2950, 1953.

151. Huss, G., "A Simple Method for Localization of Shock Waves on Three-Dimensional Surfaces," Reports from the Laboratory of Optics, No. 17, Royal Institute of Technology, Stockholm, 1951.

BIBLIOGRAPHY

Schlieren and Direct Shadow Methods

Ladenburg, R. W., Lewis, B., Pease, R. N., and Taylor, H. S., Editors, "Physical Measurements in Gas Dynamics and Combustion," Vol. 9 of High-Speed Aerodynamics and Jet Propulsion, Princeton University Press, 1954.

Schardin, H., "Die Schlierenverfahren und ihre anwendungen," Ergebnisse der exakten Naturwissenschaften, Vol. 10, 1941. Translated as British ARC 10,724.

Howarth, L., Editor, "Modern Developments in Fluid Dynamics: High-Speed Flow," Vol. 2, Chapter 11, Oxford University Press, 1953.

Melton, B. S., Prescott, R., and Gayhart, E. L., "A Working Manual for Spark-Shadowgraph Photography," Bumblebee series Report No. 90, 1948.

Light Sources and Photography

Hardy, A. C., and Perrin, F. H., "The Principles of Optics," McGraw Hill, 1932.

Cotton, H., "Electric Discharge Lamps," Chapman and Hall, 1946.

Schardin, H., and Fünfer, E., "Principles of Flash Cinematography," Z. Angew Phys., Vol. 4, p. 185, and p. 224, 1952. Translated as British MOS TIB/T4113.

Jones, G. A., "High-Speed Photography," Chapman and Hall, 1952.

Chesterman, W. D., "The Photographic Study of Rapid Events," Oxford University Press, 1951.

Mees, C. E. K., "The Theory of the Photographic Process," Macmillan, 1942.

Power Supplies, Triggering, and Delay Circuits

Ridenour, L. N., Editor-in-Chief, Massachusetts Institute of Technology Radiation Laboratory Series, Vols. 5, 19, and 22, McGraw Hill, 1948-9.

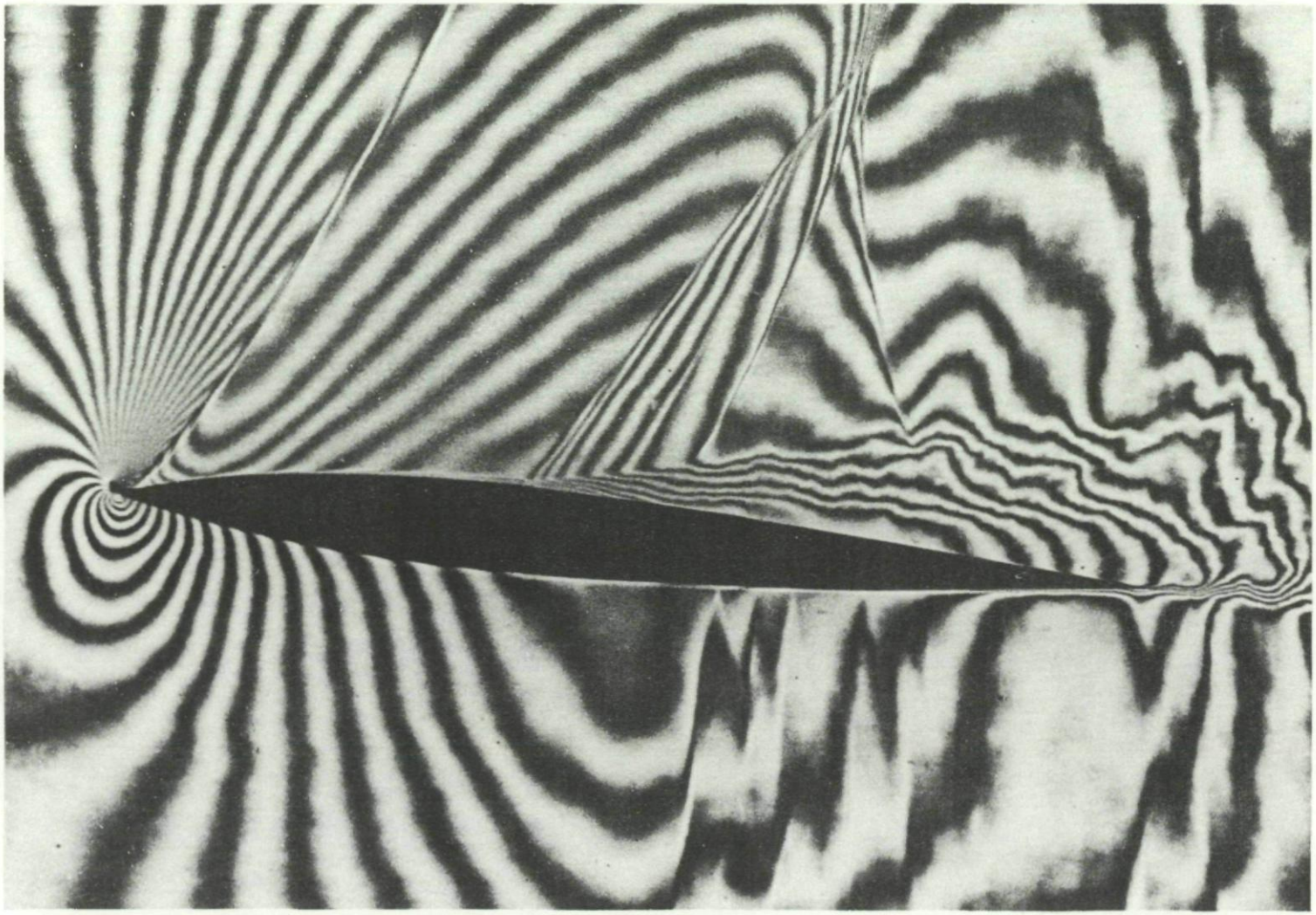

Fig. I-1a. Interferometer photograph of the flow past a two-dimensional aerofoil.

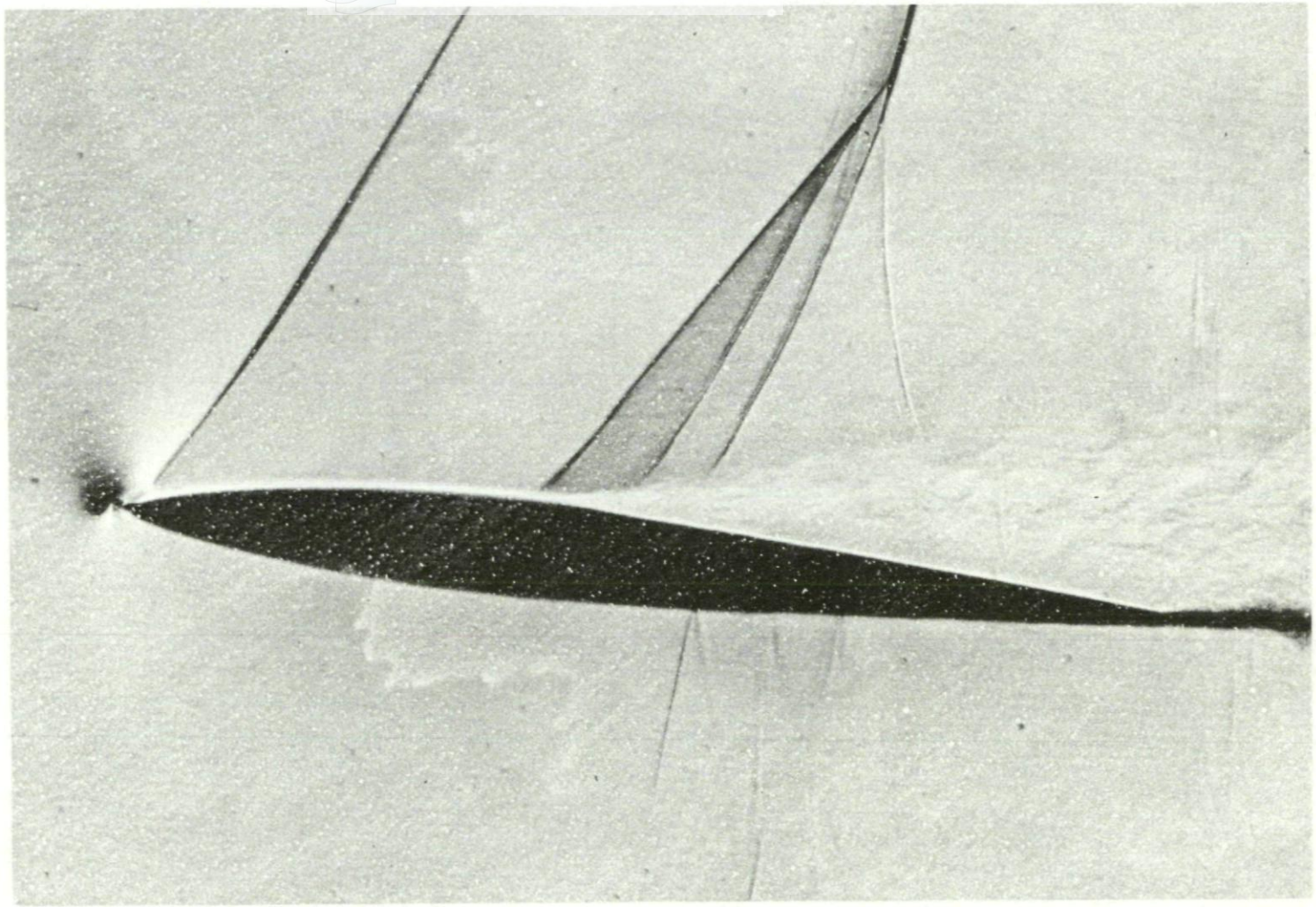

Fig. I-1b. Toepler schlieren photograph of the flow past a two-dimensional aerofoil.

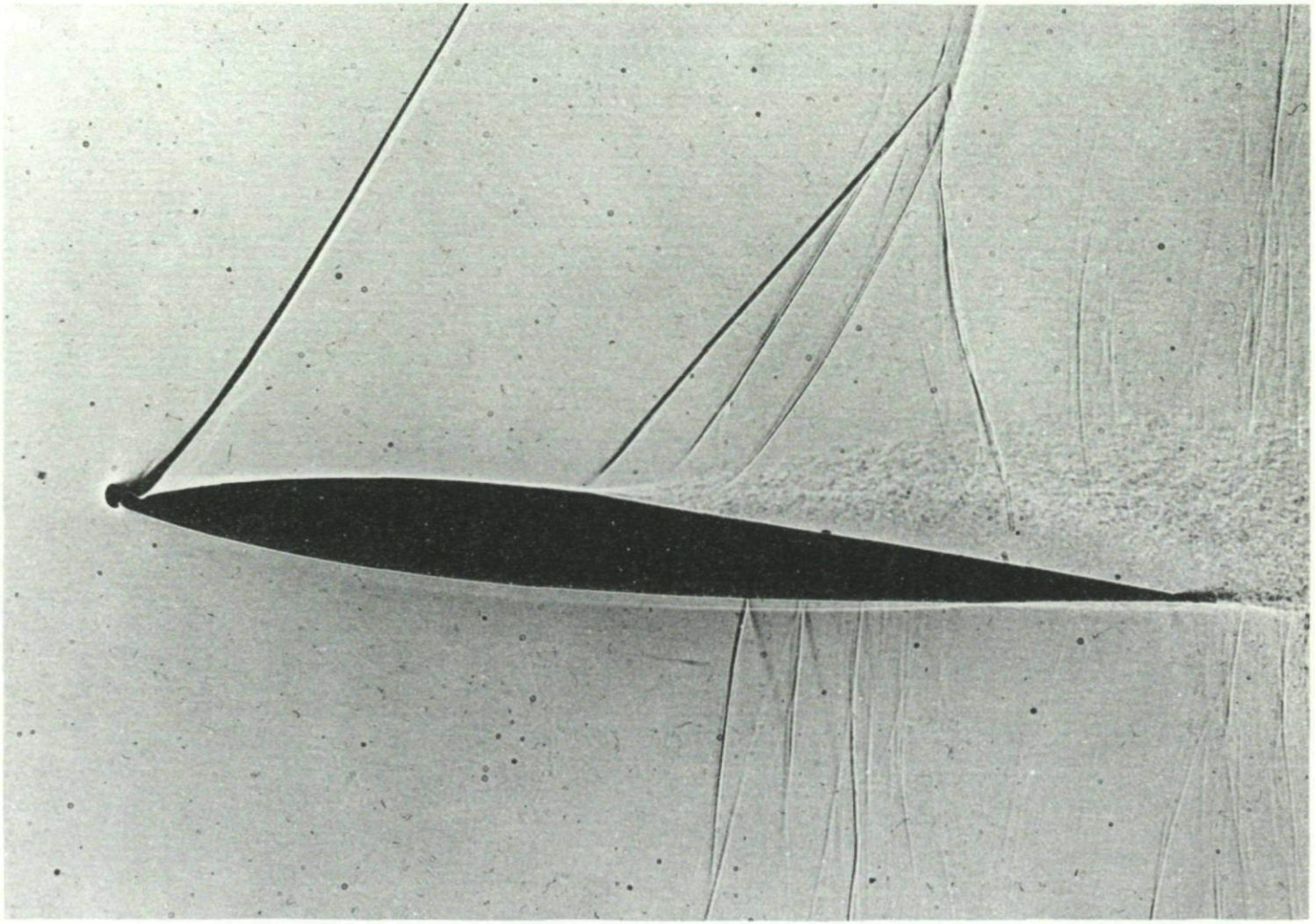

Fig. I-1c. Direct-shadow photograph of the flow past a two-dimensional aerofoil.

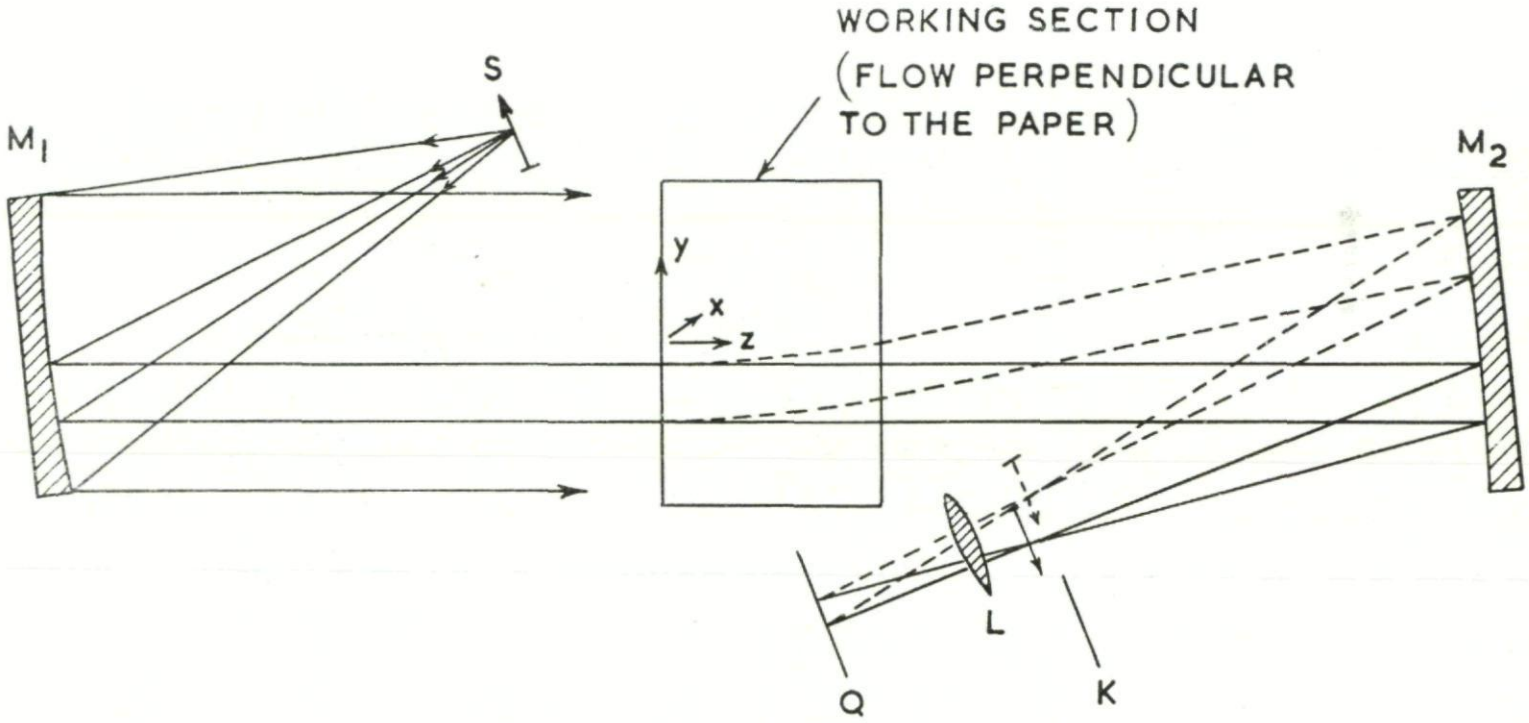

Fig. II-1. Sketch showing the arrangement of a typical schlieren apparatus. (Undisturbed rays shown full, disturbed rays shown dotted.)

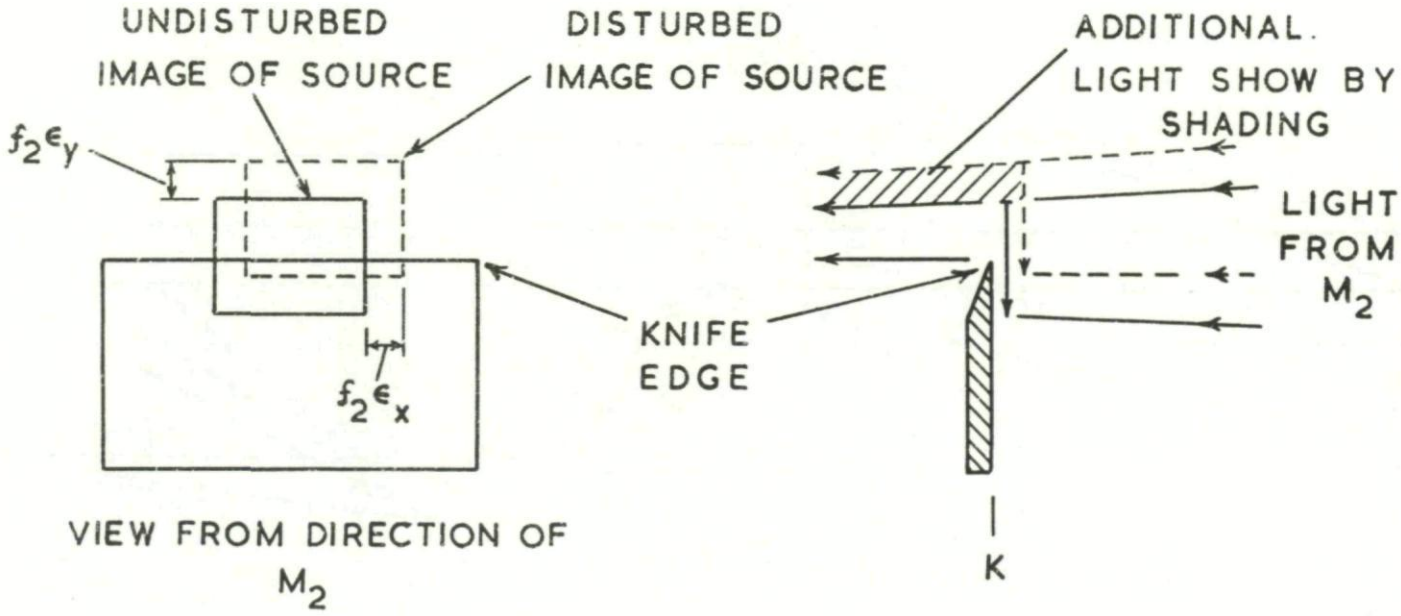

Fig. II-2. The arrangement of the knife edge in the Toepler apparatus.

(a) Knife edge perpendicular to chord

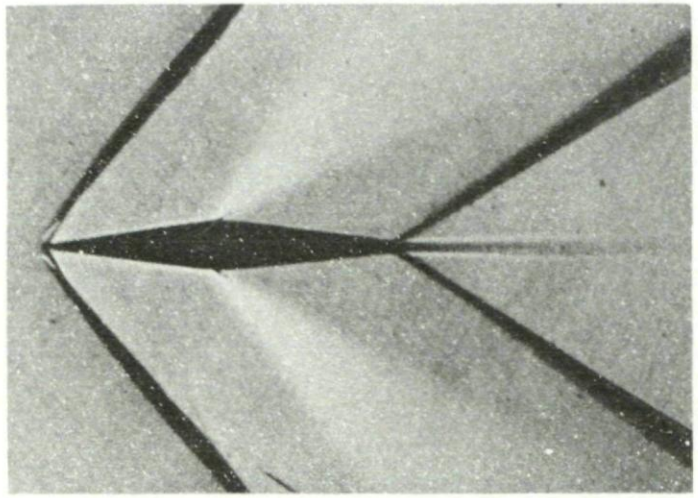

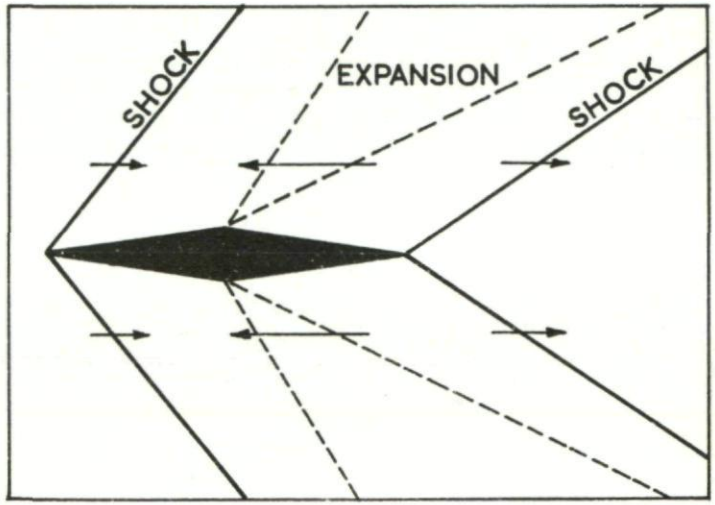

(b) Knife edge parallel to chord

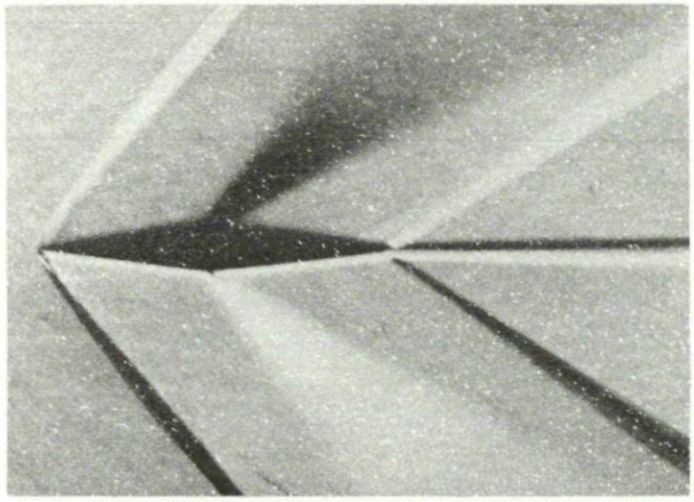

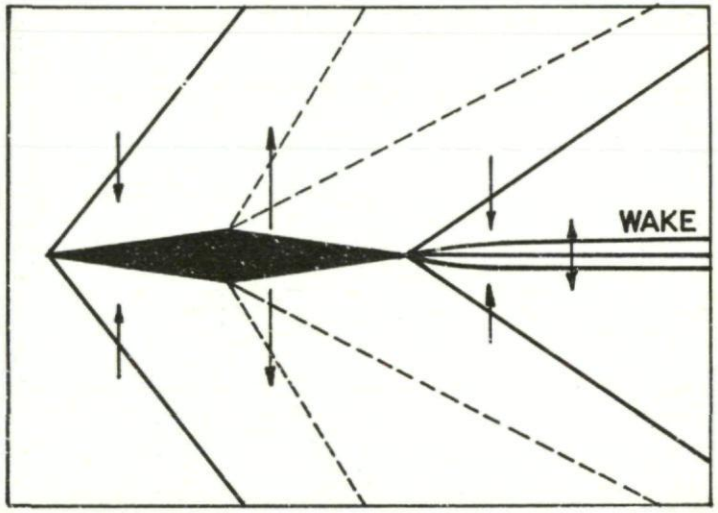

Fig. II-3. Toepler schlieren photographs of the flow round a double wedge at M = 1.6.

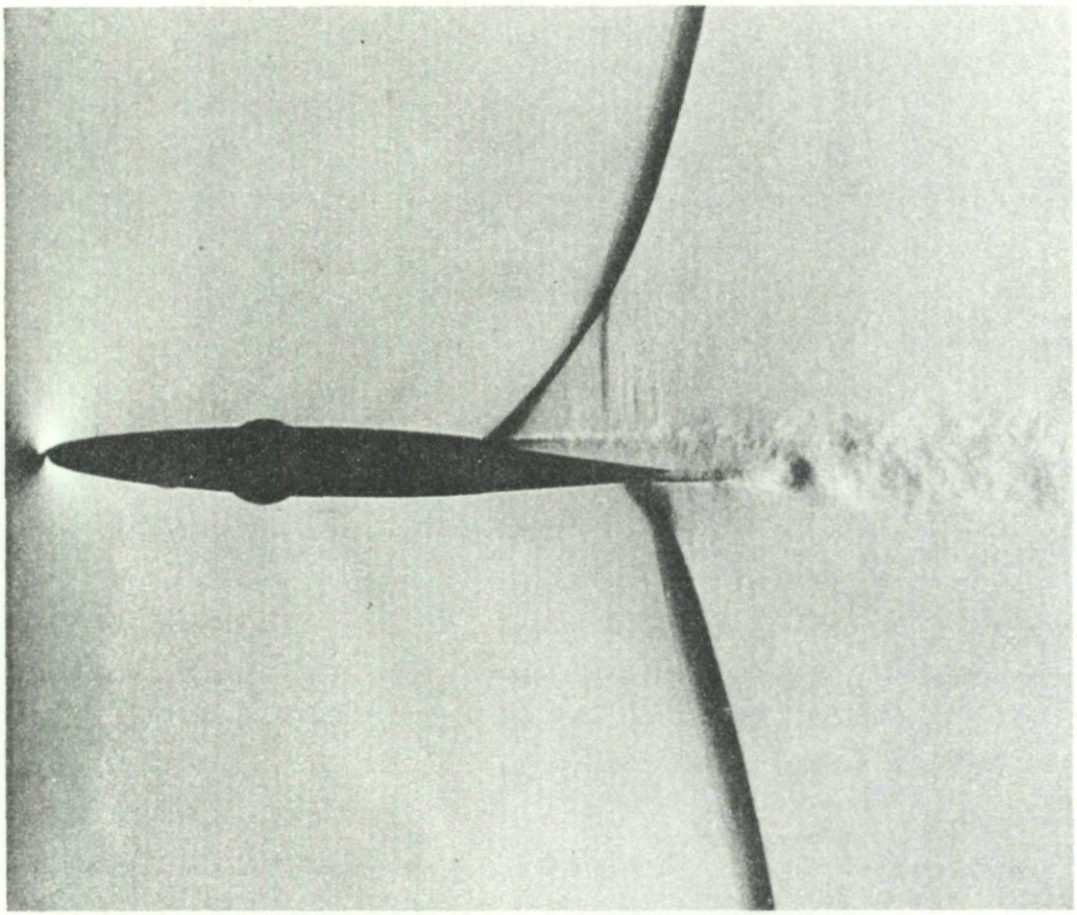

Fig. II-4. Toepler schlieren photograph of the flow past a two-dimensional aerofoil at M = 0.87.

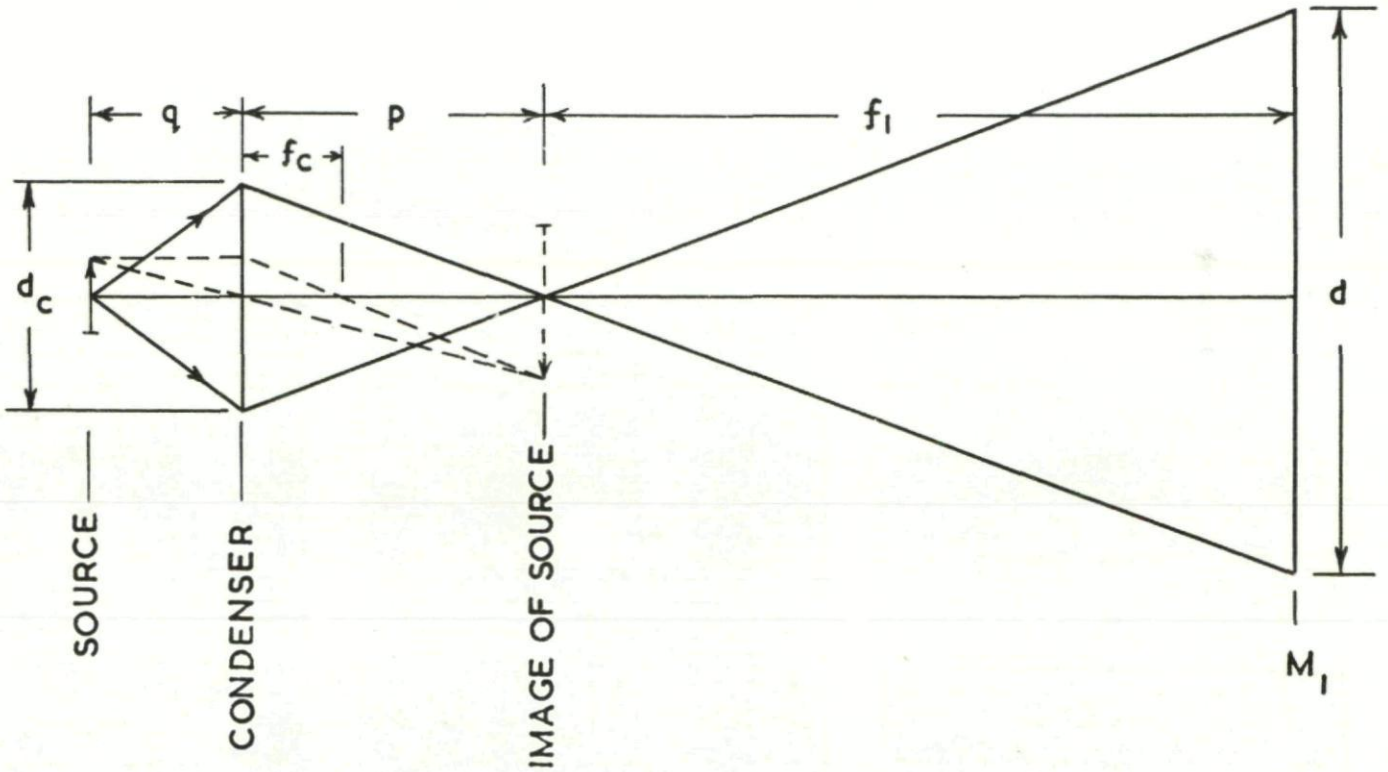

Fig. II-5. The use of a condenser lens to produce a magnified image of the light source.

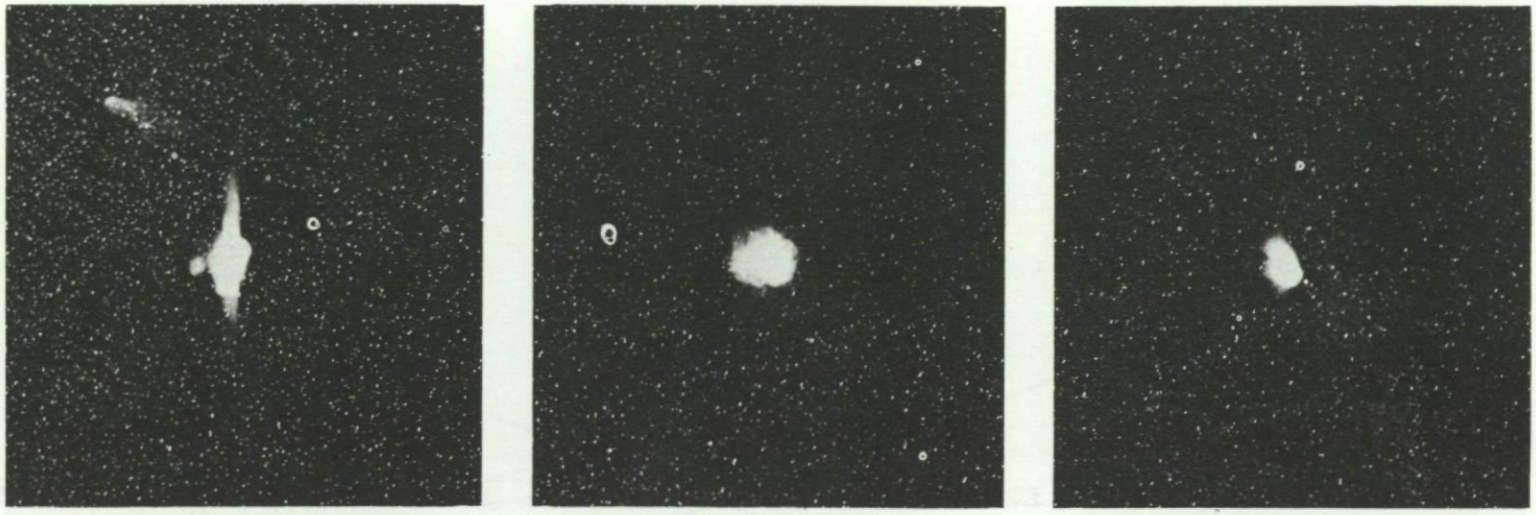

(a) Horizontal knife edge

(b) Graded filter

(c) No knife edge or graded filter

Fig. II-6. Images of a pin hole formed with various schlieren systems.

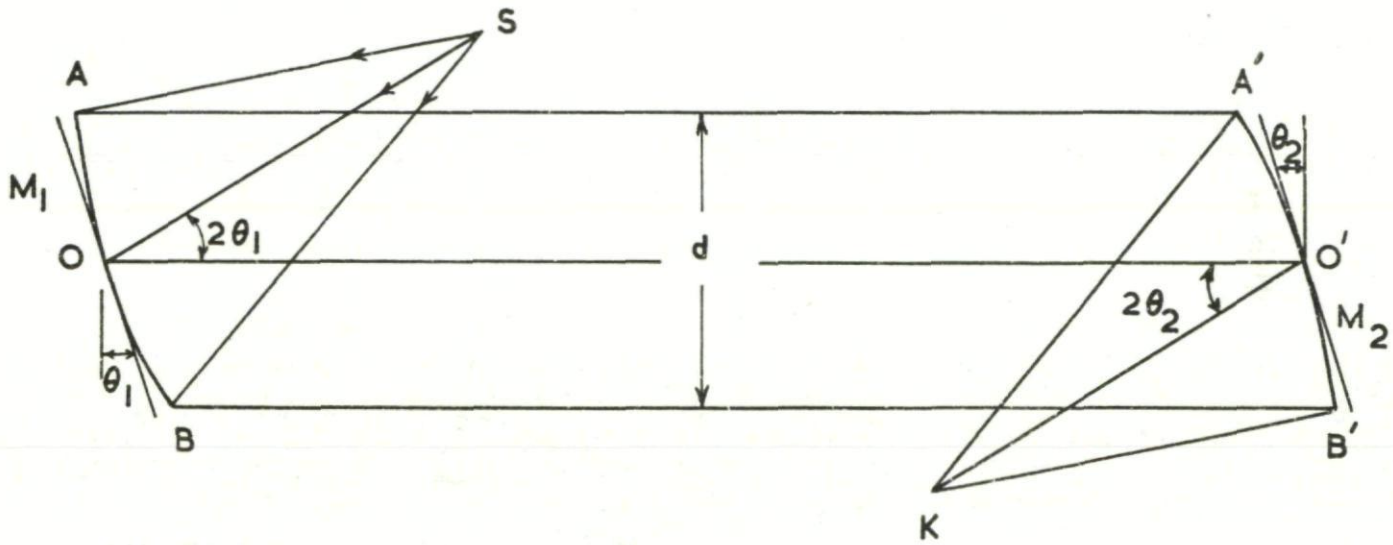

Fig. II-7. Diagram of the notation used in the discussion of coma and astigmatism.

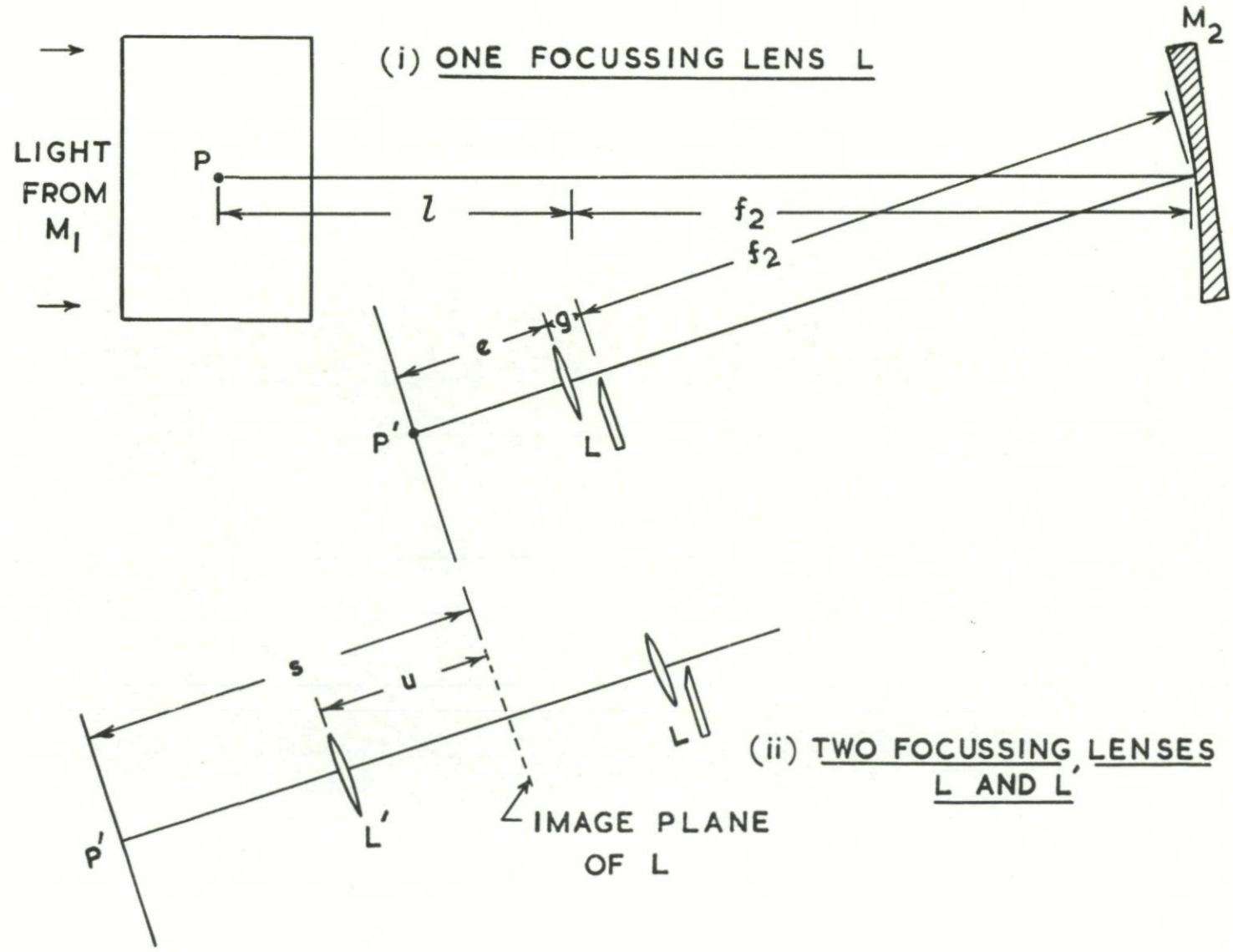

Fig. II-8. Diagram of the notation for the focussing lenses used to produce an image of p at p' .

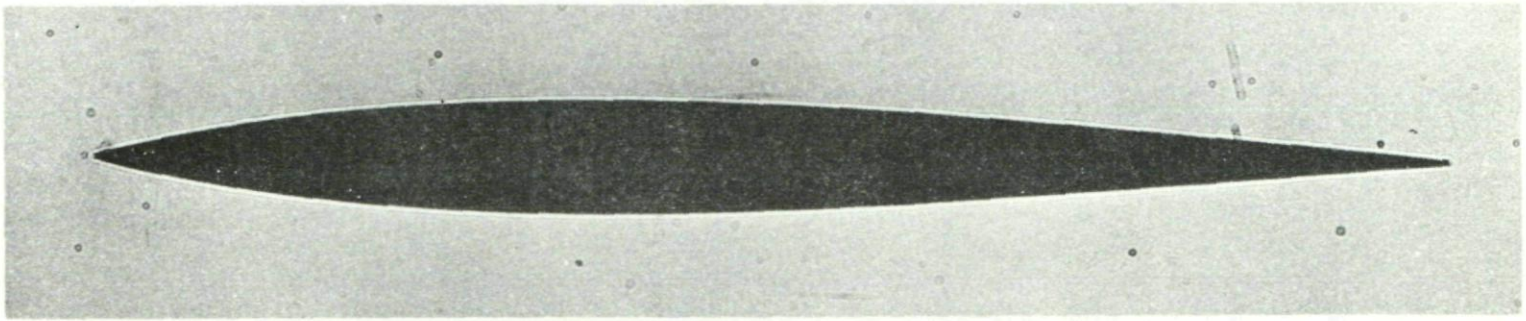

Light beam parallel to aerofoil span

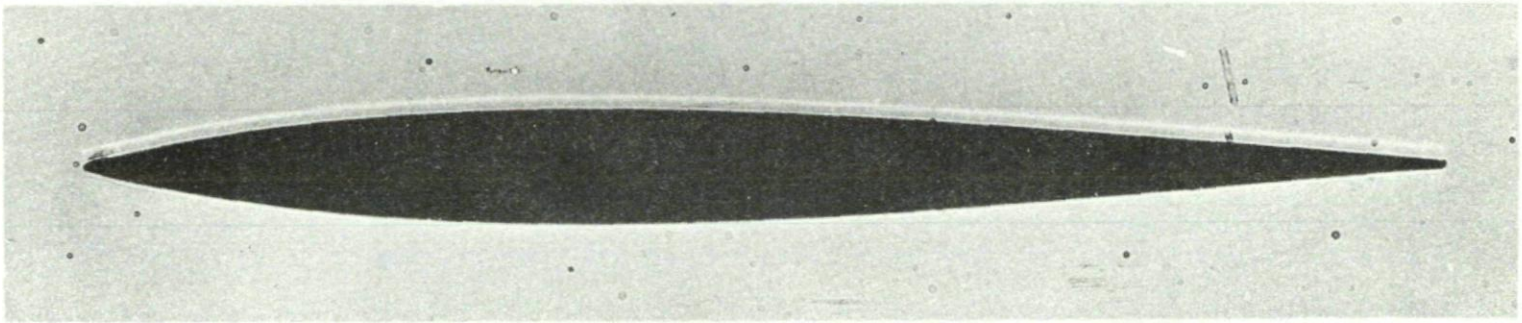

Light beam inclined towards the upper surface

Fig. II-9a. Direct-shadow photographs with no flow showing the effects of diffraction and misalignment of the light beam.

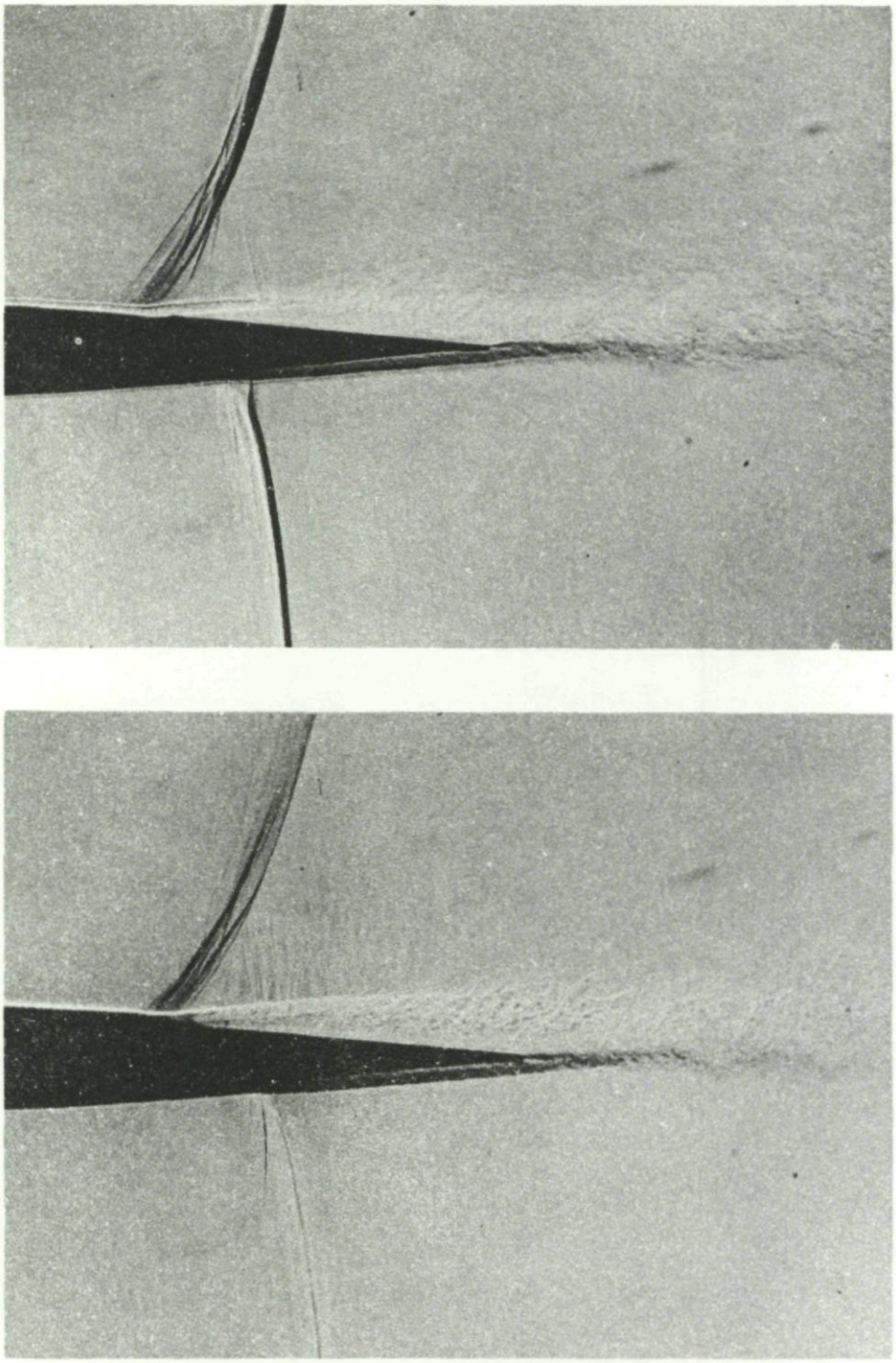

Fig. II-9b. Examples showing the effects of focussing on the image of the flow near the trailing edge of an aerofoil moving at a high subsonic speed.

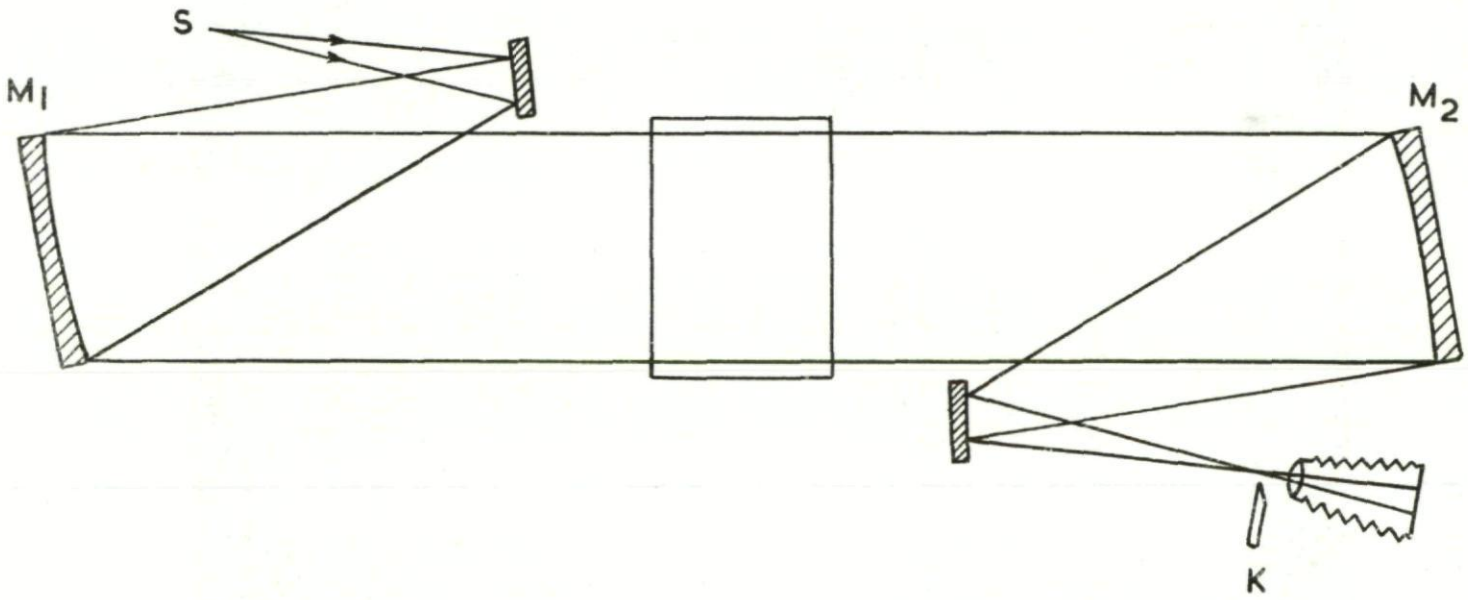

Fig. II-10. The use of plane mirrors to fold the light beam.

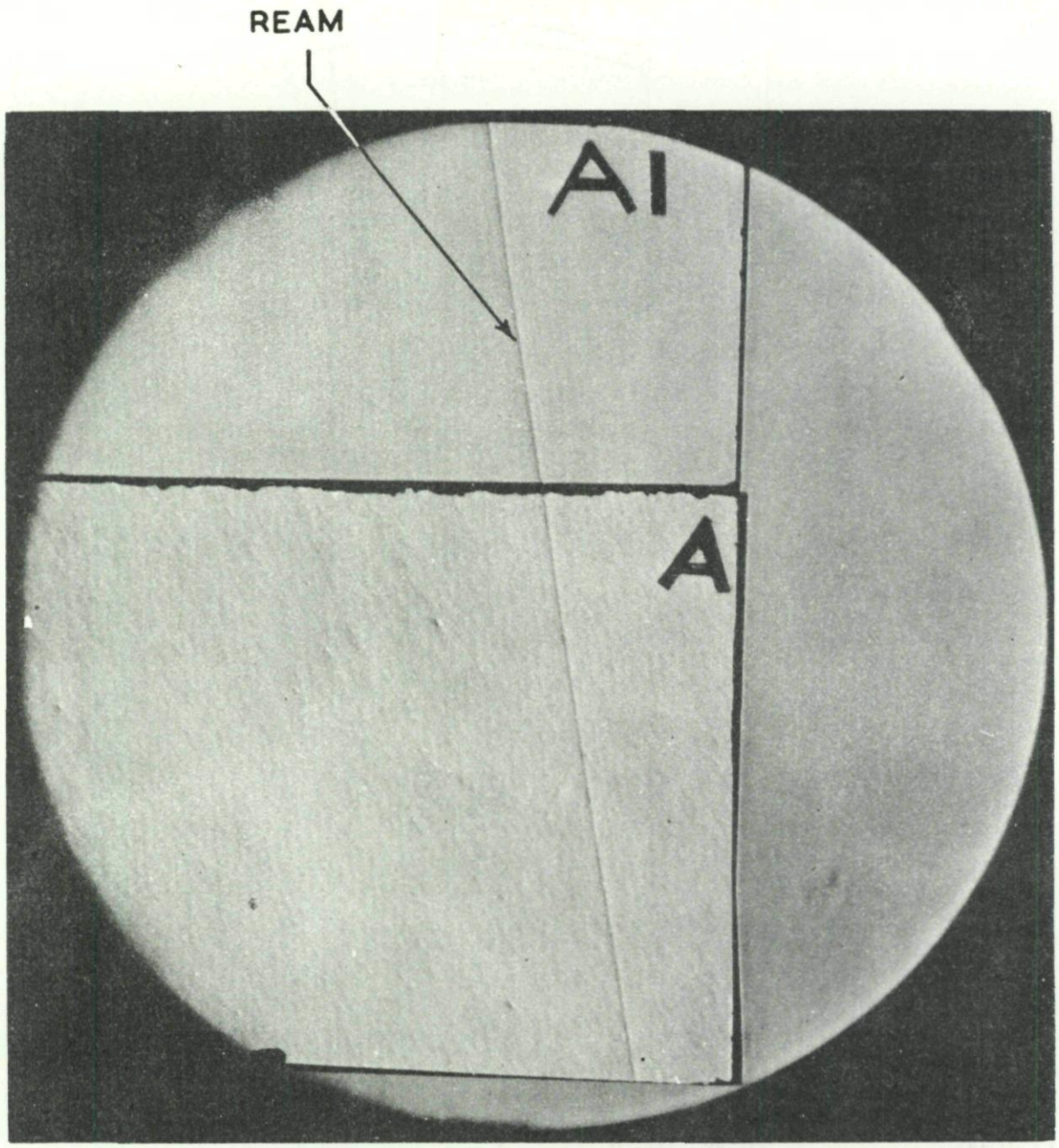

Fig. II-11. Schlieren photographs showing ream and defects in the surface polish of glass.

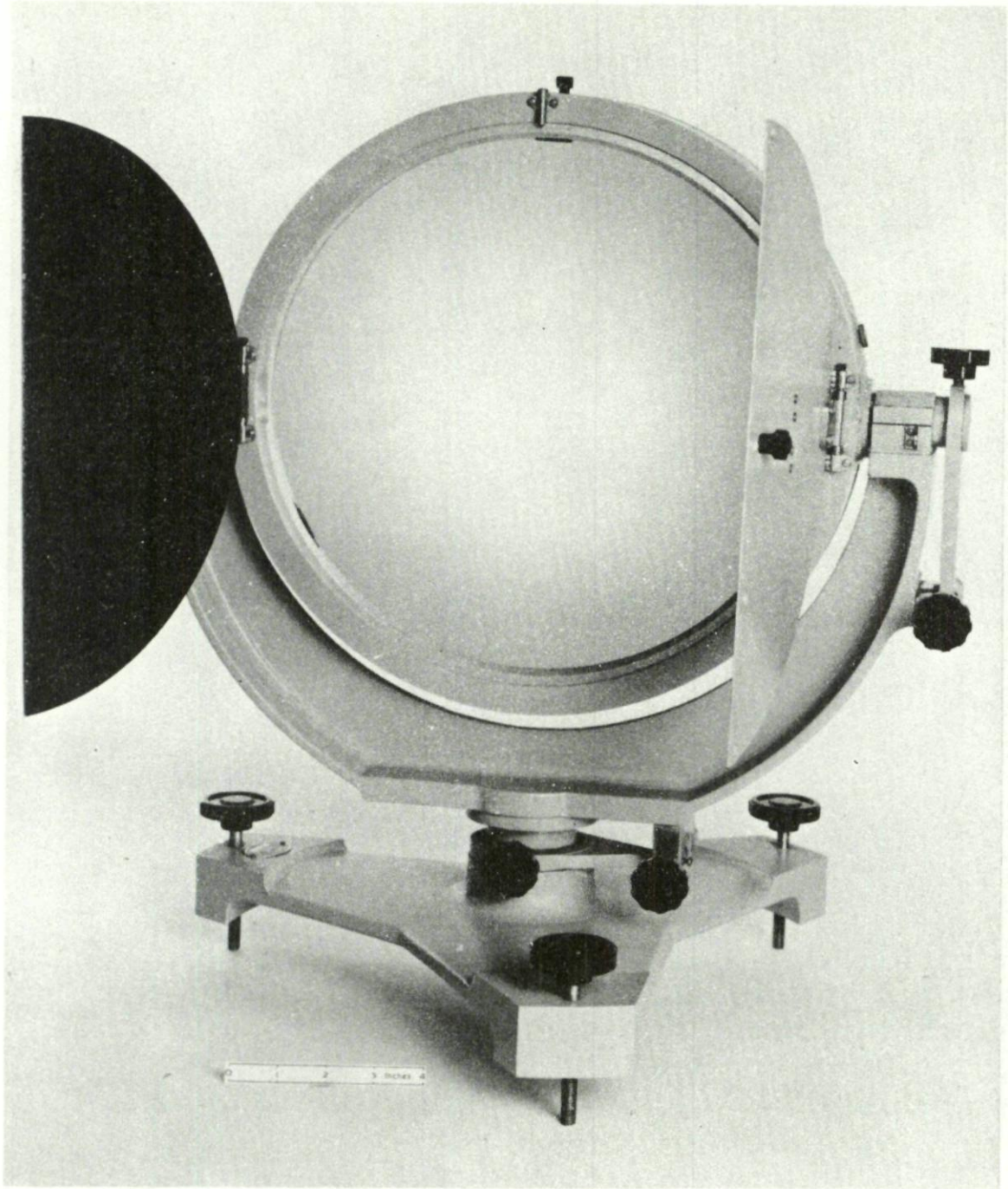

Fig. II-12. A typical schlieren-mirror mount.

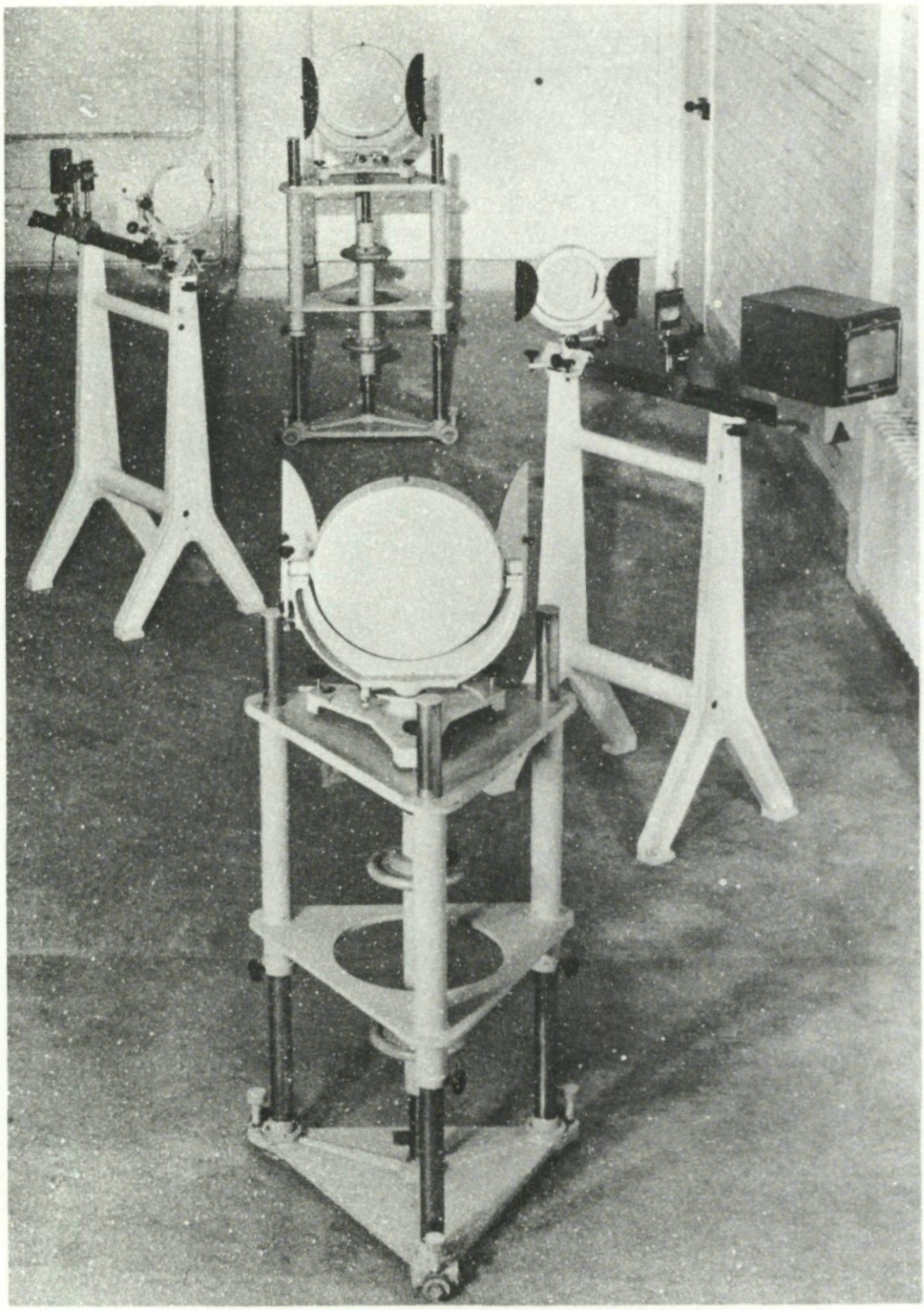

Fig. II-13. A typical schlieren apparatus.

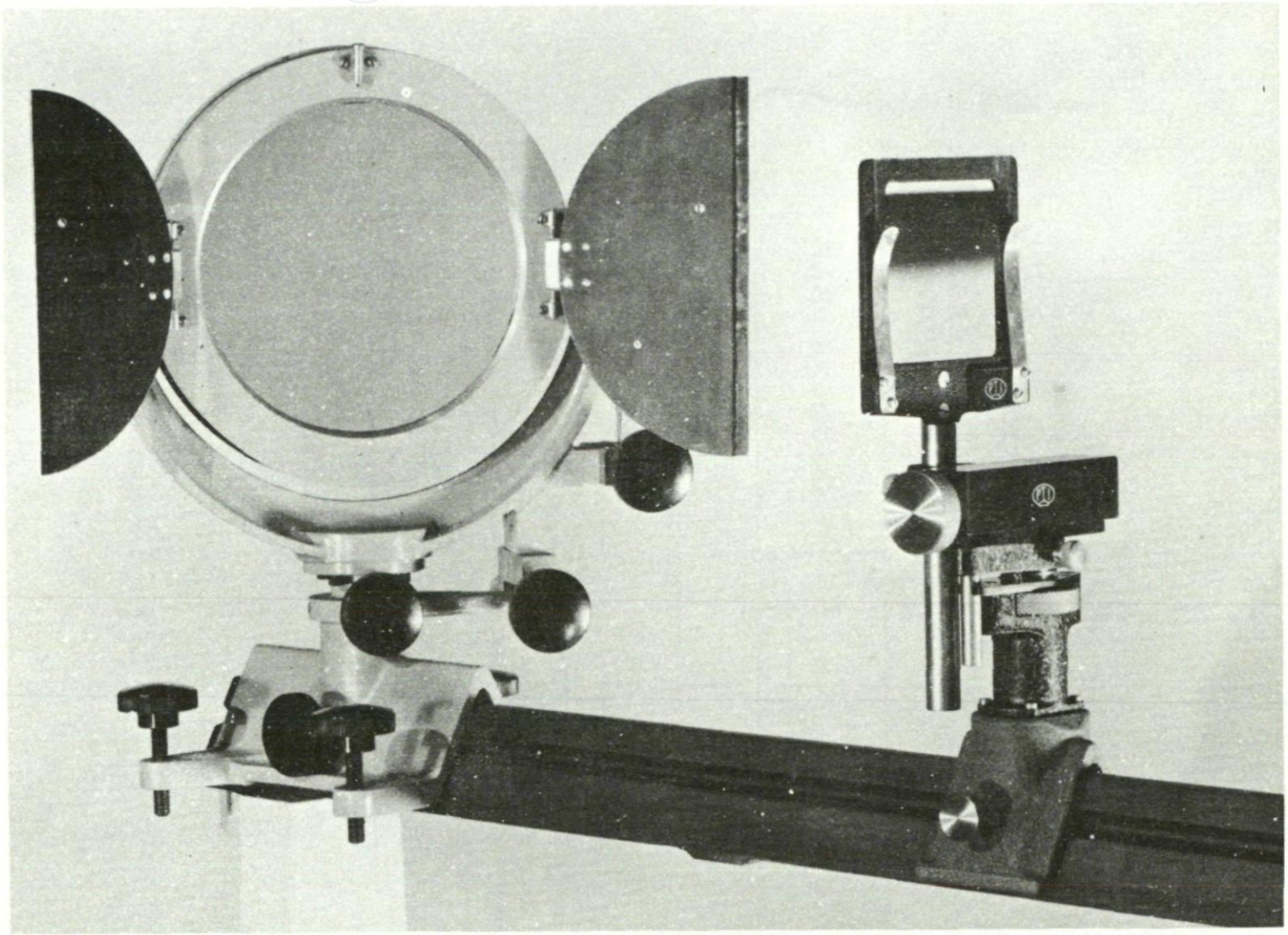

Fig. II-14. Photograph showing a graded filter and its adjustments and a plane mirror used to fold the light beam.

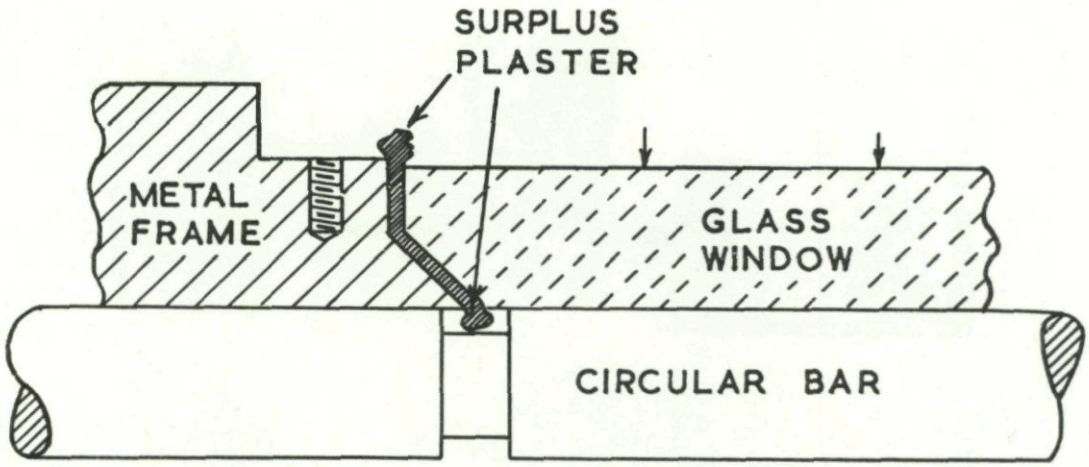

(a) Arrangement for mounting

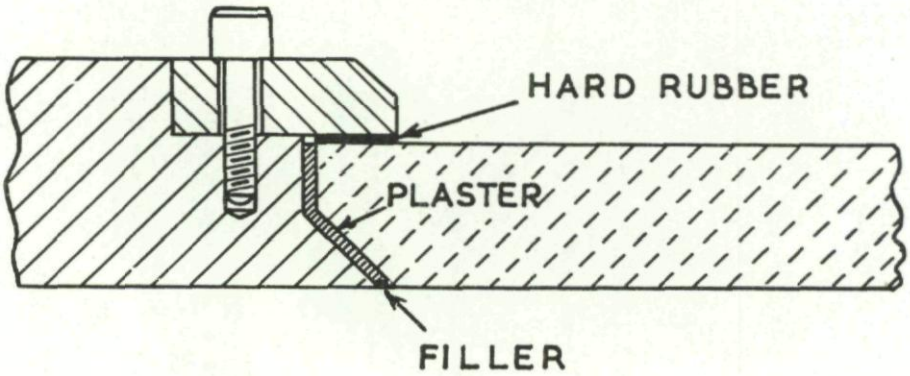

(b) Finished assembly

Fig. II-15. Sketches illustrating a typical n ethod of mounting wind tunnel windows.

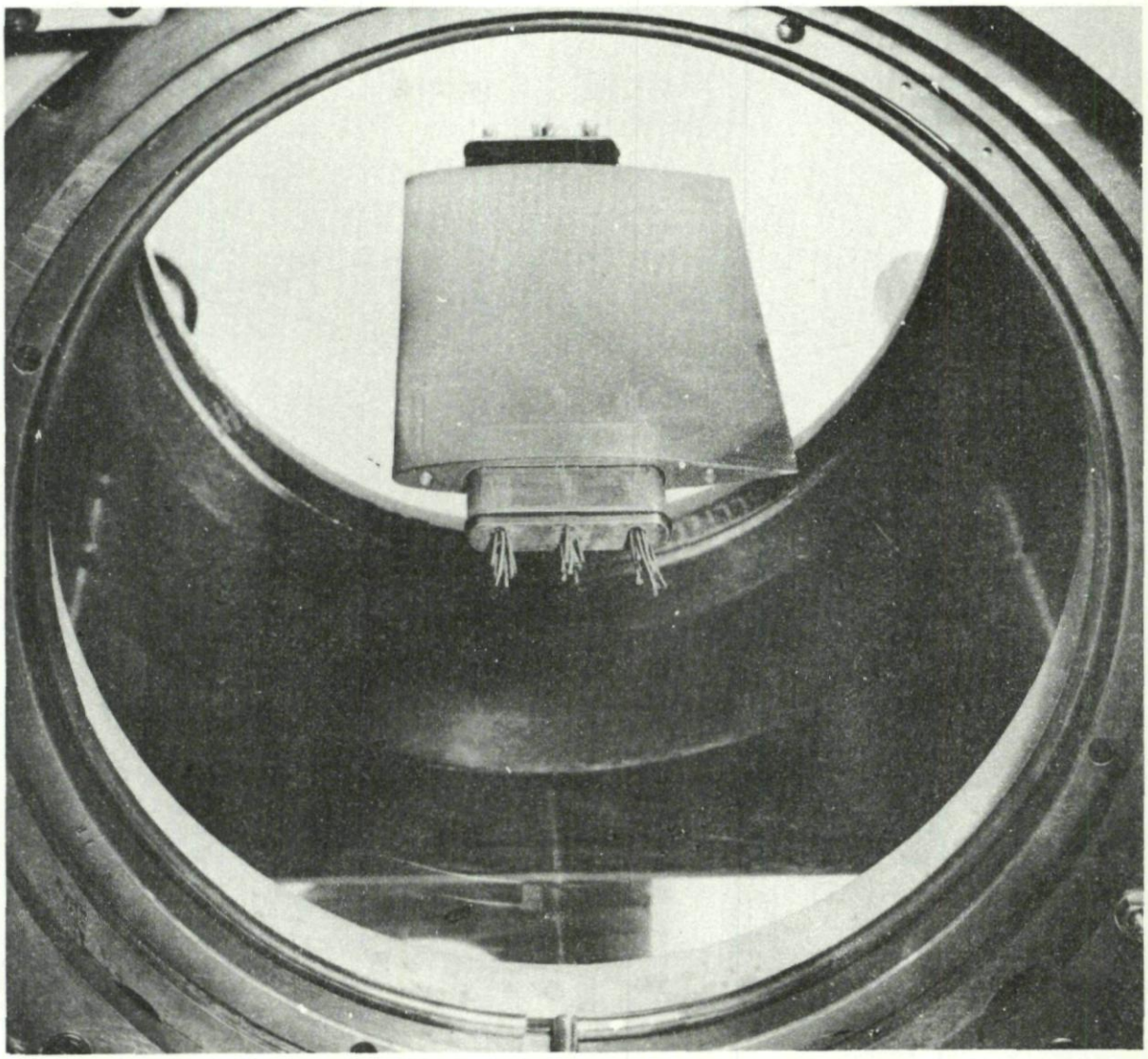

Fig. II-16. A two-dimensional aerofoil supported by tongues passing through slots cut in the glass windows of a wind tunnel.

(a) With parallel light

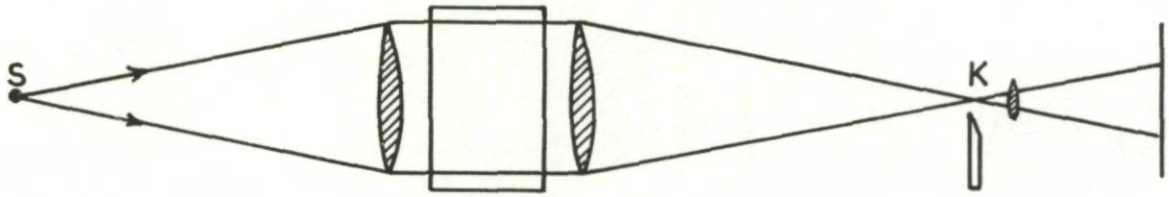

(b) With non-parallel light

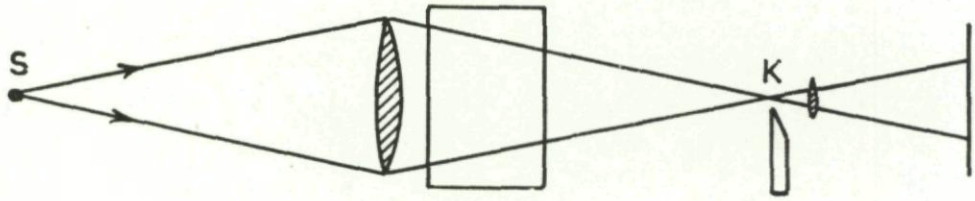

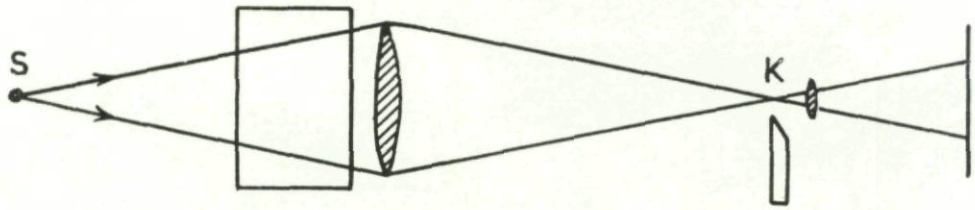

Fig. II-17. Schlieren systems based on lenses.

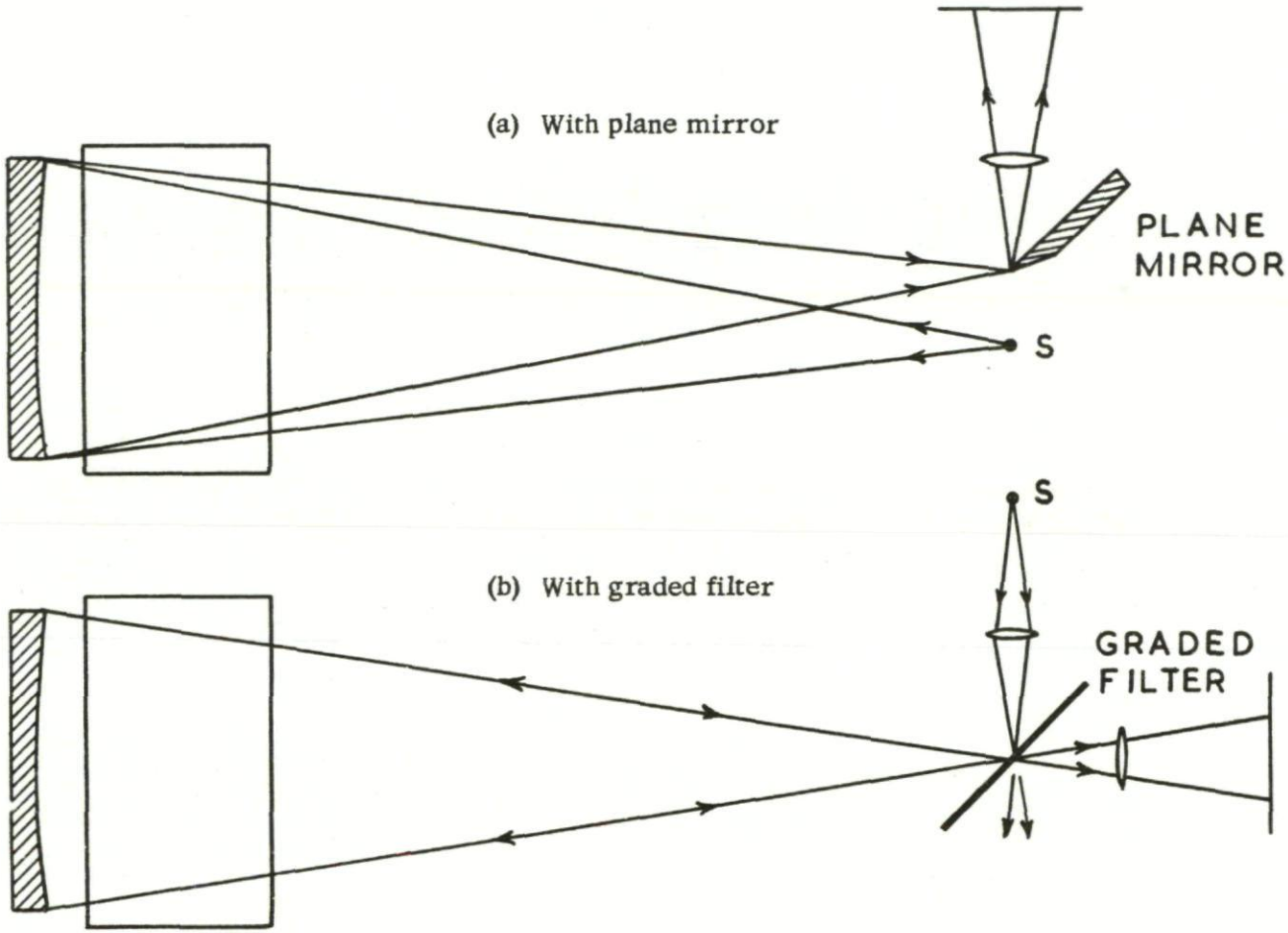

Fig. II-18. Coincidence schlieren systems.

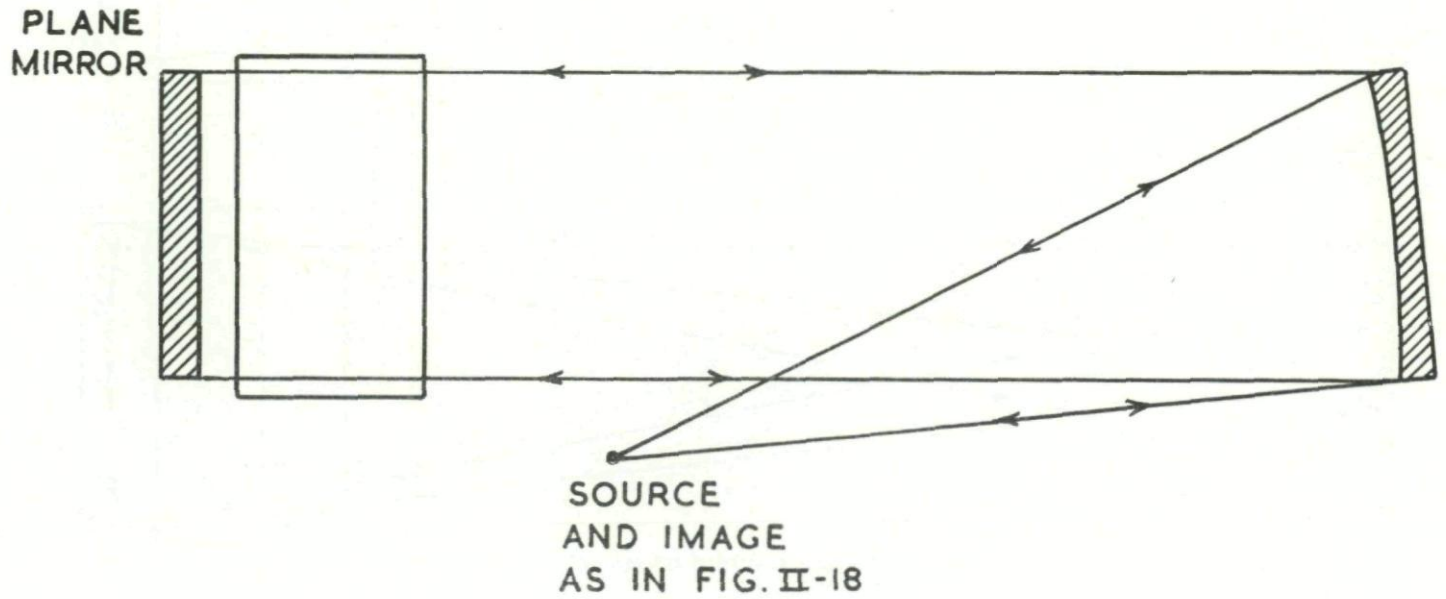

Fig. II-19. A schlieren system in which the parallel beam crosses the working section twice.

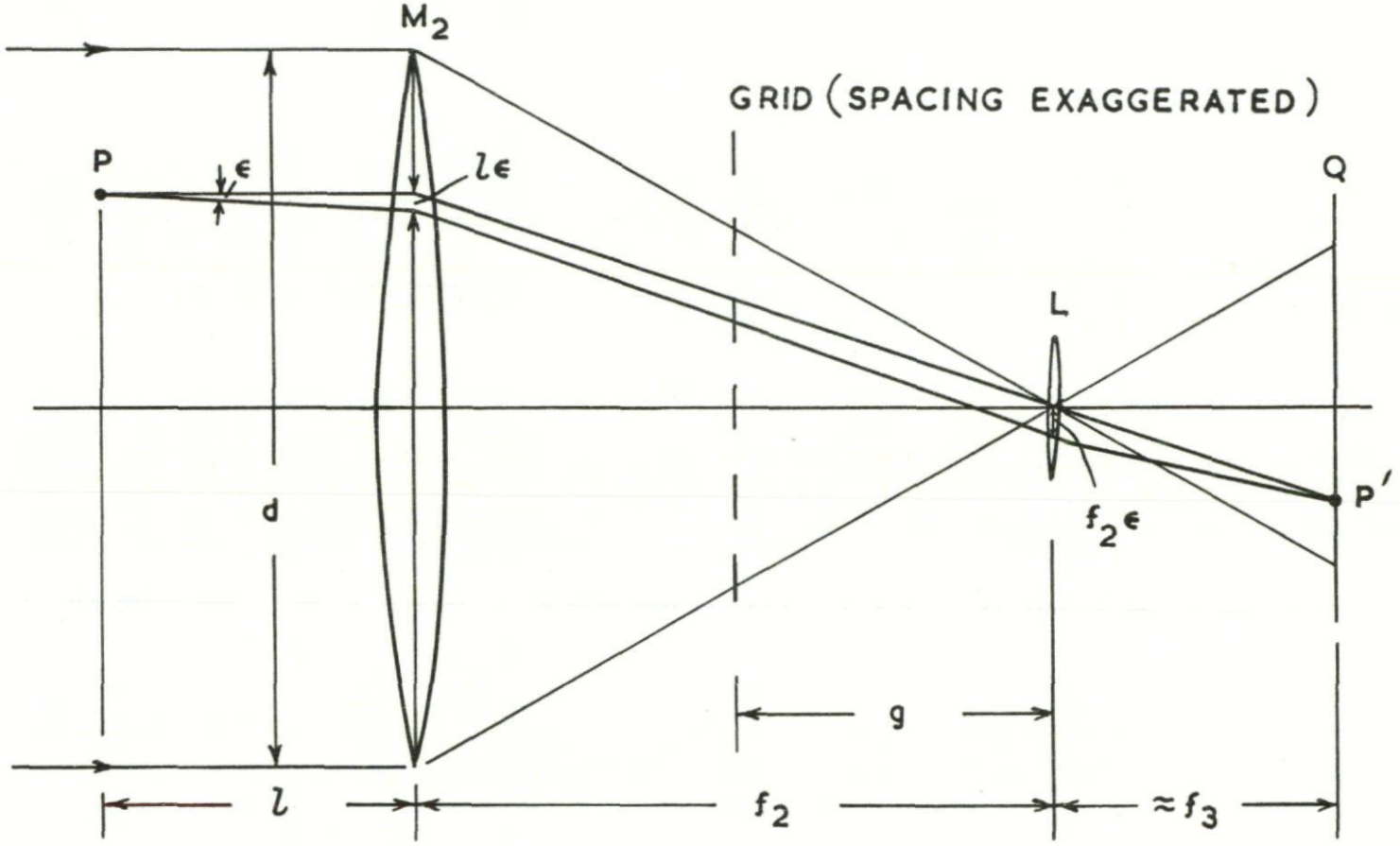

Fig. II-20. Sketch illustrating the Ronchi method.

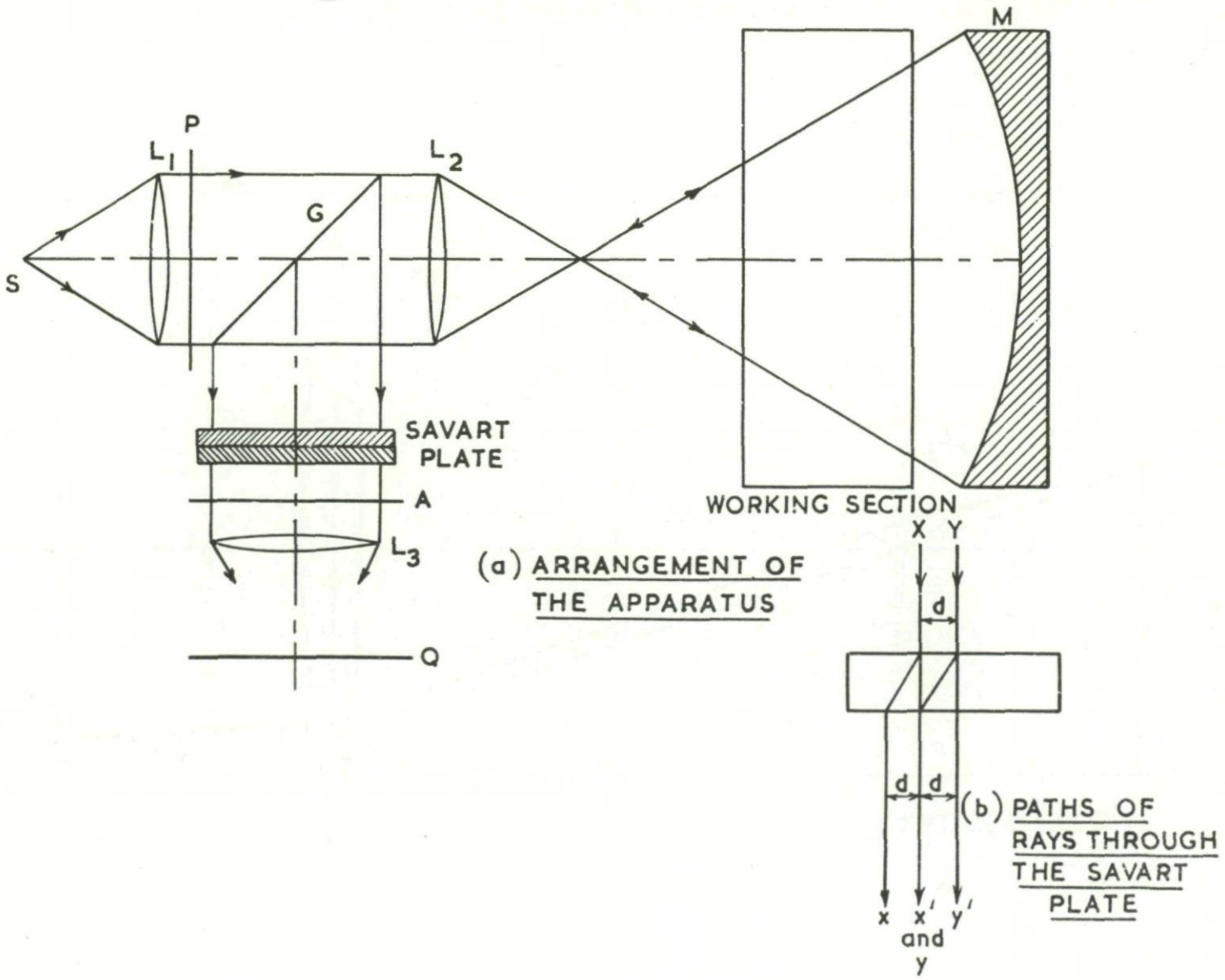

Fig. II-21 A method using polarized light.

(a) A typical arrangement of the apparatus

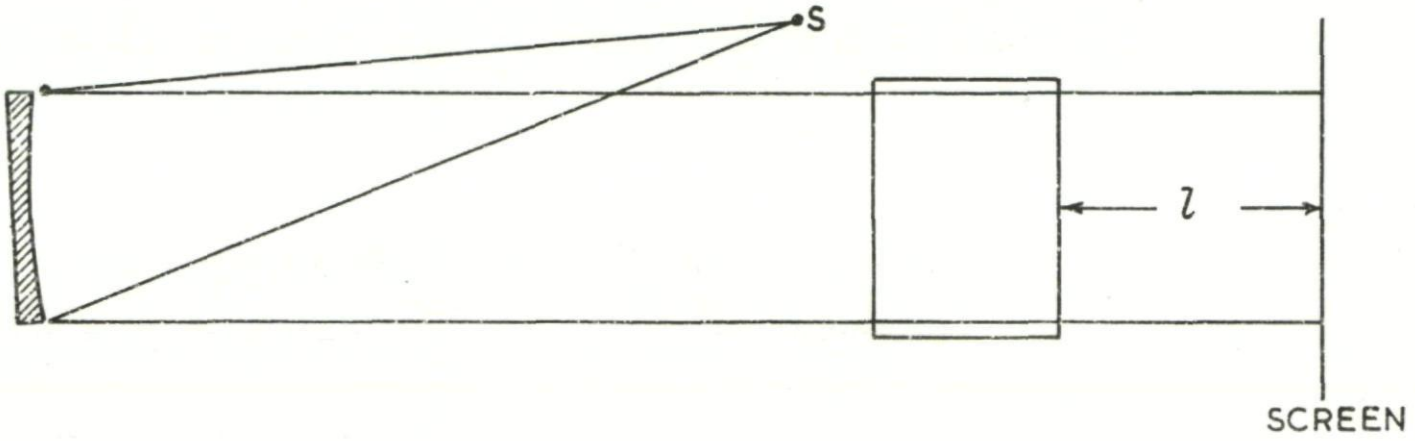

(b) Sketch illustrating the change of illumination at the screen

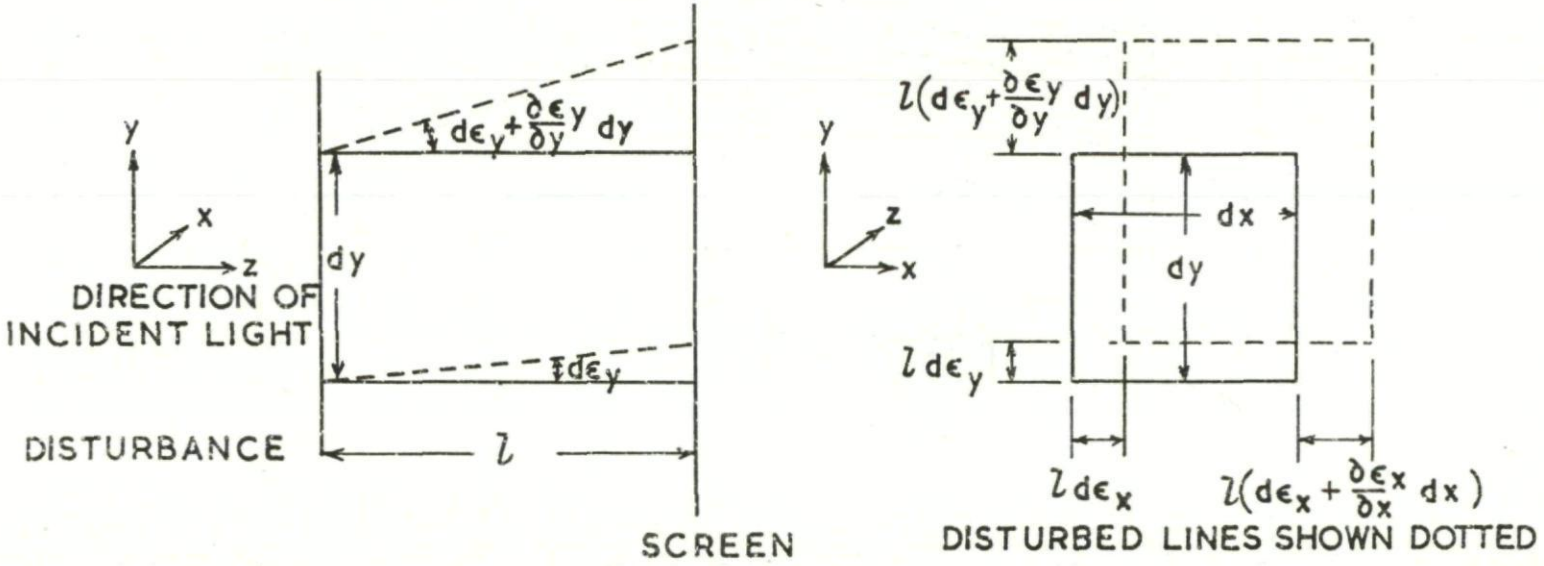

Fig. II-22. The direct-shadow method.

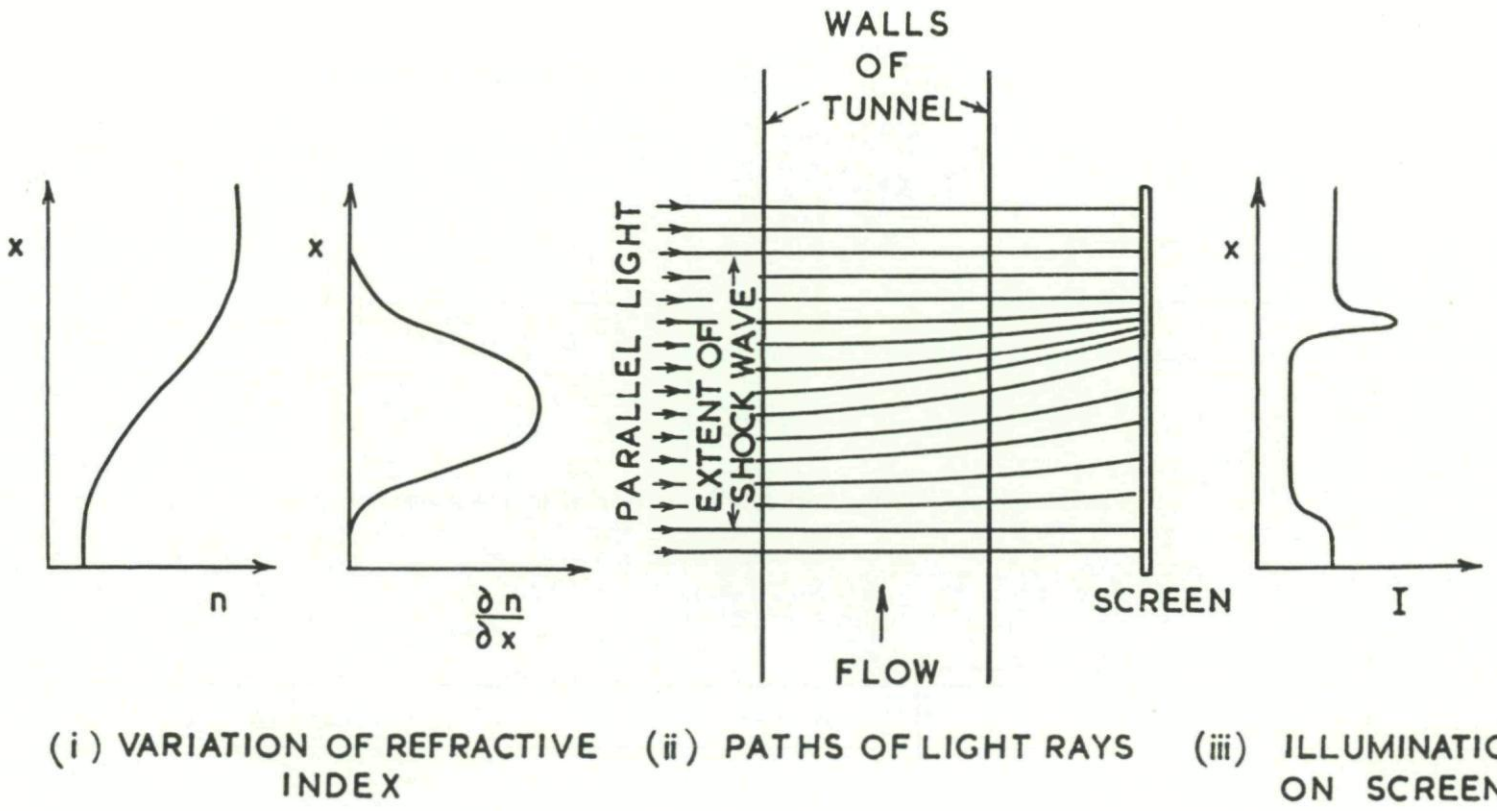

Fig. II-23. Sketches illustrating the formation of a direct-shadow image of a two-dimensional shock wave.

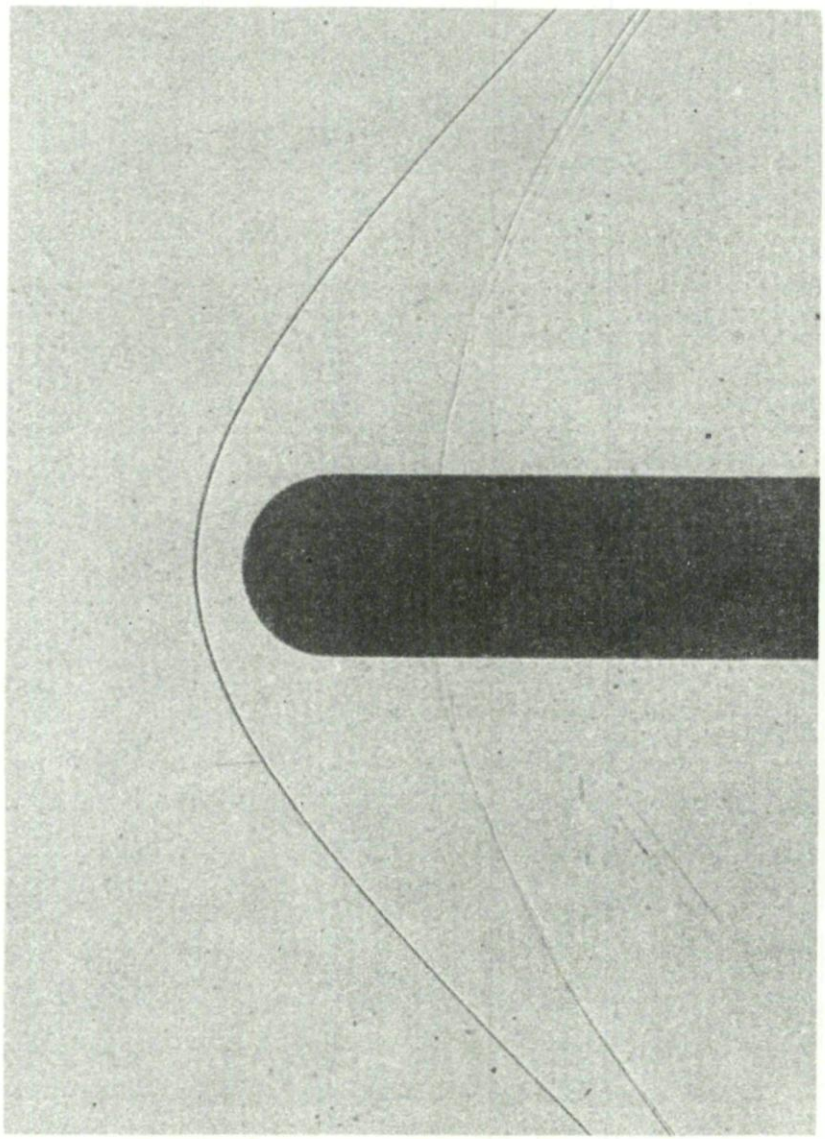

Fig. II-24. Direct-shadow photograph of the flow past a body of revolution with a hemispherical nose at M = 1.6.

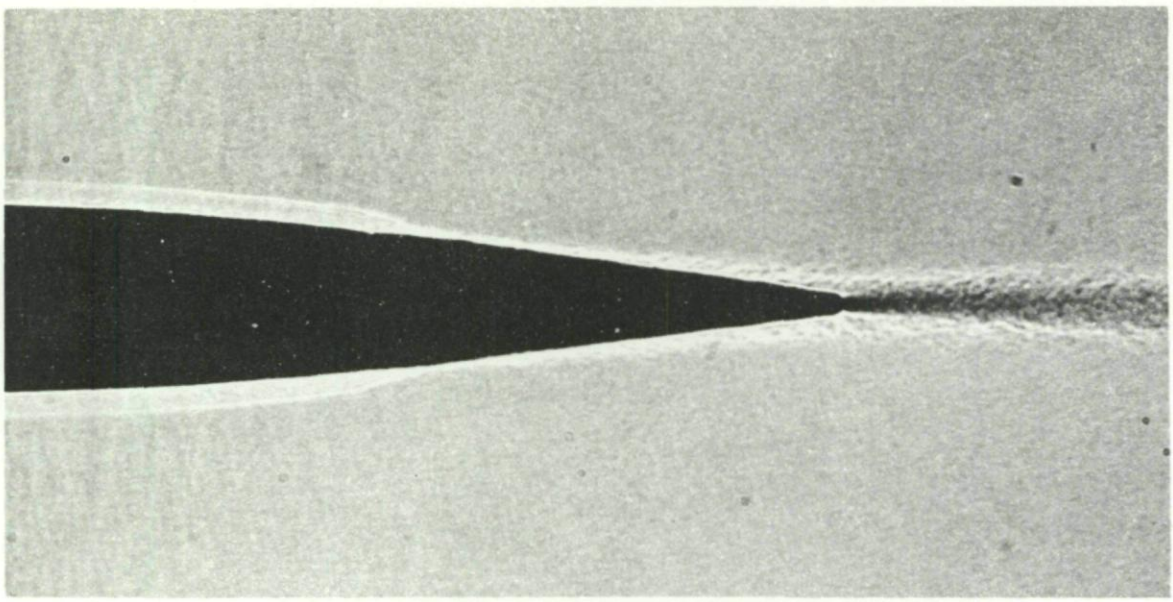

(a) Transition at 0.73 chord

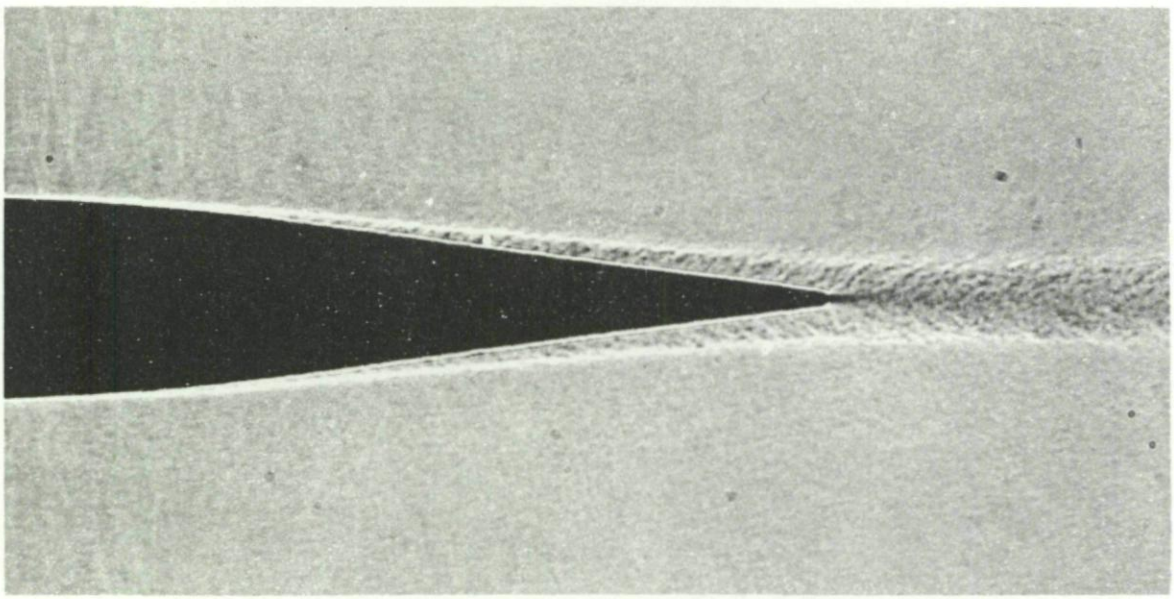

(b) Transition near the leading edge

Fig. II-25. Direct-shadow photographs of the rear half of an aerofoil showing the state of the boundary layer.

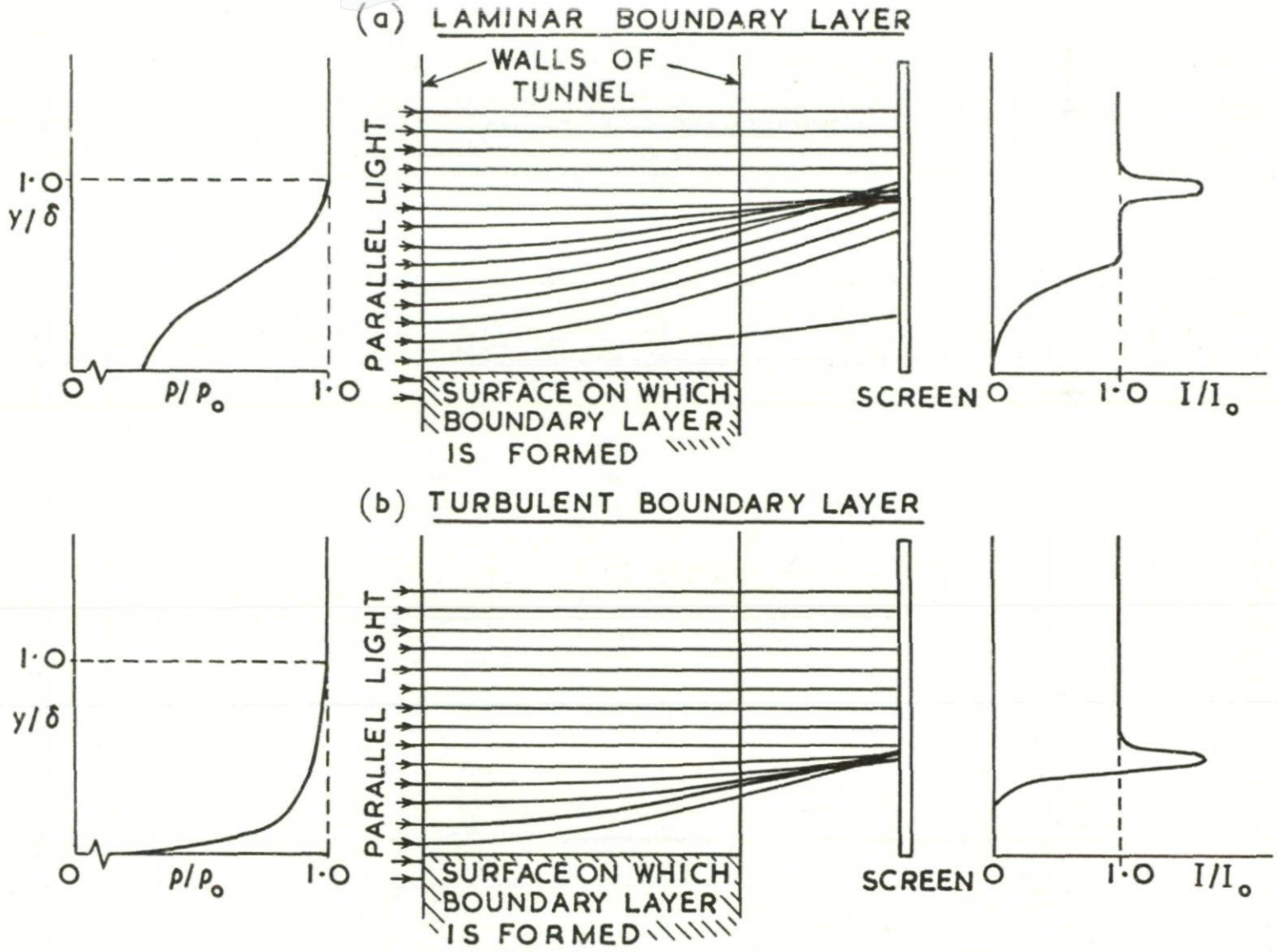

Fig. II-26. Sketches illustrating the formation of direct-shadow images of two-dimensional boundary layers. (Flow perpendicular to plane of paper.)

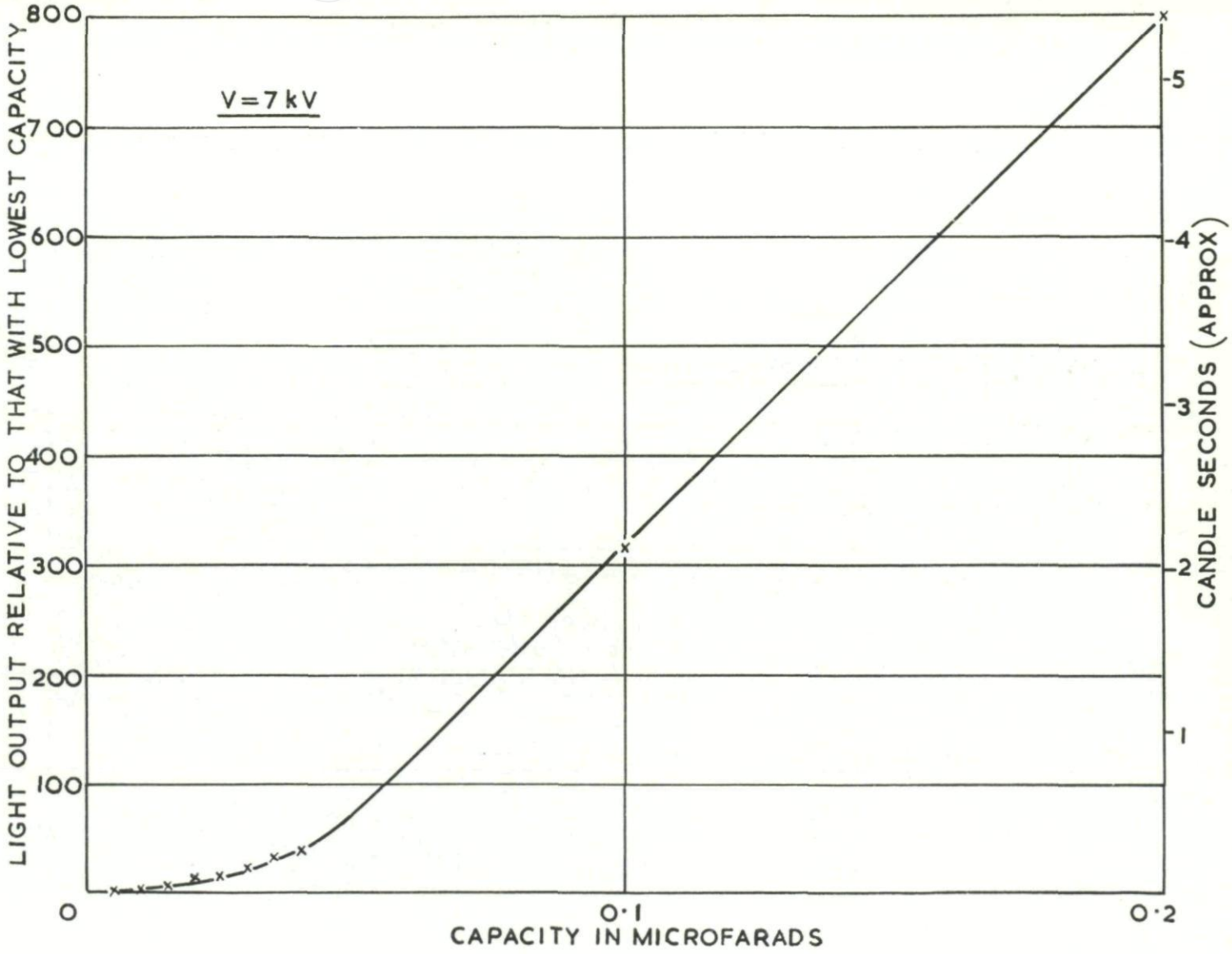

Fig. II-27. The variation with capacitor size of the light output of a spark gap.

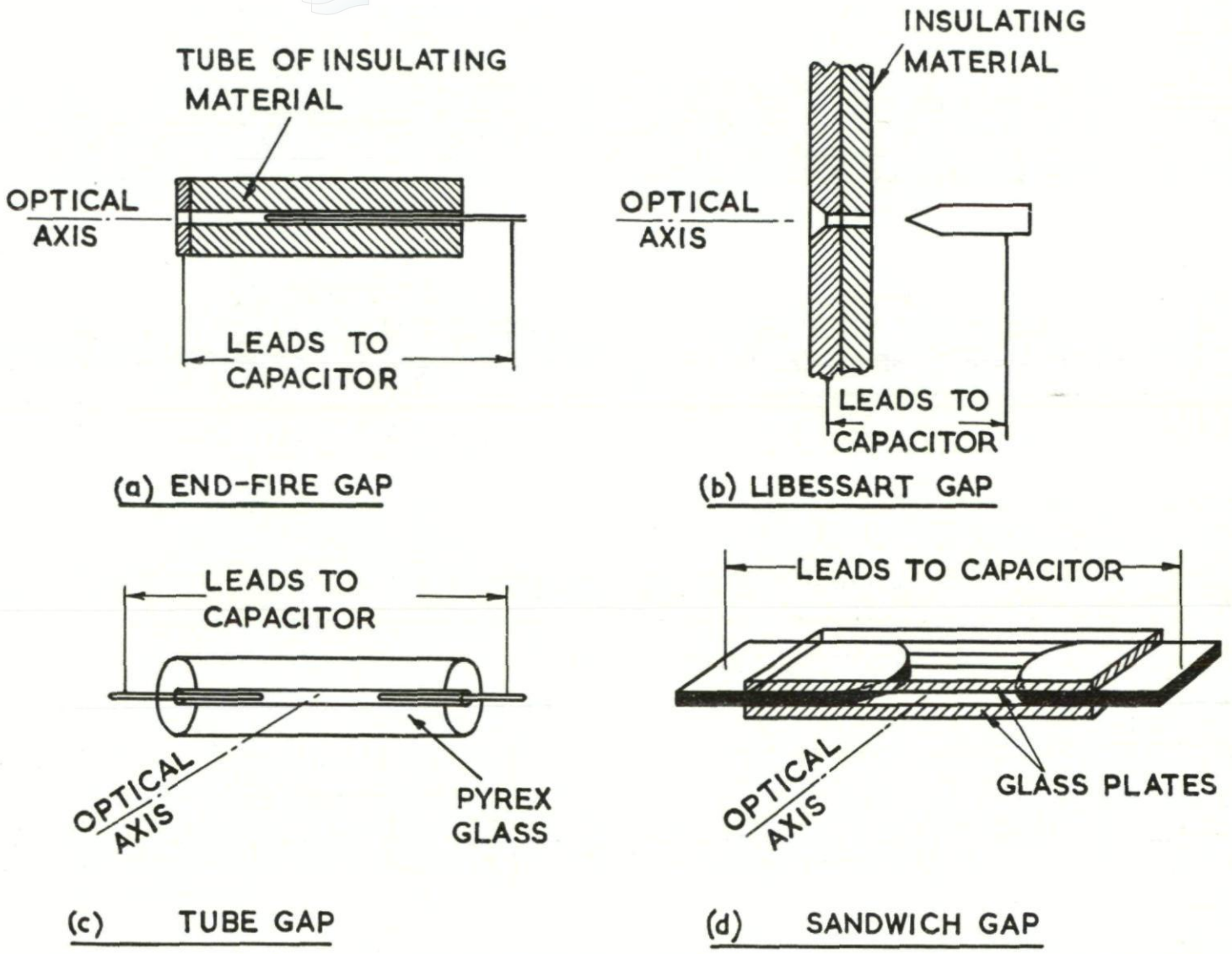

Fig. II-28. Simple types of spark gap.

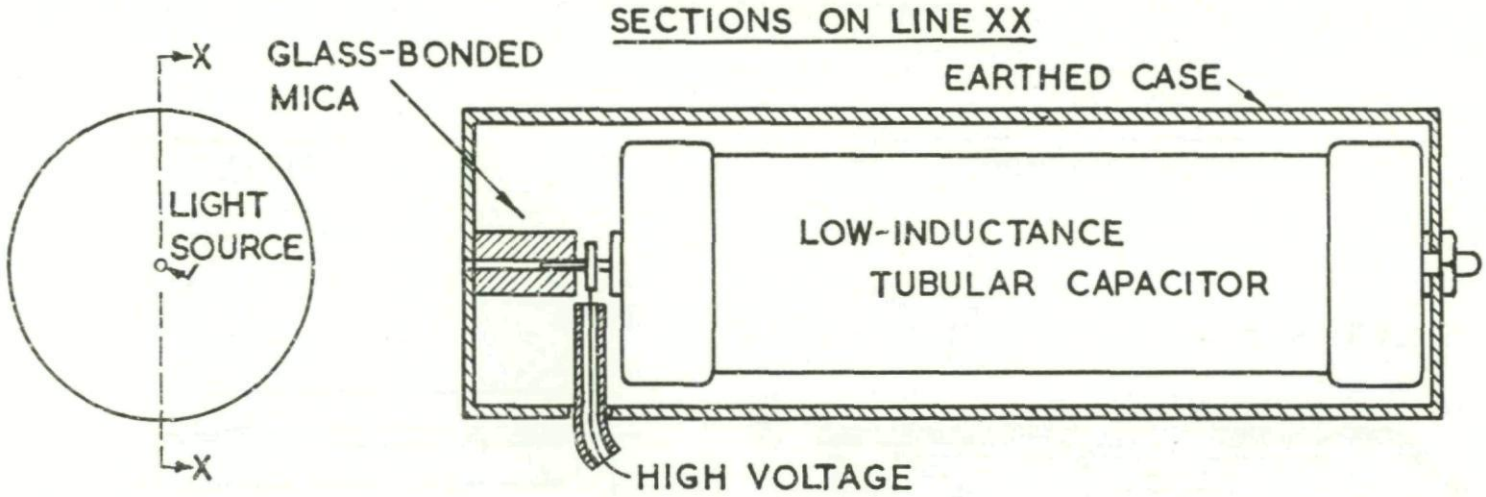

(a) With a commercial paper-dielectric capacitor

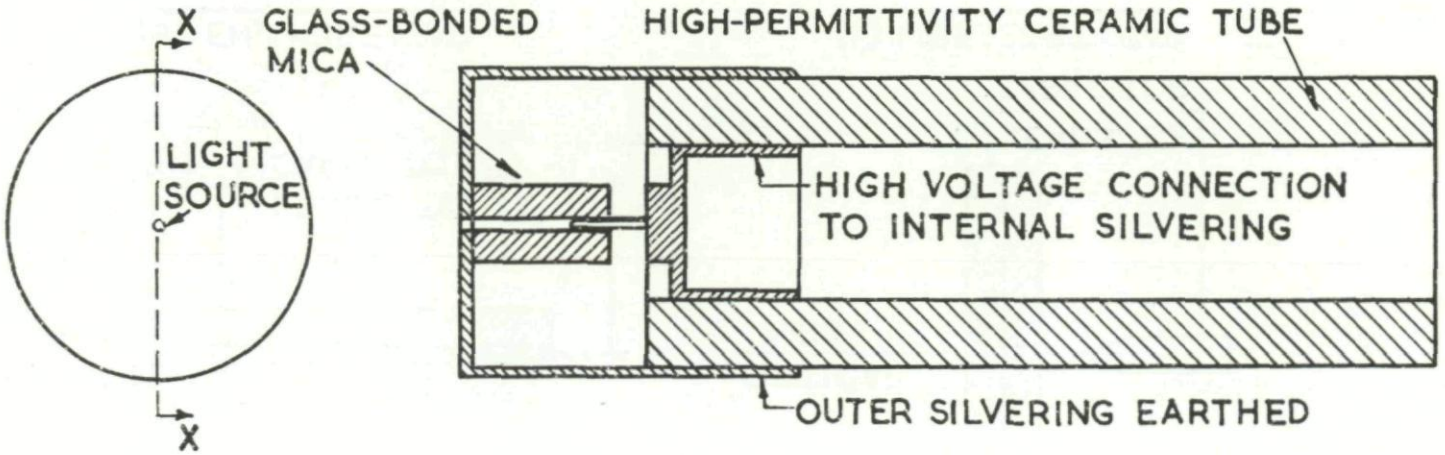

(b) With a ceramic-dielectric capacitor

Fig. II-29. Spark light source and capacitor arrangements (Refs. 40 and 41).

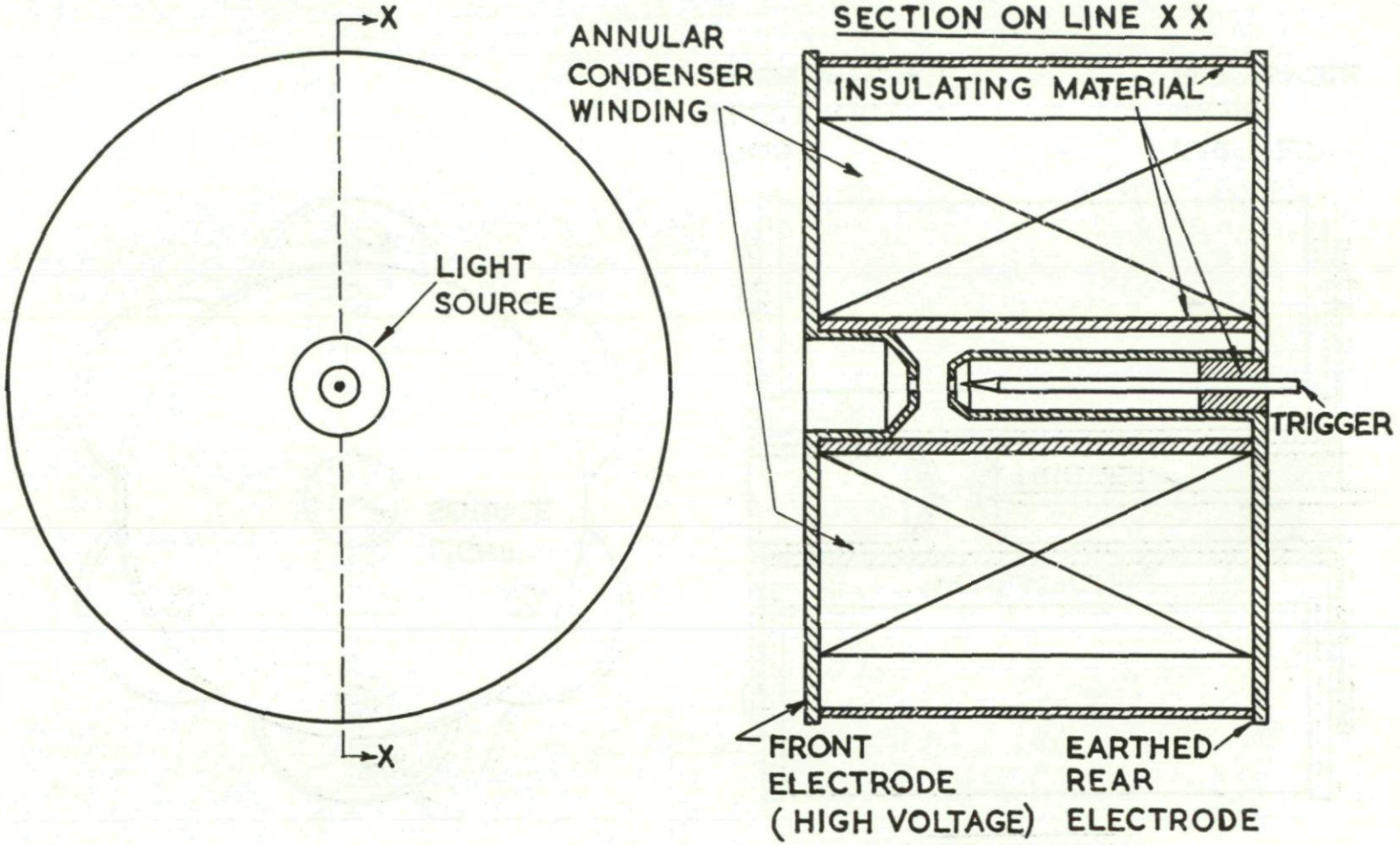

Fig. II-29c. Spark light source and capacitor arrangements (Ref. 125).

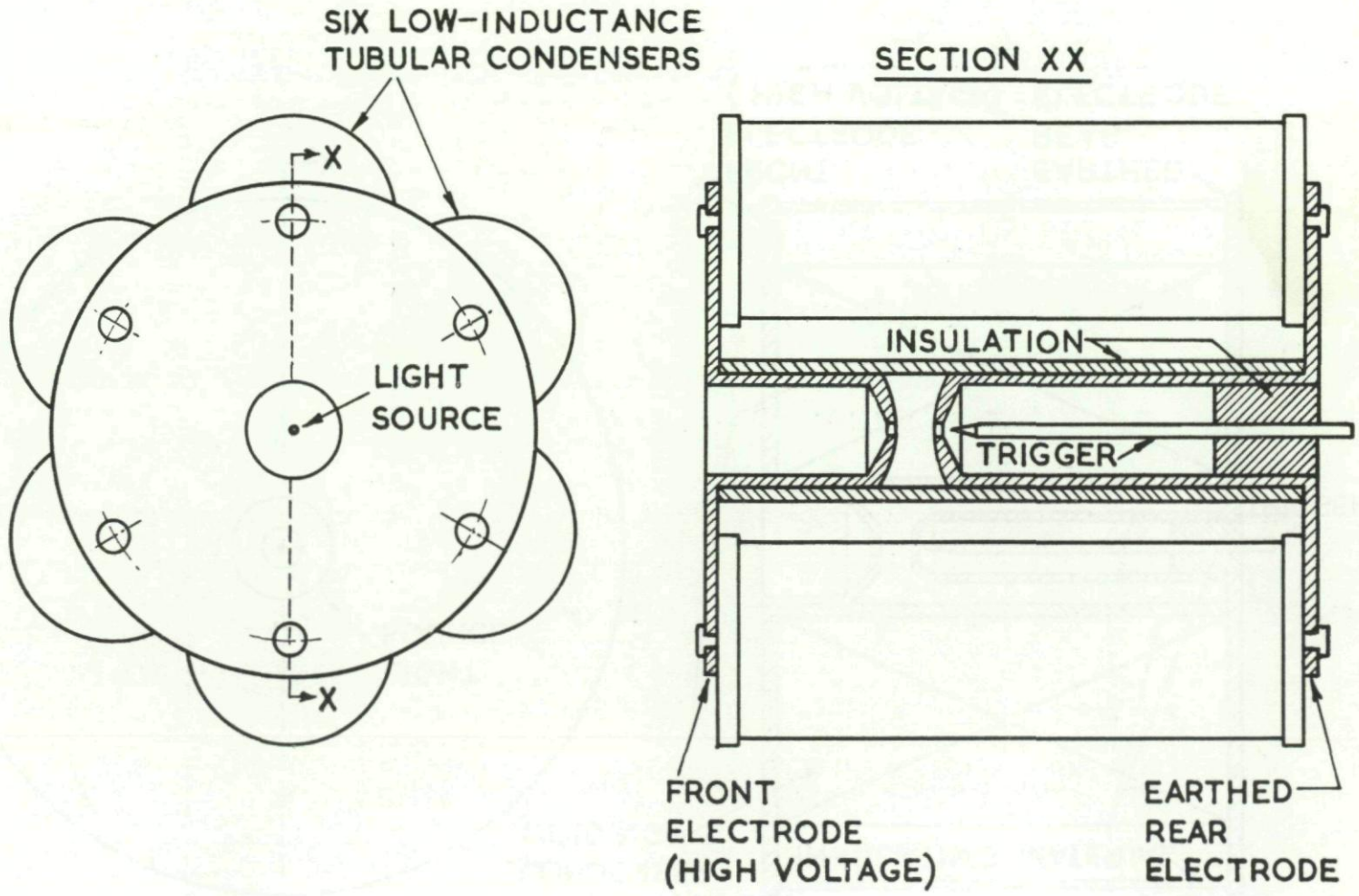

Fig. II-29d. Spark light source and capacitor arrangements (Ref. 124).

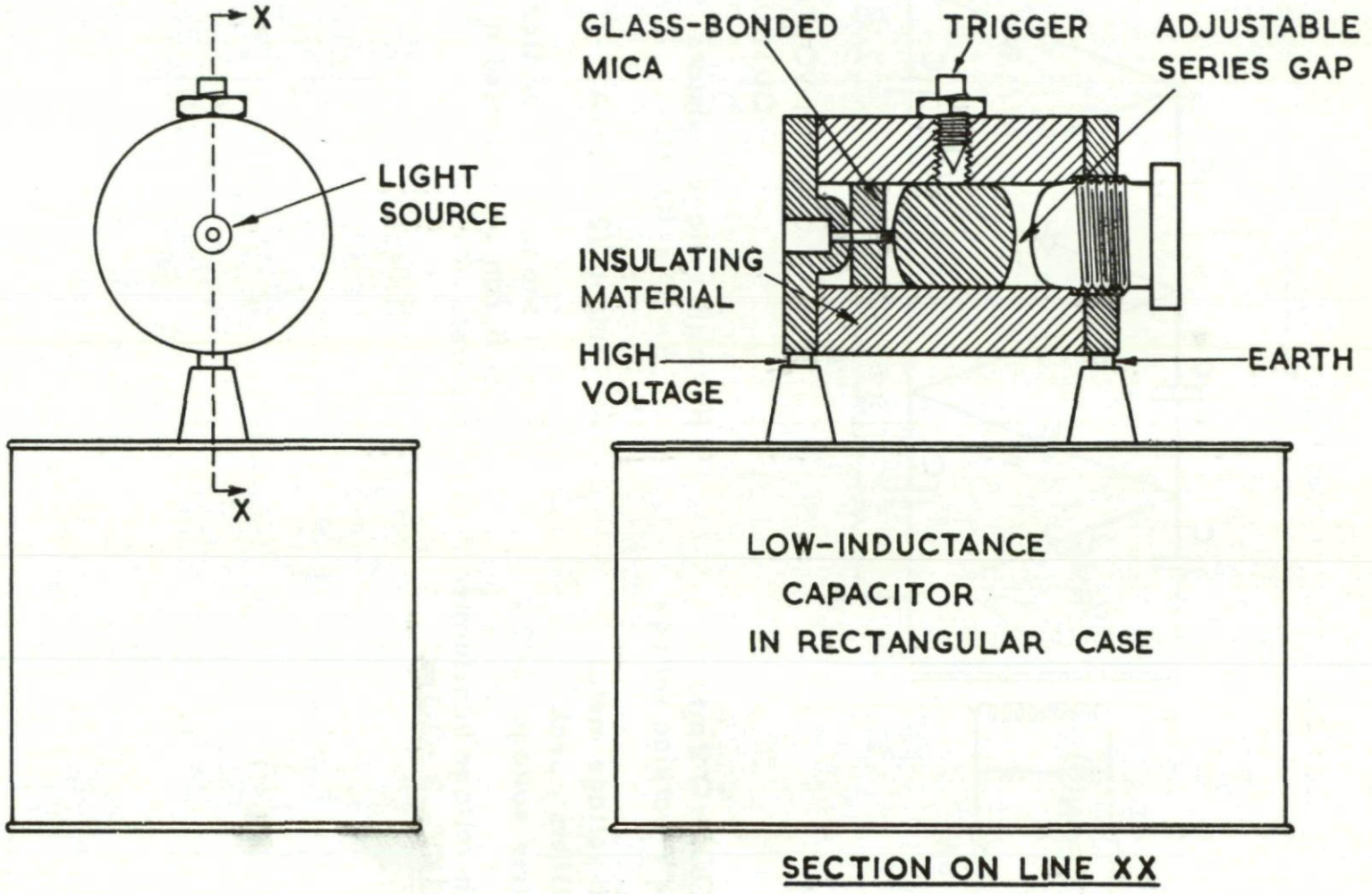

Fig. II-29e. Spark light source and capacitor arrangements (Ref. 122).

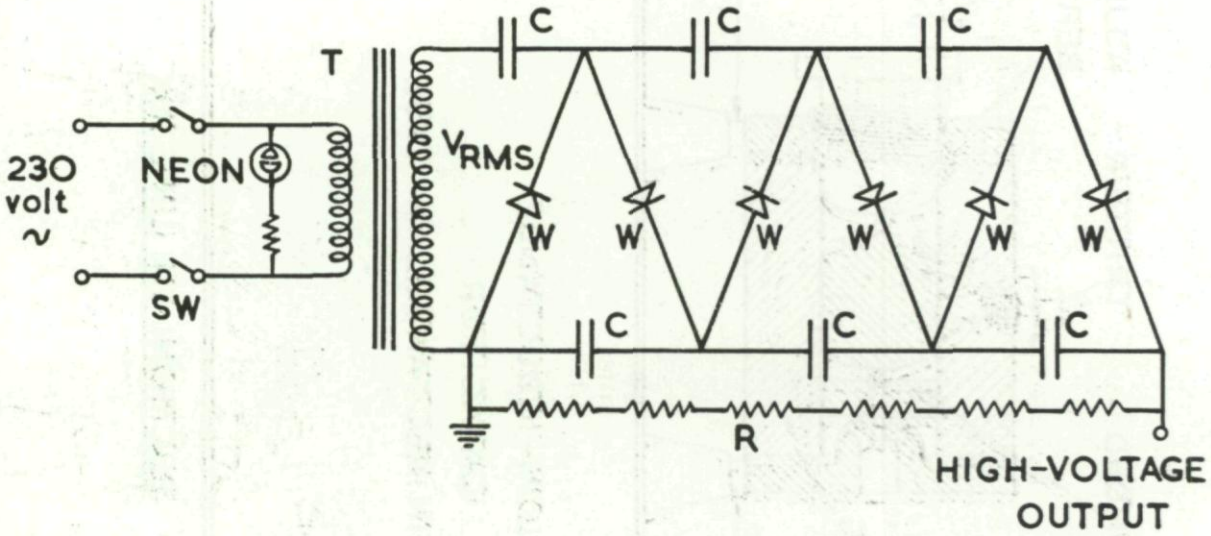

C 0·005–0·2 mfd
$2\sqrt{2}$ V working voltage

W high-voltage metal rectifiers, peak inverse voltage $2\sqrt{2}$ V

T high-voltage transformer
3–5 KV, 3 – 10 mA

R high-voltage resistors
5 – 10 x .10 MΩ

DC output 1/2 – 2 mA

Circuit shown with 6 sections: 4 or 8 can also be used if required.

Fig. II-30. A multiplying circuit used as a high-voltage supply.

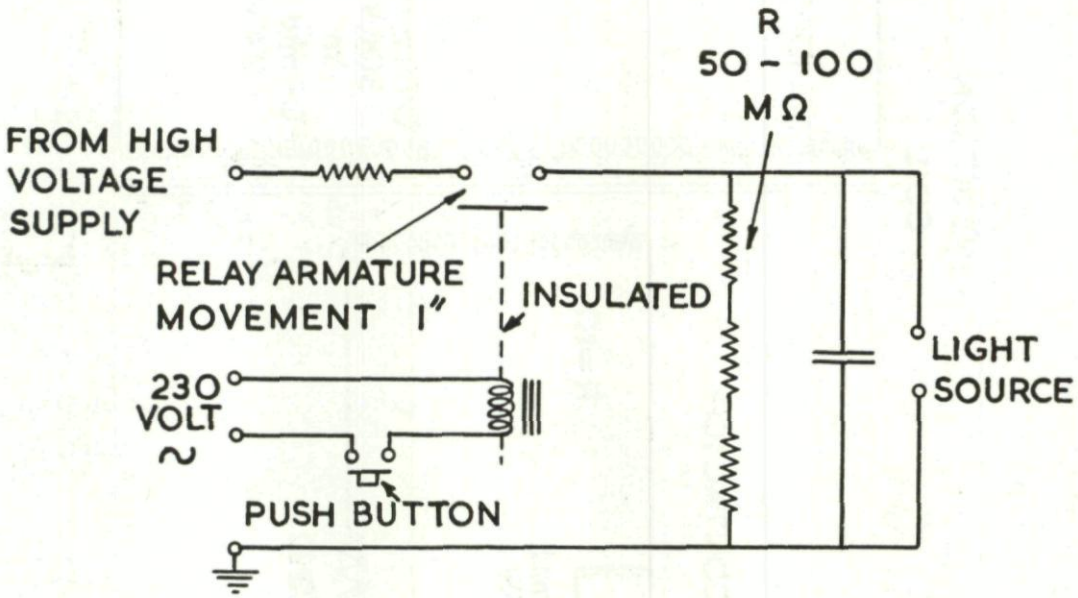

Fig. II-31. A high voltage relay used to control the charging of the spark capacitor.

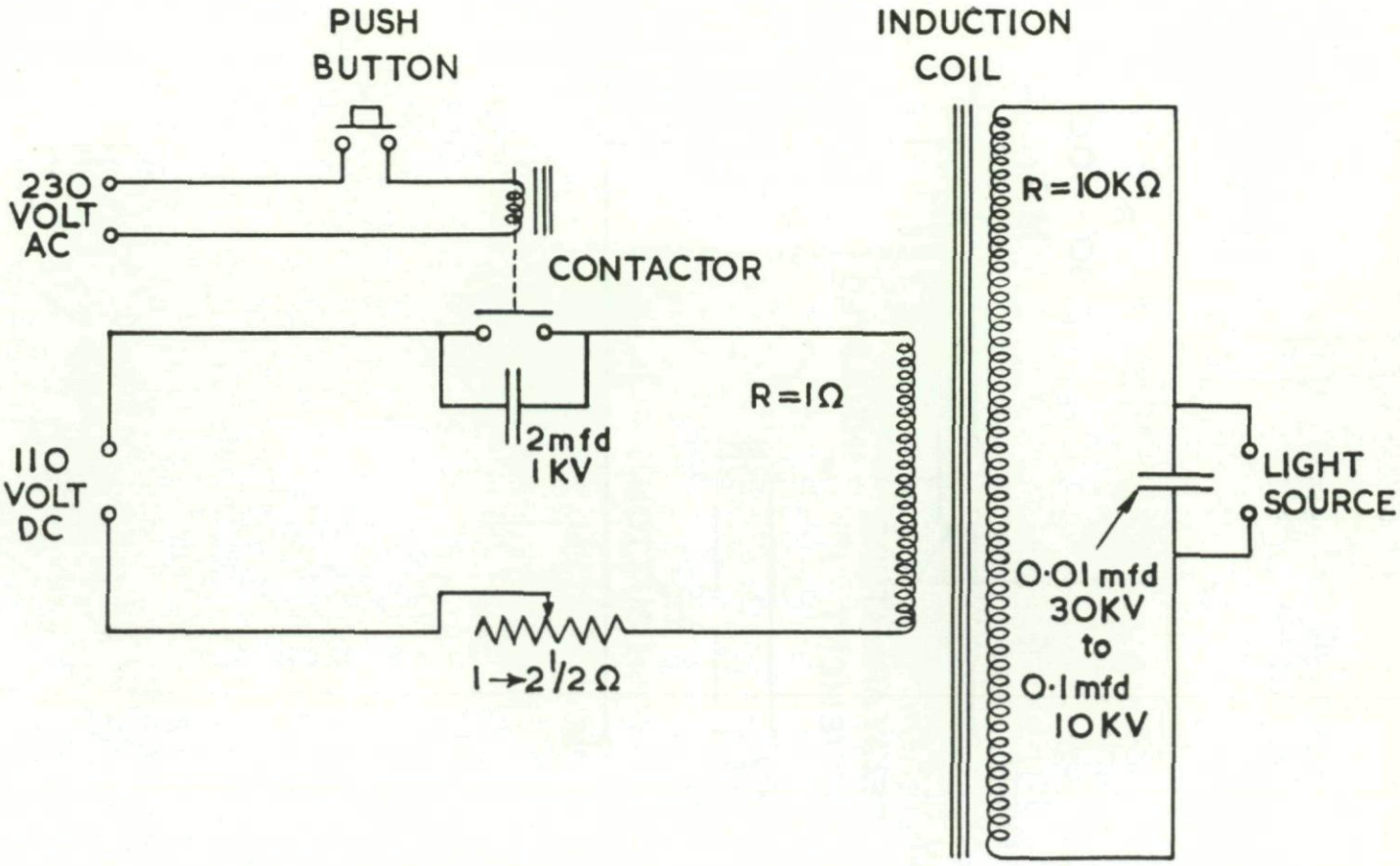

Fig. II-32. An induction coil used to charge the spark capacitor (Ref. 121).

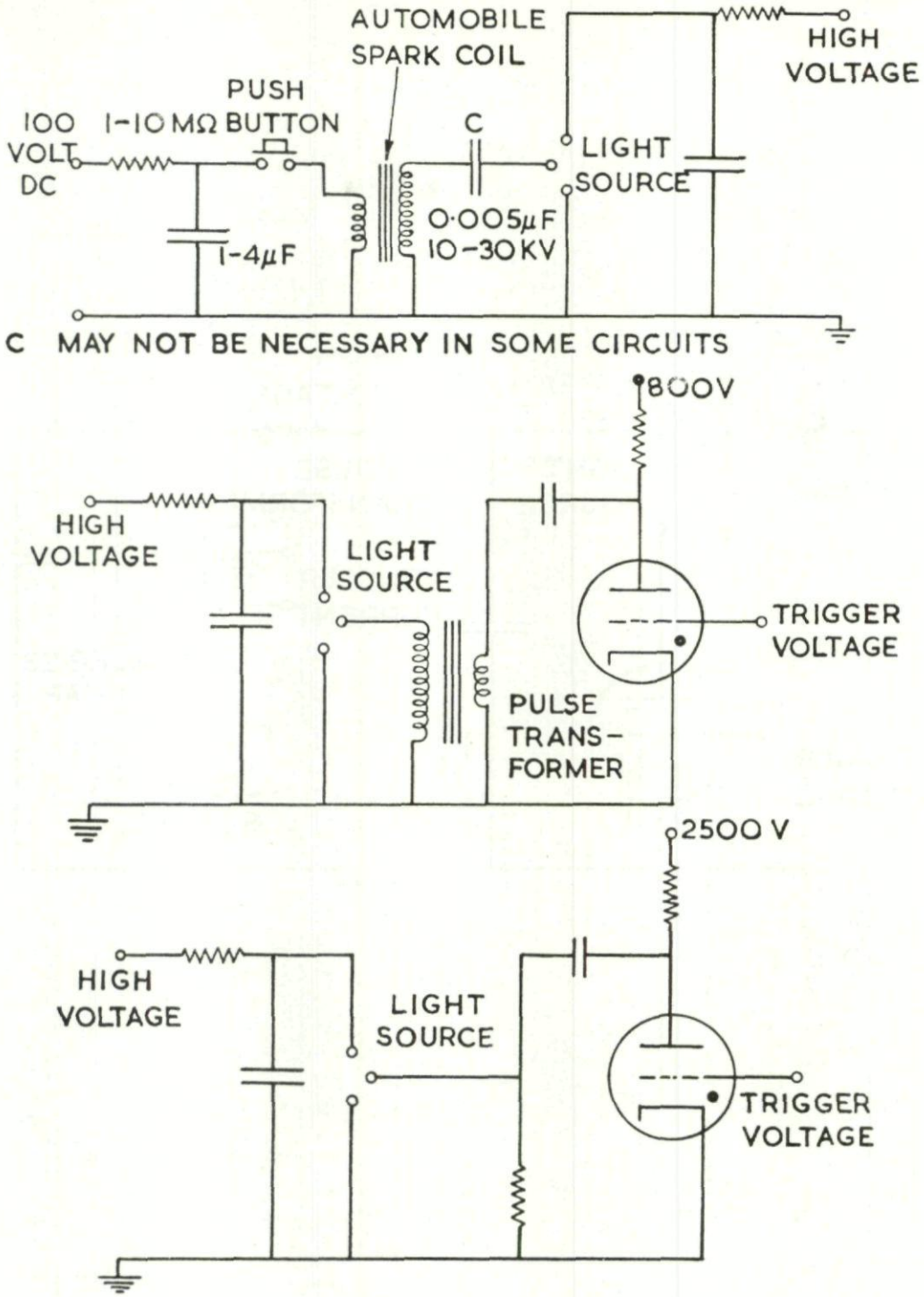

Fig. II-33a. Arrangements for triggering a third electrode in the spark light source (Ref. 128).

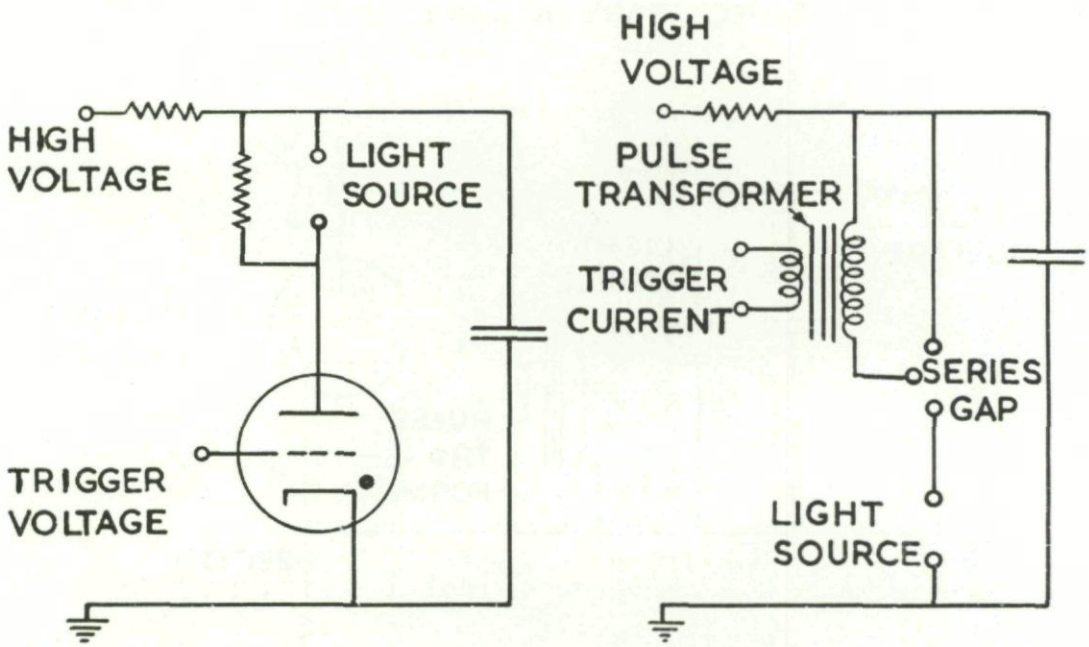

Fig. II-33b. Arrangements for triggering a thyratron or three-electrode gap connected in series with the spark light source (Refs. 104, 125, 132, and 133).

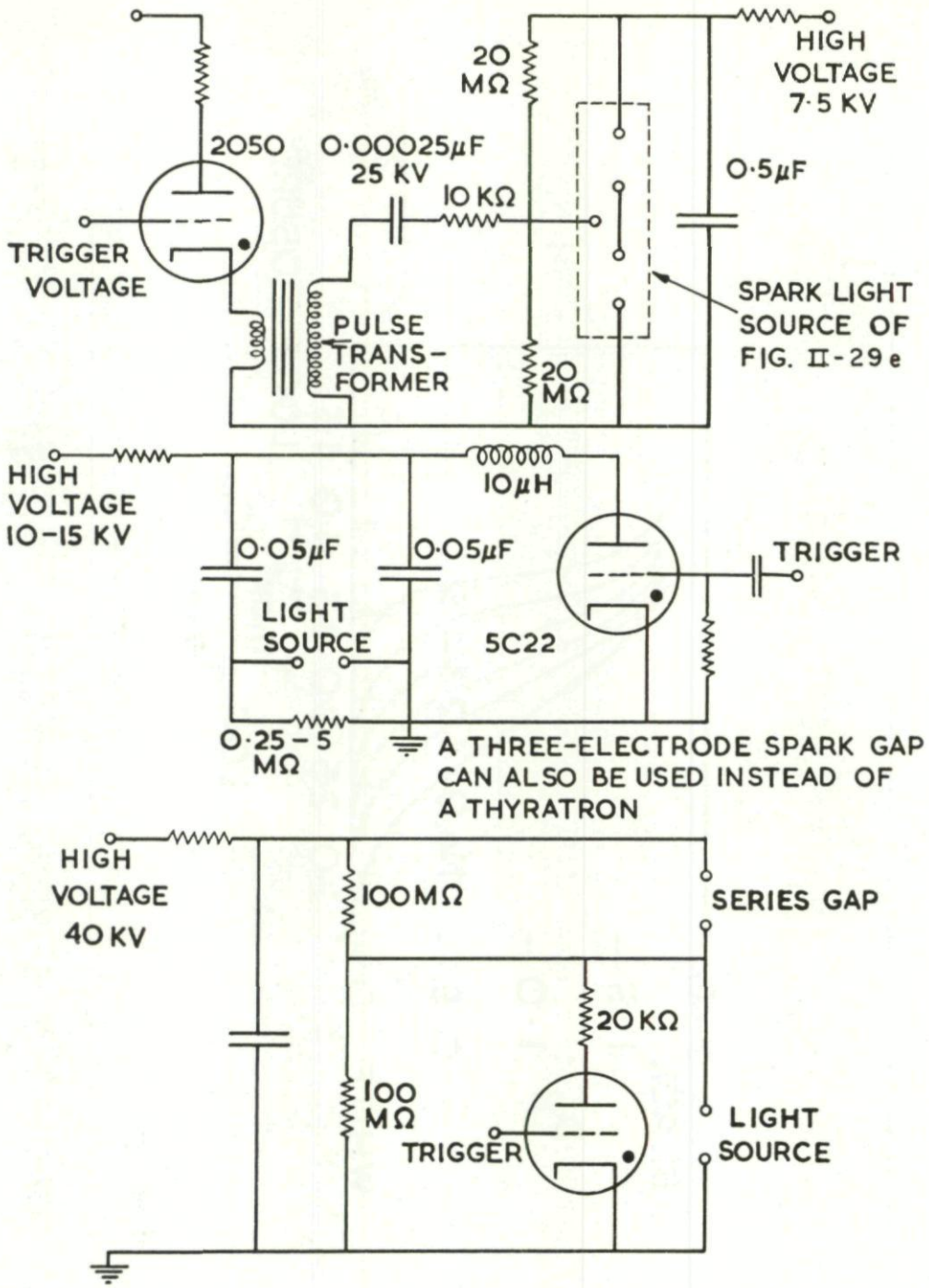

Fig. II-33c. Arrangements for triggering the spark light source by disturbing the potential across it (Refs. 90, 100, 122, and 134).

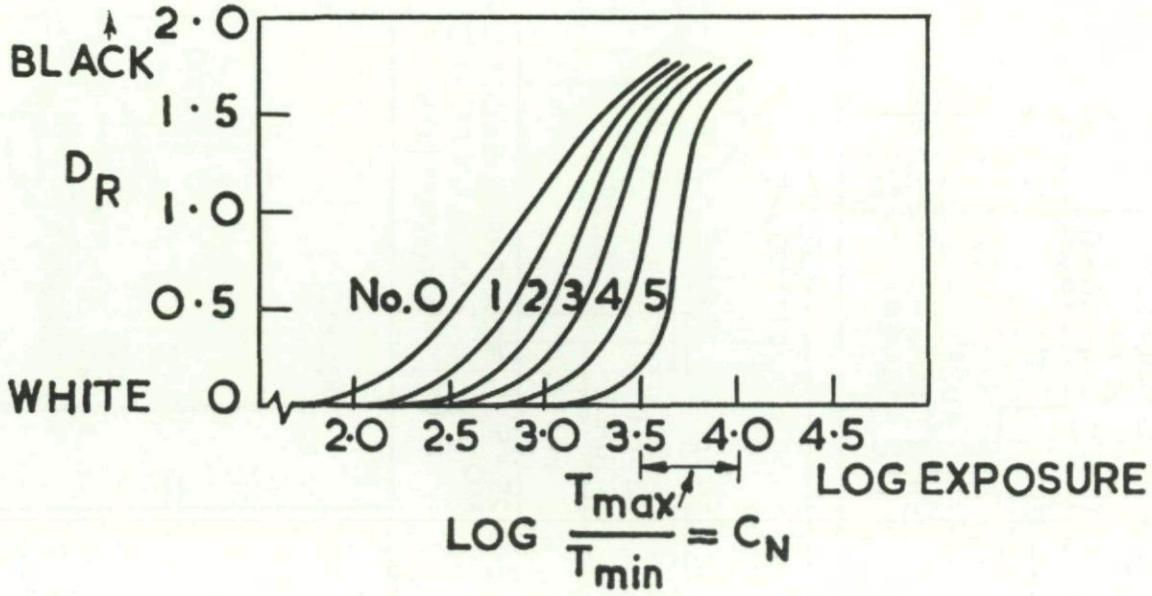

Fig. II-34. Typical characteristic curves for various grades of printing paper.

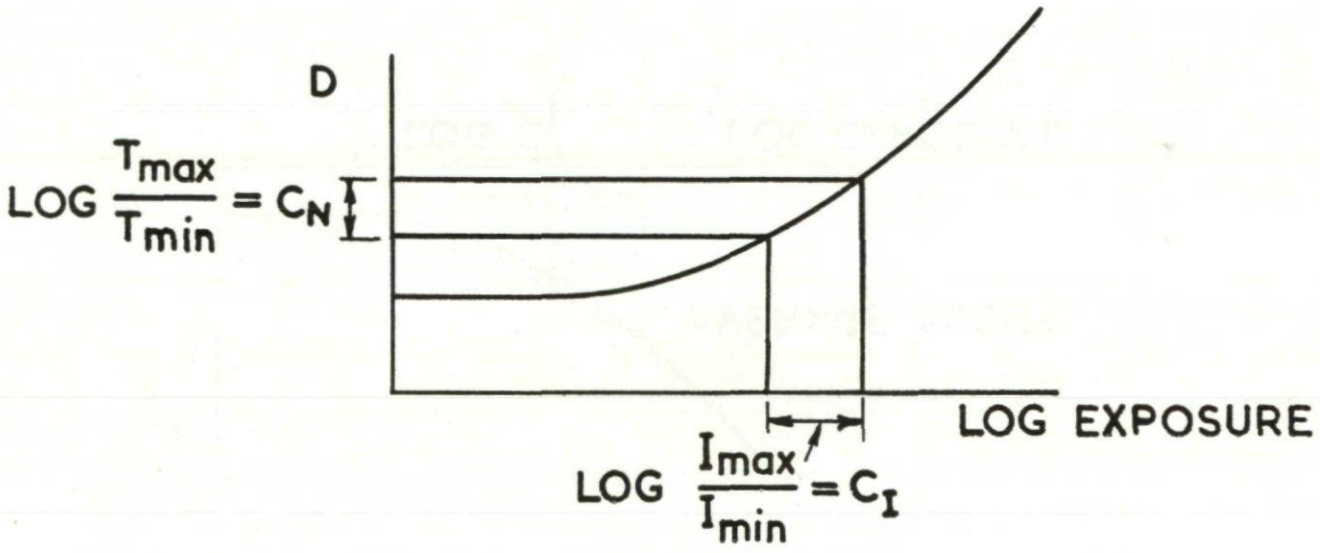

Fig. II-35. Sketch illustrating the relation of image and negative contrast.

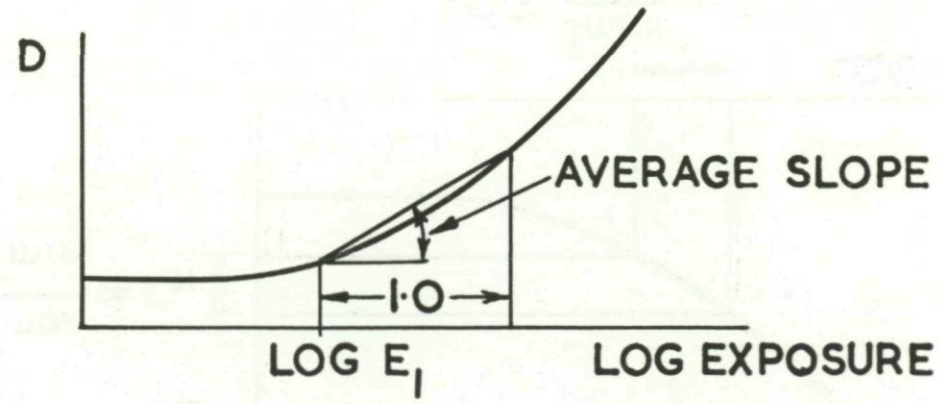

Fig. II-36. Sketch showing a definition of emulsion speed.

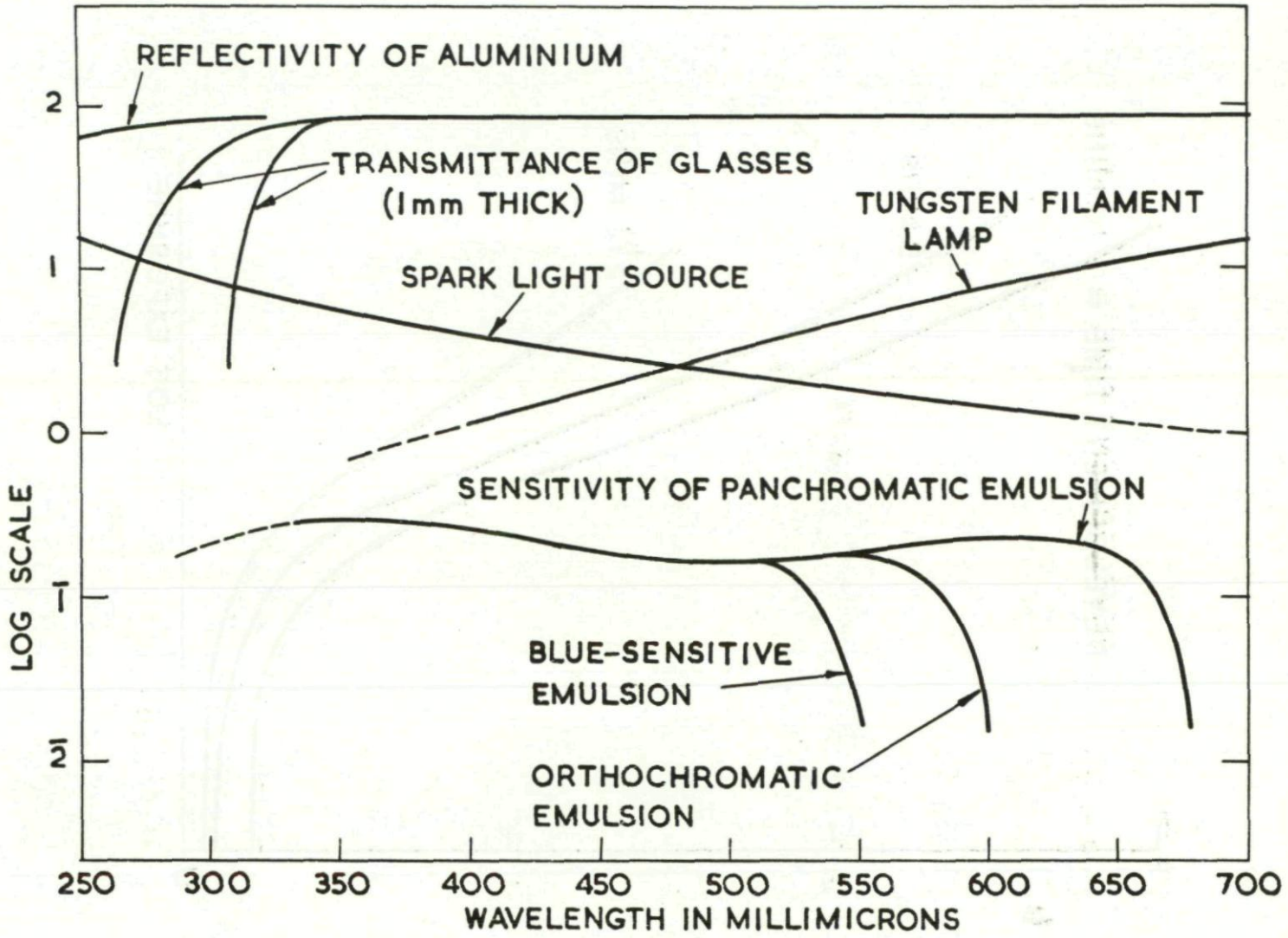

Fig. II-37. Spectral distributions of light sources and spectral sensitivities of photographic emulsions.

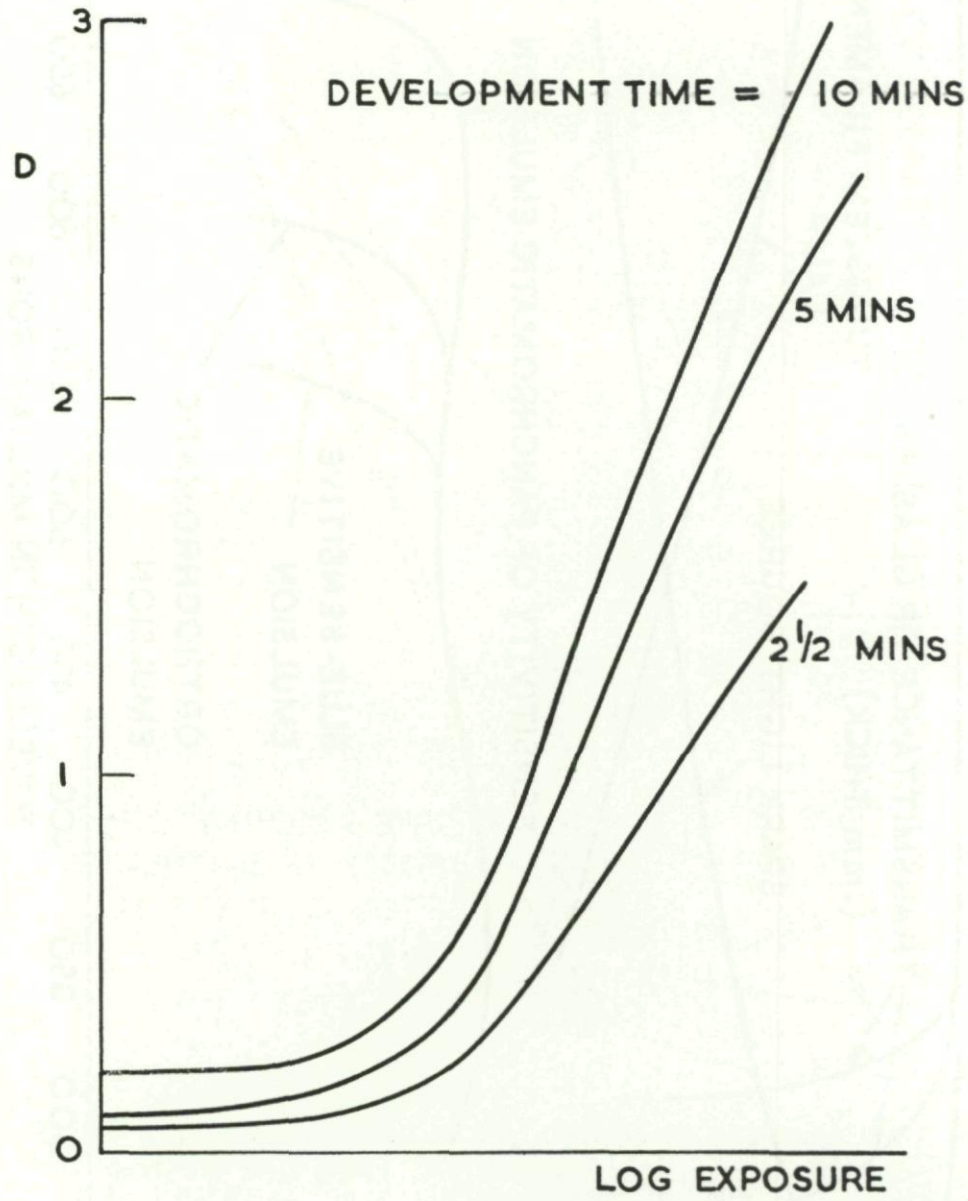

Fig. II-38. The effect of development time on the characteristic curve of Ilford type LN emulsion after exposure to a spark light source. Developer Ilford ID 19 at 68°F.

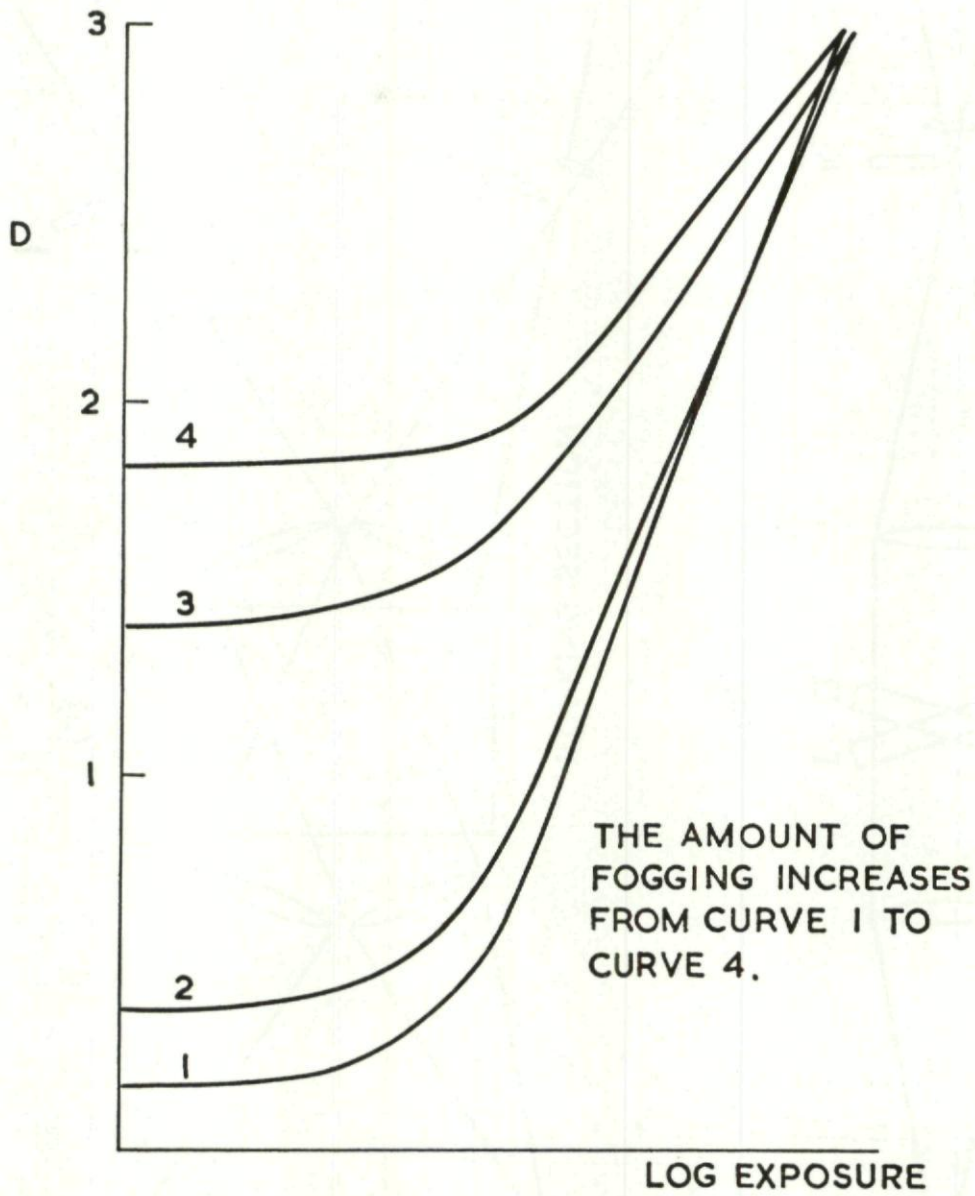

Fig. II-39. Illustration of the effects of fogging on the characteristic curve with spark exposures. Ilford type LN emulsion developed for 10 minutes in Ilford ID 19 developer at 68°F.

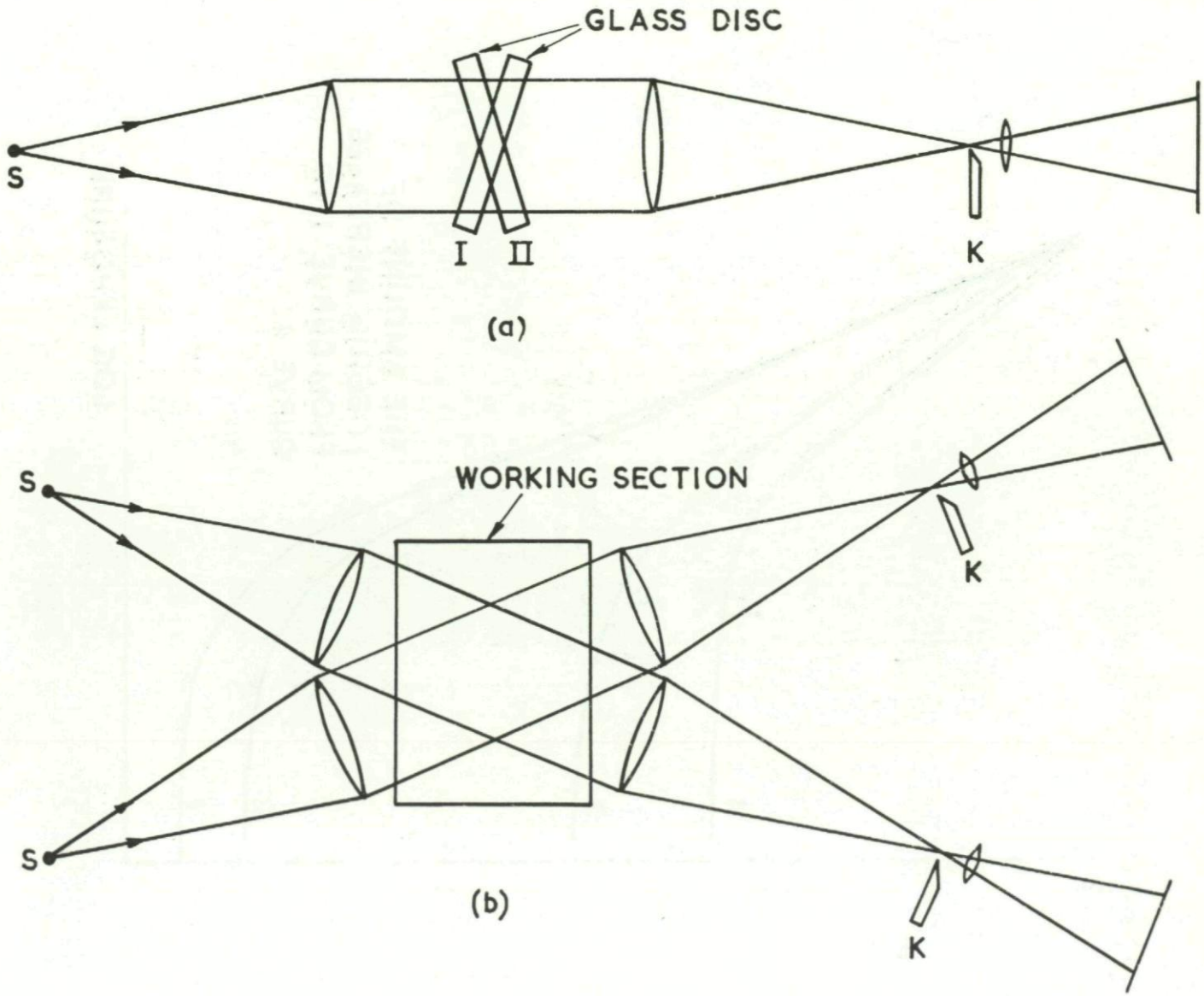

Fig. II-40. A stereoscopic schlieren apparatus.

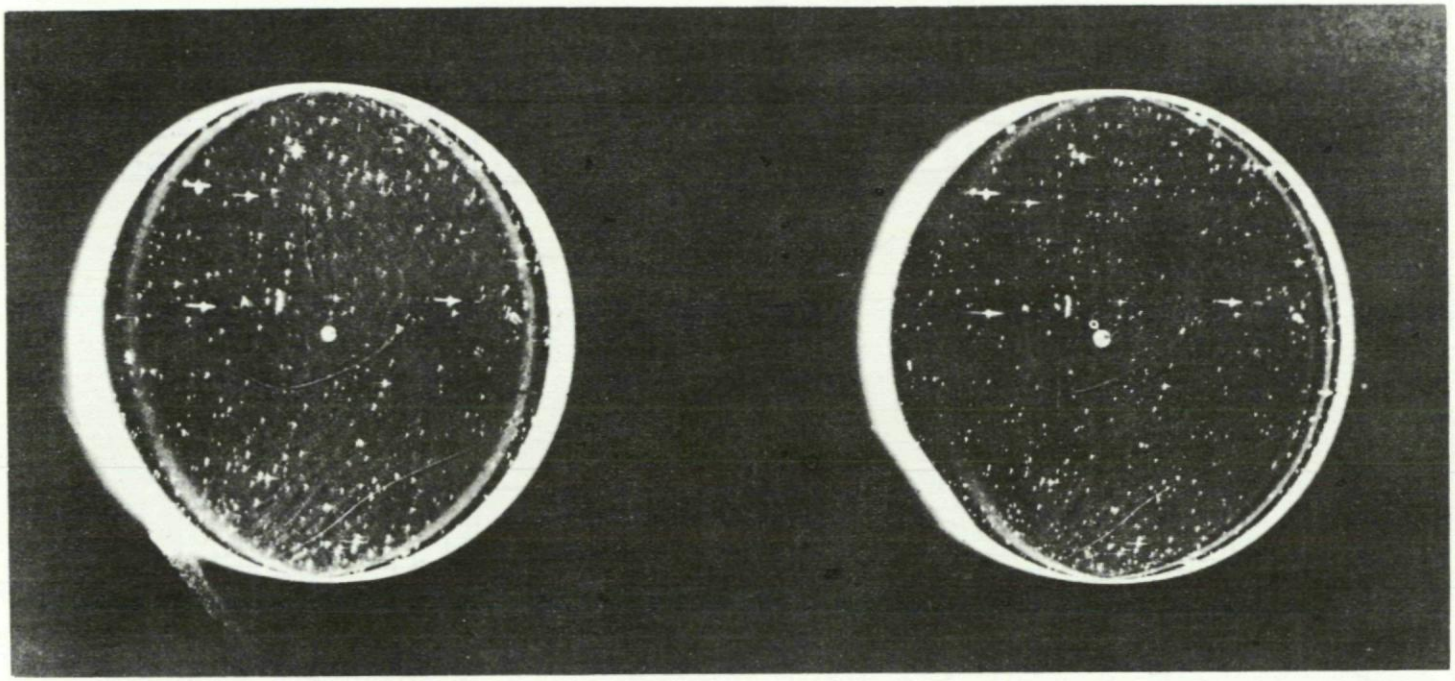

Fig. II-41. A pair of stereoscopic photographs of a glass disc.

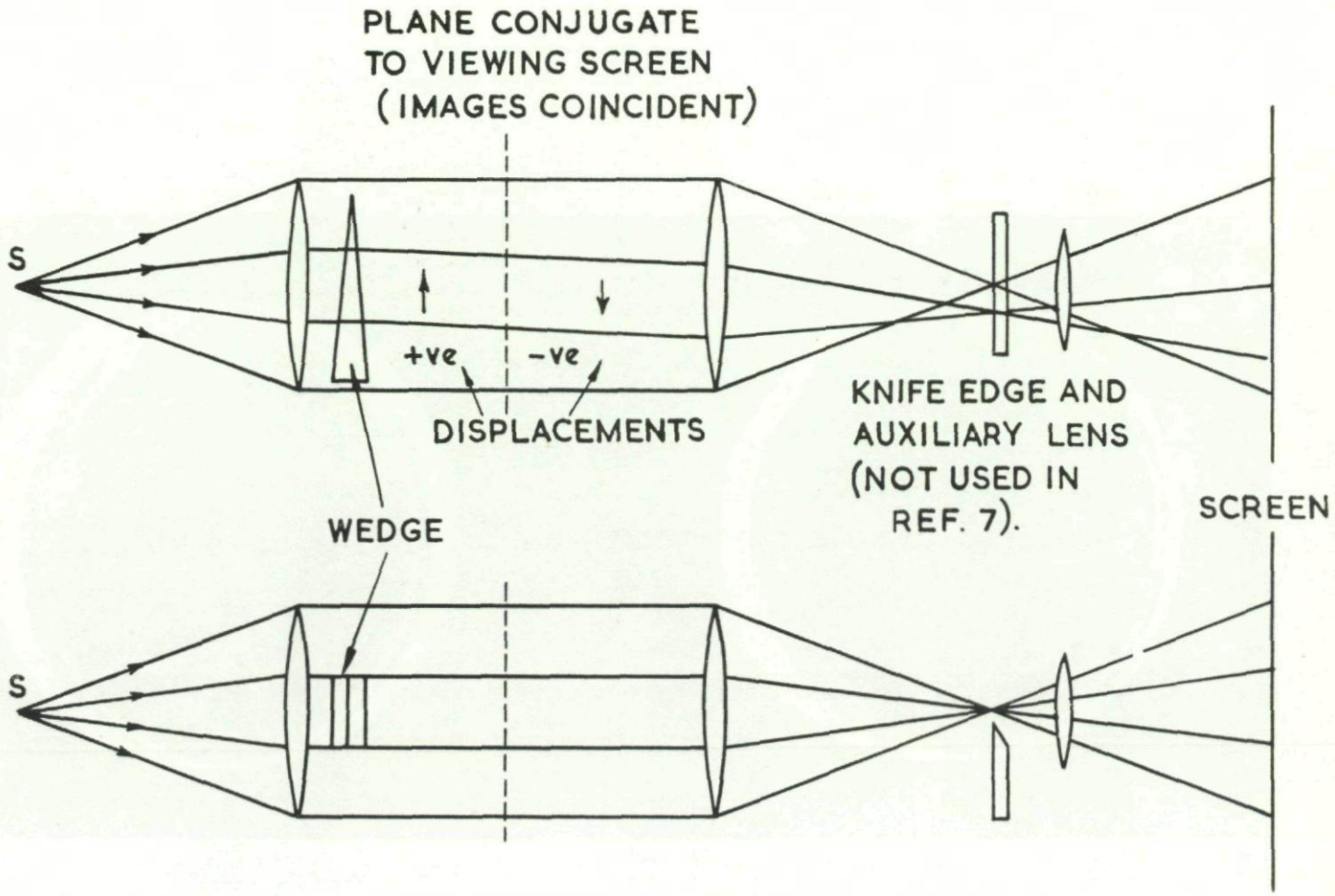

Fig. II-42. A rangefinder wedge arrangement.

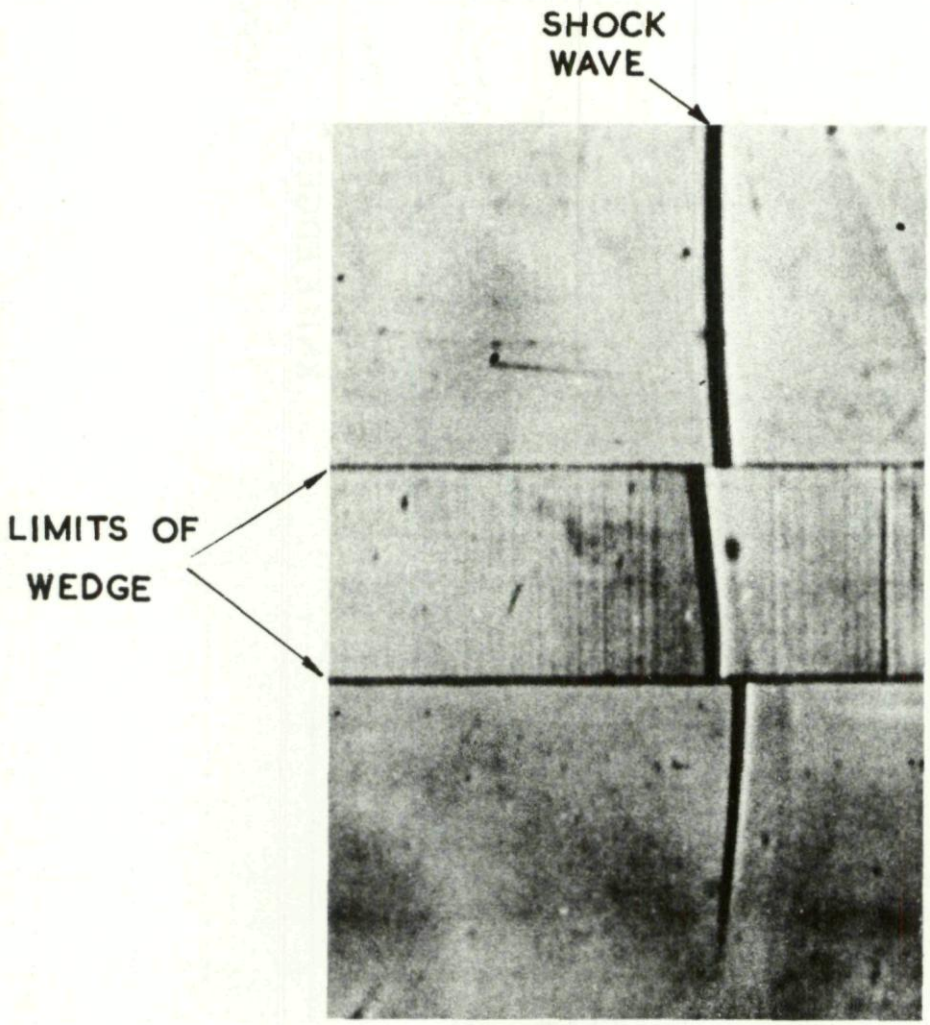

Fig. II-43. Photograph showing the displacement of the image of a shock wave by a range finder wedge.

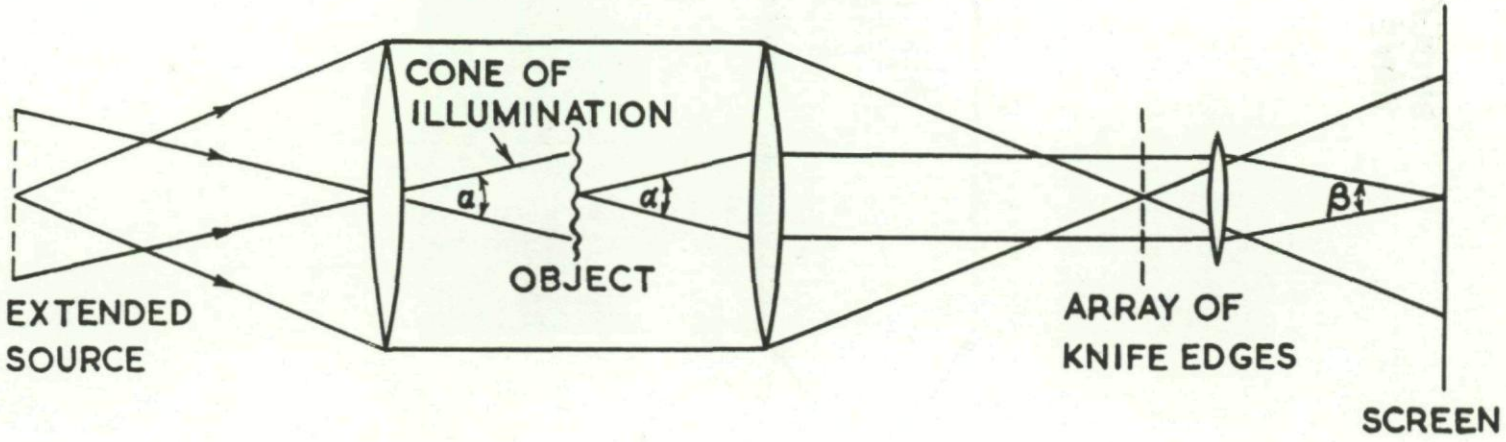

Fig. II-44. A sharp-focus schlieren apparatus.

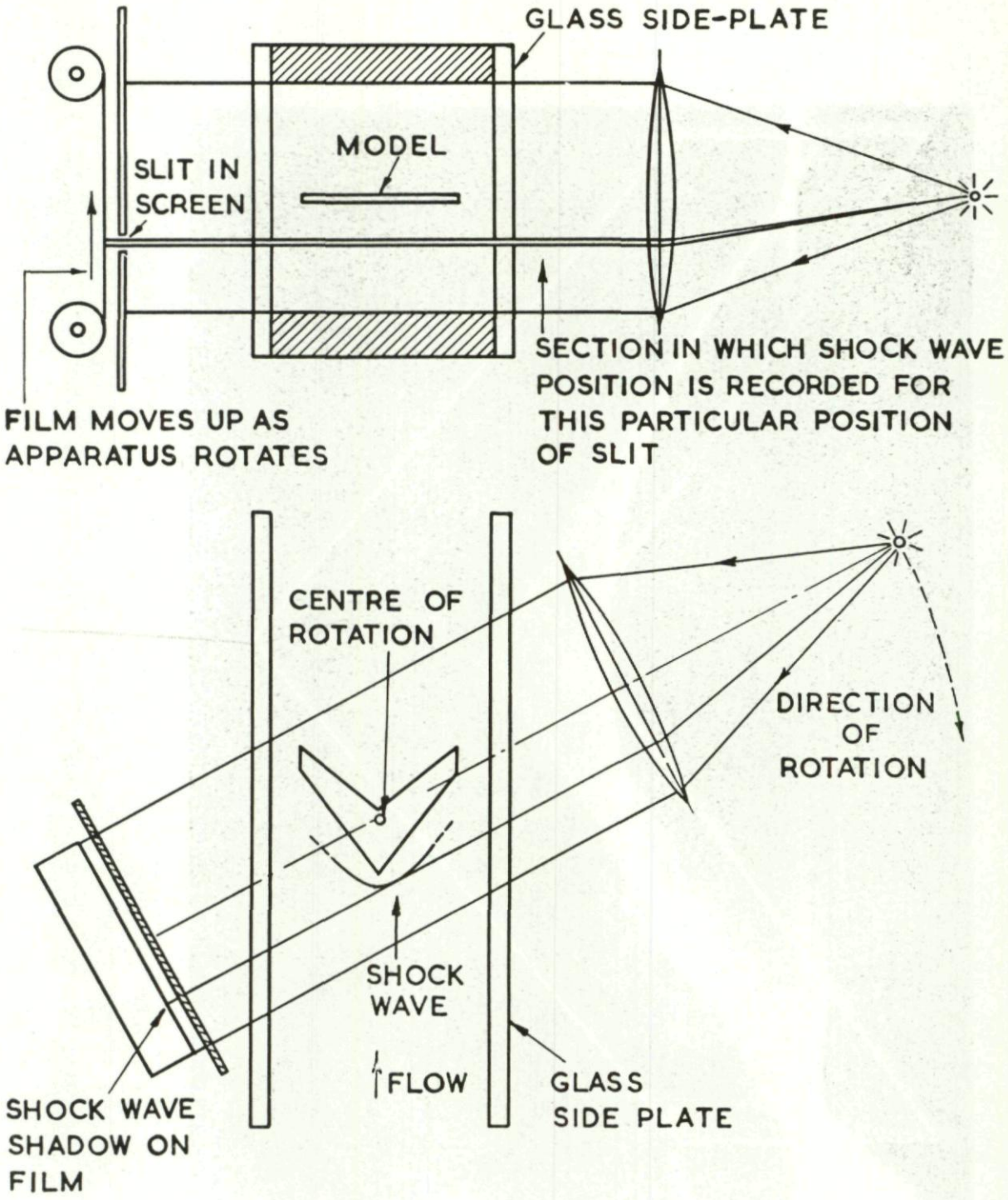

Fig. II-45. The shock wave plotting method.

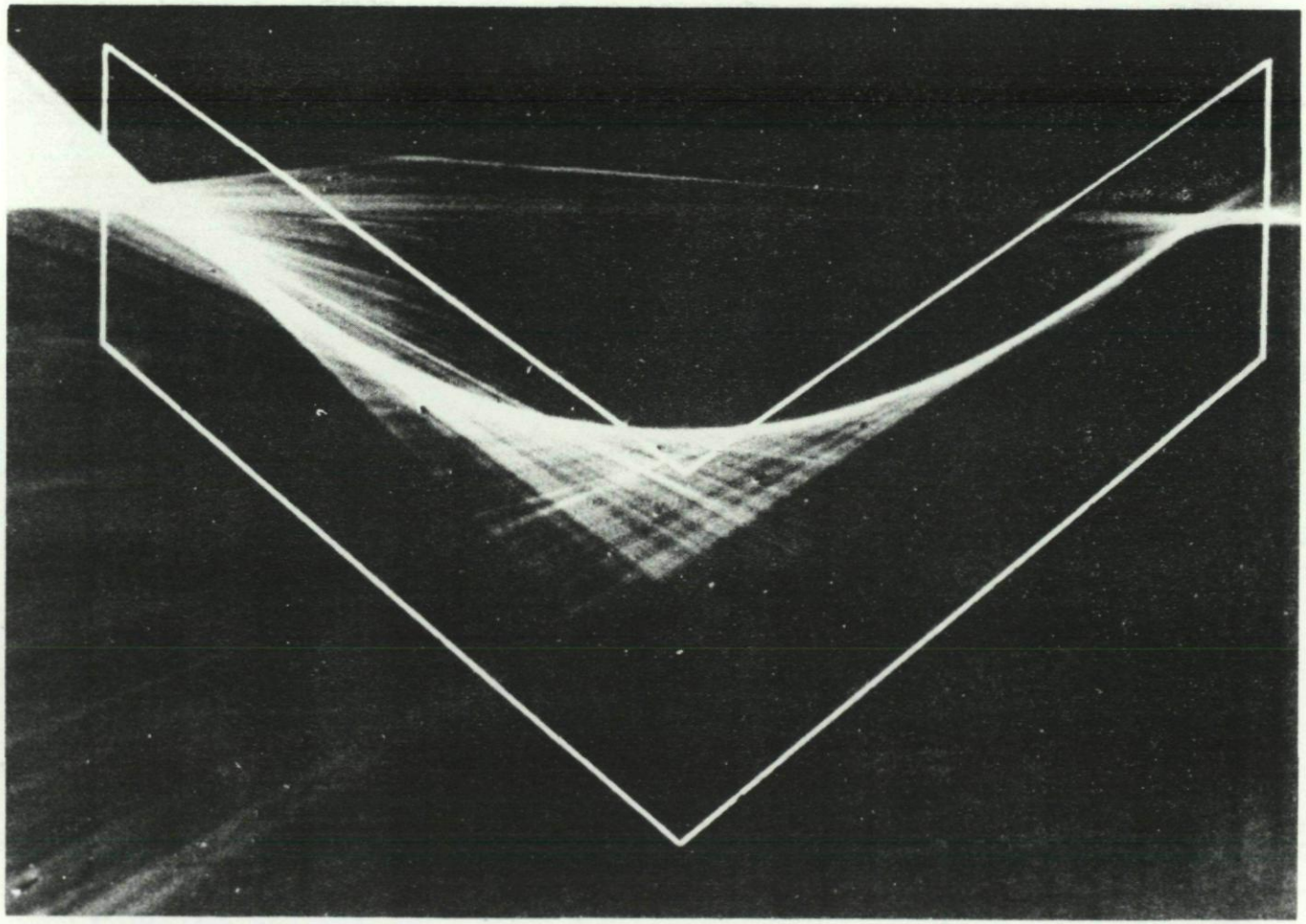

Fig. II-46. Reconstruction of the contour of a shock wave on a swept-back wing from records obtained with a shock wave plotting apparatus.

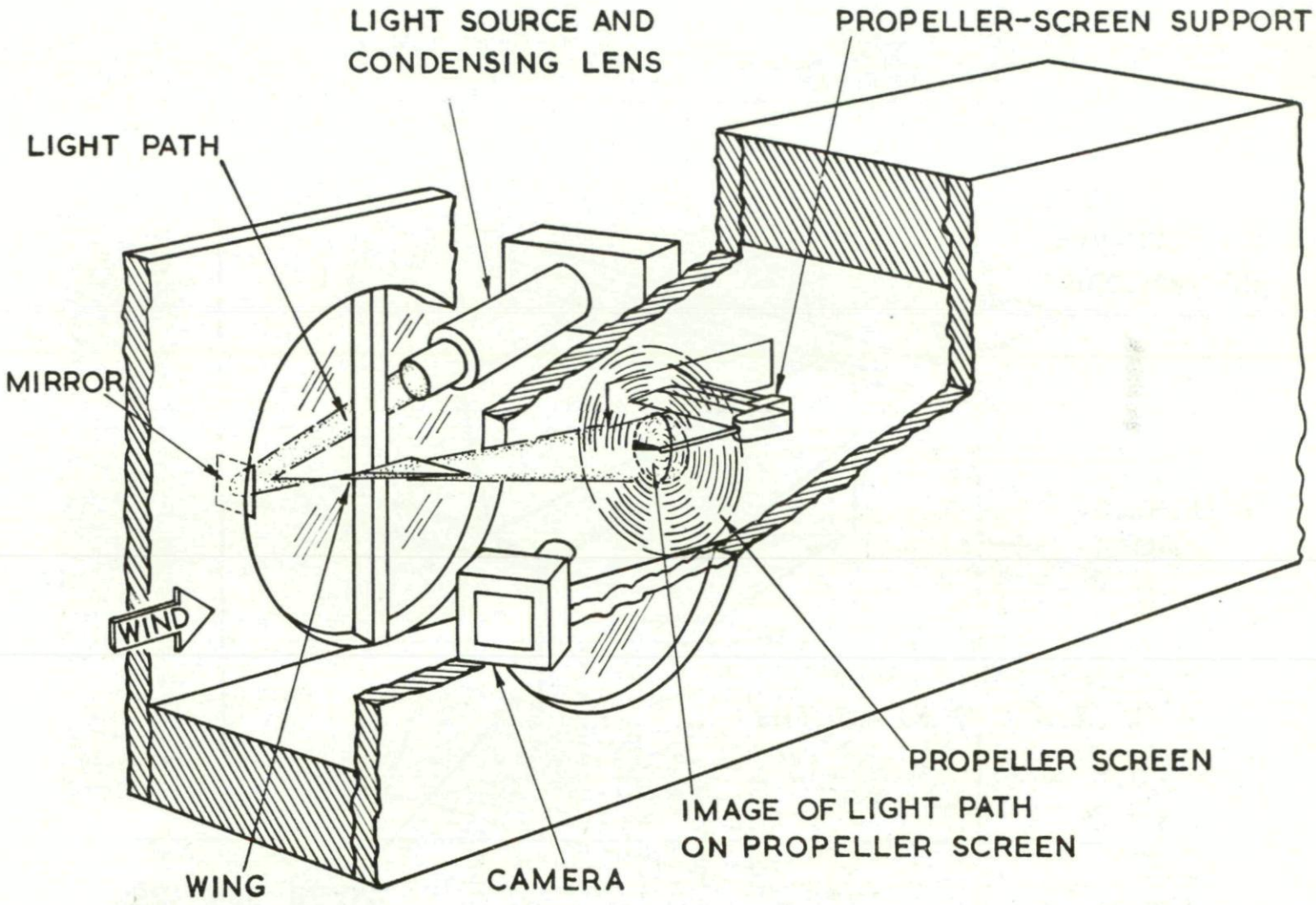

Fig. II-47. Drawing of conical shadowgraph system utilizing a half-span triangular wing and external light source.

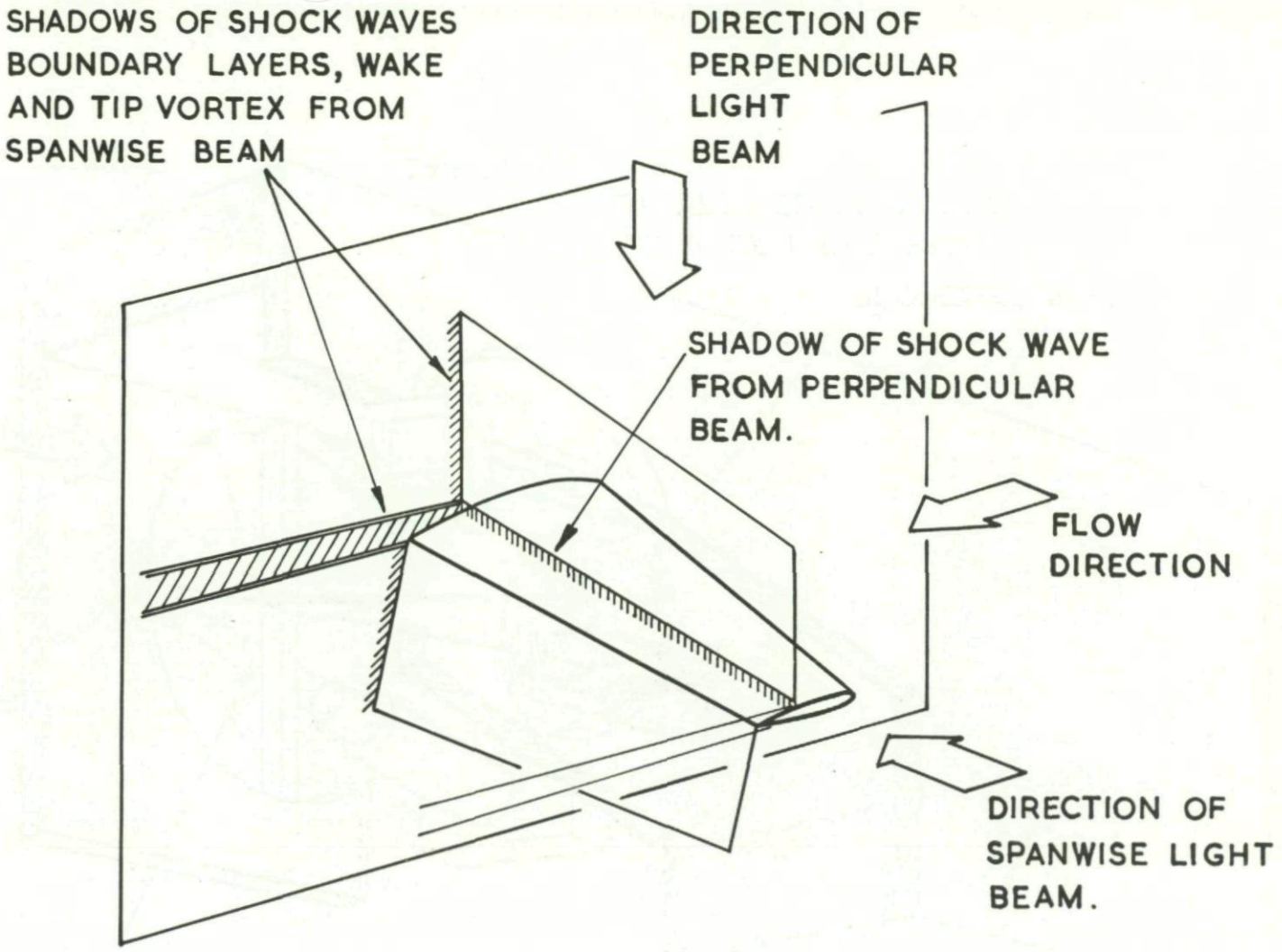

Fig. II-48. Methods for use with a half-span model.

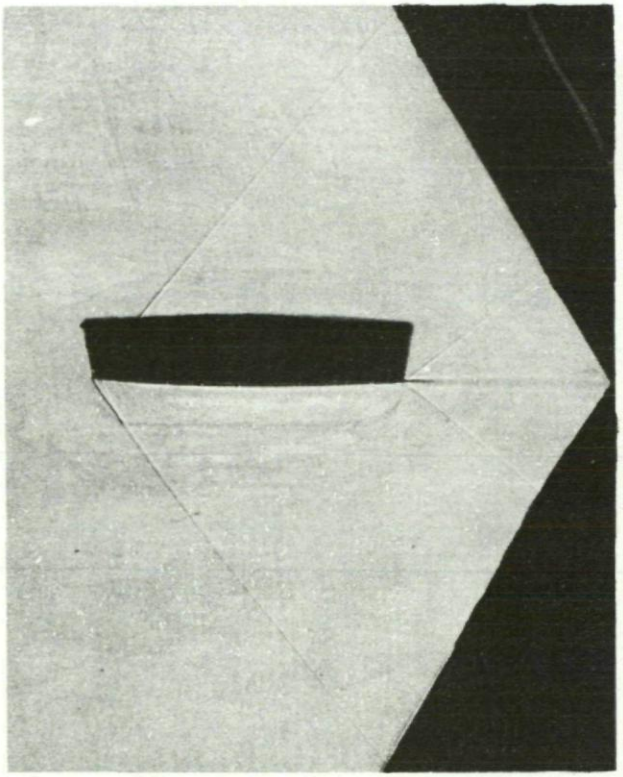

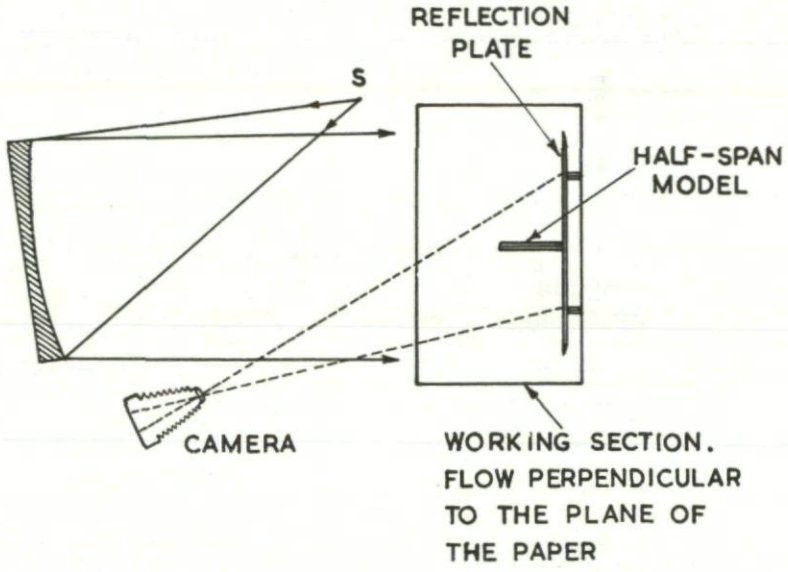

Fig. II-49. The direct shadow image of a half-span model projected on to a reflection plate.

Table I. Some Continuous Light Sources for Schlieren Systems

(a) Tungsten Filament Lamps

Type of Lamp	Voltage	Watts	Source Dimensions (mm)	Average Brightness (stilb)	References
Siemens, CF/13 Projector Lamp	12	48	6 x 1-1/2	Between 1,000 and 2,000 depending on whether the lamp is overrun.	Manufacturer's catalogues and Ref. 101
Ediswan Class F Projector Lamp	6	48	3 x 2-1/2		Manufacturer's catalogues and Ref. 101
Ediswan Class G Exciter Lamp	10	75	6 x 2		Manufacturer's catalogues and Ref. 101
Siemens A1/3 Solid Source Projector Lamp	12	150	6 x 4-1/2		Manufacturer's catalogues and Ref. 101
Siemens A1/4 Solid Source Projector Lamp	12	250	6 x 6		Manufacturer's catalogues and Ref. 101
Philips Class F Ribbon Filament Projector Lamp	6	108	7 x 2		Manufacturer's catalogues and Ref. 100

Table I. Some Continuous Light Sources for Schlieren Systems

(b) Discharge Lamps

Type of Lamp	Watts	Source Dimensions (mm)	Maximum Brightness (stilb)	Remarks	References
Mazda BH-6 Mercury-Vapour Lamp	1,000	25 x 1	30,000	Brightness and burning position similar to MD/H below	Refs. 45, 102, 54, 103, 104
Ames Type "A" Mercury-Vapour Lamp		63 x 1	60,000	Water cooled	Private communication from NACA
Ames Type "B" Mercury-Vapour Lamp			120,000	Water cooled	Private communication from NACA
B.T.H. MD/H Mercury-Vapour Lamp	500 1,000	13 x 1 25 x 1	30,000 30,000	Brightness quoted for water-cooled lamp, it is somewhat lower for forced air cooling. Larger source dimension must be horizontal.	Manufacturer's literature and Refs. 105, 55, 106
B. T. H. ME/D Mercury-Vapour Lamp	250	3.4 to 4.1 x 1.5	20,000	Larger source dimension must be vertical.	Manufacturer's literature and Refs. 105, 106
B. T. H. FA5 Xenon Lamp	150	4.5 to 5.5 x 2.6	600	Larger source dimension must be vertical	Manufacturer's literature and Ref. 107
Western Union Telegraph Co. Zirconium Arc Lamp	2 to 100 300	0.075 to 1.5 dia. 2.9 dia.	10,000 to 4,000 5,200		Manufacturer's literature and Ref. 108

Table II. Some Flash Tube Light Sources for Schlieren Systems

Type of Tube	Continuous Operation (watts)	Flash Voltage V (kv)	Capacity C (μF)	Flash Energy $1/2CV^2$ (watt-sec)	Flash Duration (μ secs)	Source Size (mm)	References
		7.5	Up to 2	Up to 56	1 to 2	30 long	Manufacturer's catalogues
Siemens SF7		8	0.1	3	2 to 3 above 1/2 amplitude of "photographic" effect		Refs. 111, 116
		7.5	2	56	About 1	30 long	Ref. 119
Mullard LSD 2		7.5	2	56	3 above 1/2 amplitude of "photographic" effect		Refs. 99, 111, 116
Krypton Tube		15	0.01	1	0.3 above 1/2 amplitude		Ref. 92
Mazda Type B-H6 Mercury-Vapour Tube	1,000	2	2	4	3	25 x 1	Ref. 102
		2	2	4	6 above 1/10 amplitude		Ref. 104
		2	3	6	10-15		Ref. 120
B. T. H. MD/H Mercury-Vapour Tube	500 or 1,000			4 to 8	4	25 x 1	Information from B.T.H. and Ref. 105
B. T. H. FA5 Xenon Tube	150			Max. 200		4 to 5 x 2.6	Information from B. T. H.
		10	0.25 to 1	12 to 50	3-12		Ref. 107

Table III. Some Spark Light Sources for Schlieren Systems

Type of Spark Gap	Electrode Material	Voltage V (kv)	Capacity C (μF)	Energy $1/2CV^2$ (watt-sec)	Duration* (μ secs)	Method for Measuring Duration	References
Open	-	20	about 0.0003	about 0.06	0.1 "total" duration	Rotating mirror	Ref. 127
Confined (Libessart)	Tungsten and steel	10	0.12	6	1 above 1/2 amplitude	Rotating mirror	Ref. 114
Confined (Libessart)	-	6	0.1	1.8	7.5 above 1/50 amplitude	Rotating mirror	Ref. 124
Open	Aluminium	6	0.5	9	4 above 1/50 amplitude	Rotating mirror	Ref. 124
Open	Aluminium	6	0.12	2.2	0.8 above 1/50 amplitude	Rotating mirror	Ref. 124
Open	-	20	0.01	2	0.1	Photo-electric	Ref. 128
Open	Tungsten	10	0.25	12.5	1 "total" duration, 0.5 "photographic" duration	Photo-electric	Ref. 122
Confined	Tungsten	10	0.25	12.5	3 to 4 "total" duration, 2 "photo-graphic" duration	Photo-electric	Ref. 122
Confined	Tungsten and stainless steel	10	0.024	1.2	1.2 "total" duration 0.18 above 1/2 amplitude	Photo-electric	Ref. 123

Table III. Some Spark Light Sources for Schlieren Systems (Continued)

Type of Spark Gap	Electrode Material	Voltage V (kv)	Capacity C (μF)	Energy $1/2CV^2$ (watt-sec)	Duration* (μ secs)	Method for Measuring Duration	References
Open	Platinum-iridium	6 to 10	0.15	2.7 to 7.5	2 "total" duration 0.2 above 1/2 amplitude	Rotating mirror	Private communication from Svenska Flygmotor AB, Sweden
Open	-	15	0.5	56	1 above 1/2 amplitude	Rotating mirror and photo-electric	Ref. 120
Confined (Libessart)	-	15	0.1	11	3 above 1/2 amplitude		Ref. 120
Confined (Libessart)	-	15	2	225	8 above 1/2 amplitude		Ref. 120
Confined (Sandwich)	Magnesium	15	0.1	11	0.2 above 1/2 amplitude		Ref. 120
Confined (Sandwich)	Magnesium	15	2	225	4 above 1/2 amplitude		Ref. 120
Open	-	3	0.1	0.5	0.2 above 1/2 amplitude	Photo-electric	Ref. 115
Open	Brass	5	0.25	3.1	0.75 above 1/2 amplitude	Photo-electric	Ref. 125
Open	Magnesium	5	0.25	3.1	2 above 1/2 amplitude	Photo-electric	Ref. 125
Confined (Libessart)	Brass	5	0.25	3.1	3 above 1/2 amplitude	Photo-electric	Ref. 125

Confined	Tungsten and tantalum	6	0.005	0.2	0.1	Photo-graphic and photo-electric	Ref. 126
Open	Steel	6	0.2	3.5	0.8 above 1/2 amplitude	Photo-electric	Ref. 129
Open	Steel	13	0.01	0.8	0.3 above 1/2 amplitude	Photo-electric	Ref. 129
Confined	Steel	13	0.01	0.8	0.4 above 1/2 amplitude	Photo-electric	Ref. 129
Confined	Steel	17	0.01	1.5	0.6 above 1/2 amplitude	Photo-electric	Ref. 129
Open	-	10	0.25	12.5	0.5 above 1/2 amplitude	Photo-electric	Ref. 21
Open	Steel	9	0.025 Barium-strontium titanate dielectric	1	0.1 about 1/2 amplitude	Photo-electric	Ref. 129

*Various criteria have been used to define the duration of a spark light source, and because of inadequate data it has not always been possible to quote in the table values for a consistent definition. In many cases the duration is quoted as the time for which the intensity of the light exceeds half the peak value. Even on the basis of this definition, however, it is difficult to compare the performance of different sparks because of differences of the waveform of the emitted light. It is preferable to quote the duration in terms of the print contrast or the contrast sensitivity of the eye (Ref. 124).

Table IV. Exposures Required for Typical Emulsions

Emulsion Speed		Required Exposure (metre candle secs)
B. S. I. or Scheiner	Weston ASA GE	
38°	400	0.001
28°	40	0.01
18°	4	0.1

Table V. Relative Speeds of Certain Emulsions Manufactured in the U.S.A. (From Ref. 137)

Emulsion	Density = 0.1 + fog			Density = 1.0		
	Mercury Arc (2 μ sec)	Flash Tube (20 μ sec)	Tungsten (1/64 sec)	Mercury Arc (2 μ sec)	Flash Tube (20 μ sec)	Tungsten (1/64 sec)
Tri-X Aerial Recon*	100	80	100	47	19	72
Super-XX Panchromatic	100	47	40	12	4	20
Super Panchro Press	98	65	62	17	7	30
Ortho-X	92	65	30	10	5	14
Super Ortho Press	88	71	38	18	10	24
Linagraph Pan*	65	80	62	43	22	100
Blue Brand X-Ray*	63	100	23	100	100	59
Linagraph Ortho*	55	60	28	60	68	60
Tri-X Panchromatic	43	32	32	9	4	15
Photoflure Green Sens.*	38	54	27	39	35	45

*Developed for 5 minutes in Kodak D-19 developer at 68°F; the remainder were developed with the same time and temperature in Kodak DK-50 developer.

Table VI. Relative Speeds of Certain Emulsions Manufactured in the United Kingdom

Emulsion	Density = 0.1 + fog		Average slope = 0.25 (see Fig. II-36)		Average slope = 0.5 (see Fig. II-36)	
	Spark (1/2 μ sec)	Tungsten (1/25 sec)	Spark (1/2 μ sec)	Tungsten (1/25 sec)	Spark (1/2 μ sec)	Tungsten (1/25 sec)
Kodak Experimental Plate No. 68981	56	32	80	32	100	40
Kodak Experimental Plate No. 68979	79	32	100	36	100	40
Kodak Experimental Plate No. V.1015	56	25	71	28	50	32
Kodak P.2000	100	100	100	100	50	100
Kodak Experimental Plate No. V.1002	32	22	28	20	16	20
Ilford Fast Blue Sensitive Plate Type LN	36	11	40	11	25	13
Ilford Zenith Plate	8	6	11	7	8	10
Ilford Orthotone Plate	16	16	20	20	16	20
Ilford H.P.3. Plate	50	40	80	63	32	79
Ilford H.P.S. Plate	63	80	71	63	40	100
Ilford H.P.S. Film	71	80	89	63	40	100
Ilford H.P.3. Film	45	50	40	63	25	63
Ilford Hyperchromatic Film	20	22	25	23	16	25
Kodak Ortho-X Film	20	20	28	23	20	25

All developed for 10 minutes in Ilford ID. 19 or Kodak D. 19. b developer at 68°F.

PART TWO (SECTION III)*
INTERFEROMETER METHODS

The interferometer is useful in the study of gas-flow problems for the same reasons that the shadowgraph and the schlieren apparatus are useful: namely, it permits the flow to be visualized or observed, it provides a photographic record that can be studied at leisure, it permits rapid flow fluctuations to be "stopped," and it does not require the insertion into the flow of pressure probes or other tangible measuring instruments that would disturb the flow. The interferometer has the additional advantage over the other two methods in that it gives quantitative, as well as qualitative, results. Under the proper conditions, the density distribution in the flow around a test object can be determined with an interferometer. Along with this advantage of the interferometer go several disadvantages that will be pointed out later in this section.

(a) The Mach-Zehnder Arrangement

The commonly used type of interferometer is the Mach-Zehnder arrangement originated by L. Mach and Zehnder in the 1890's for use in studying phenomena of airflow and of ballistics. Not much application of the interferometer to problems in airflow was made until after its revival in Germany during World War II (Ref. 152). Since the war, Mach-Zehnder interferometers have been designed, constructed, and put to use in the study of supersonic flow phenomena in several American laboratories and universities (Refs. 153 to 166). The basic arrangement of the Mach-Zehnder interferometer is shown in Fig. III-1. Light from a source is made into a beam of parallel rays by the collimating lens system, L_1. This beam falls onto the splitter plate, S_1, where it is split into two beams. Part of the original beam of light is reflected by the splitter plate, S_1, and part is transmitted by it. The part that is transmitted goes to the mirror, M_1, where it is reflected onto the splitter plate, S_2. A portion of the beam is transmitted by S_2 and is not used. The other portion is reflected by S_2, passes through the lens, L_2, and falls on a screen or a photographic plate, P. The light that was reflected by S_1 likewise goes to a mirror, M_2, from which it is reflected onto the splitter plate, S_2. At S_2 a part of the beam is reflected and is not used, and the remainder is transmitted, passes through the lens, L_2, and falls on the screen or the photographic plate, P. This arrangement fulfills one of the necessary conditions for the interference of the waves in two beams of light: namely, that the two beams originate in the same light source. From a practical standpoint the arrangement also permits the condition to be met that the two beams be widely enough separated in space that the disturbance to be studied can be introduced into one of the beams without disturbing the other. The disturbance, or the "test section," can, of course, be located anywhere in either of the two beams. In the apparatus described in the present paper the test section was situated midway between the mirror, M_2, and the splitter plate, S_2.

(b) Theory of Ideal Fringe Formation

The two beams of light that reach the photographic plate, P, appear to come from separate sources, l_1, and l_2, situated to the left of the mirror, M_2. By proper orientation of the two splitter plates and the two mirrors, the

*For purposes of continuity, Part Two of this paper is also considered Section III.

two beams of light can be made to appear to cross each other, as is shown. If, for the moment, it is assumed that each beam is composed of strictly parallel and monochromatic rays, then the wavefronts can be represented by equally spaced straight lines perpendicular to the direction of propagation, as in Fig. III-2. Here the straight lines represent the "crests" of the waves. Midway between two successive "crests" are the troughs" of the waves. Where two lines intersect, two crests occupy the same position in space, reinforce each other, and cause an increase in the amplitude of vibration and an increase in the intensity of the light. Where a line intersects a point that is midway between two adjacent lines of the other beam, a crest and a trough interfere destructively, and a decrease in the amplitude of motion and in the intensity of the light results. The plate, P, will therefore be crossed by parallel lines of alternately weak and strong intensity. These lines are the interference fringes. They can be oriented in any direction by proper rotation of the two splitter plates and the two mirrors about two axes, one in a plane parallel to that of the paper and one perpendicular to the plane of the paper.

When a disturbance is produced in the air in the test section, changing the speed of the light in the beam that actually traverses this section, then the wavefronts in that beam will be advanced or retarded and therefore shifted with respect to the corresponding wavefronts in the other beam, thereby shifting the positions of the fringes down or up. From the shift in the fringes, the average speed of the light can be calculated; from that the average density of the air can be calculated.

(c) Theory of Practical Fringe Formation

So far it has been assumed that the light is strictly monochromatic and is a beam of parallel rays. But parallel light can be obtained only from a true point source. Because in practice neither monochromatic light nor a point source is used (because, with available means of approximating these to a very high degree, the intensity of the light would be too small), neither condition is actually met. With a point source and a strictly parallel beam, fringes are formed at all points along the two axes, $I_1 - I_1'$ and $I_2 - I_2'$, where the two beams overlap (see Fig. III-1). But in an actual case in which a light source of finite extent is used, the axes $I_1 - I_1'$ and $I_2 - I_2'$ become very numerous. The most distinct fringes are then formed where the various axes intersect. The interferometer should be so adjusted, by rotation of the splitter plates, that this intersection is centered in the test section.

For obtaining the greatest contrast between fringes, it is also necessary that the optical-path length through the interferometer be the same for the two beams. This condition becomes the more important the more the light departs from being monochromatic. For a given setting of the splitter plates and the mirrors, the fringes have a given spacing for each wavelength. The greater the wavelength, the greater the spacing between wavefronts and consequently between fringes. Thus, fringes produced by a large number of wavelengths coincide only at one point, the center of the band of fringes. On either side of this center the fringes get out of step with each other and the contrast between light and dark becomes less and less. The optical paths should be so adjusted that the center of the band of fringes, where the contrast is greatest, appears to be located in the test section.

(d) Design of the Interferometer

Because differences in the optical path lengths for the two light beams in an interferometer, as evidenced by fringe shifts, can easily be detected when they are of the order of only one-tenth of a wavelength of light, or 5×10^{-6} cm, the interferometer

is a very sensitive instrument and, as such, is subject to being thrown out of adjustment by temperature changes and by mechanical vibrations.

There are two philosophies with regard to the desirability of trying so to design an interferometer that the effects of these disturbances on the adjustment will be minimized. Some of the universities appear to feel that it is not particularly necessary to go to great lengths to design an instrument that will stay in adjustment day after day, but that valuable experience is gained by the students in readjusting the interferometer each time they use it. On the other hand, in government laboratories where full time is spent on research, the point of view is taken that time spent in readjusting an interferometer is time wasted, therefore efforts are made at the design stage to incorporate stability of adjustment against the effects of changes in the ambient temperature and of ever-present vibrations.

The writer has participated in the design and use of an interferometer (Ref. 163) that has stayed in adjustment for more than 12 months, during which time no readjustment of any kind was made despite variations in temperature and location near several sources of rather severe vibration. In this instrument, shown in Fig. III-3, the base on which the mirrors and the splitter plates are mounted is a heavy one-piece iron casting in the form of a four-leaf clover. (A rigid base is of prime importance in achieving stability.) The base is therefore symmetrical, has a low coefficient of thermal expansion, and has a large heat capacity. The base is supported at its center in a vertical plane by a single mount that is attached to a framework of steel welded to a steel table. Although isolating the instrument from vibrations by mounting from springs had been recommended, it was found that the instrument could be kept in adjustment when the table on which it was mounted was merely set on the floor. This arrangement also obviated the difficulty, which occurred when the interferometer was spring mounted, of keeping the beam of light oriented parallel to the surface of a two-dimensional model.

Each of the two splitter plates and two mirrors must be rotatable about two mutually perpendicular axes. Each rotation can be effected by turning two opposed screws, and the adjustment can be maintained by a very tight adjustment of the screws. The customary method of providing an adjustment of the difference in optical path length of the two light beams is to provide for the translation, in a direction perpendicular to the plane of the mirror, of the entire housing of mirror, M_1 or M_2. An additional adjustment that is usually provided for fine adjustment is that afforded by inserting a compensating plate in each beam and by making one of these plates rotatable in such a way that the path length in glass can be changed by rotating the plate.

The front surface of each of the two mirrors should be polished flat within about one-tenth wavelength of light. Probably the best coating for the mirrors is aluminum. The two splitter plates, the two compensating plates, and the two test-section windows should be free of striae and should be polished flat on both sides to a tolerance of about one-tenth wavelength. The two sides of each plate should be parallel to each other within about 2 seconds of arc. One side of each splitter plate should be coated with a semi-reflecting material. Some years ago the conventional coating was a thin partially reflecting and partially transparent layer of silver. A metallic coating has the disadvantage that a considerable portion of the light is absorbed. Available today are dielectric materials (for example, zinc

sulphide) that are transparent (do not absorb) and that form satisfactory beam splitters when deposited on glass in the proper thickness.

(e) Design of the Light Source

A satisfactory light source for application of interferometry to the study of flow phenomena must provide nearly monochromatic light in a nearly parallel beam of sufficient intensity and of sufficiently short duration. A satisfactory compromise among these four contradictory requirements is not always easy. If the region to be studied is in a free or open supersonic jet which inherently contains high frequency vibrations, then exposure times of only a few microseconds must be used. With a completely enclosed supersonic test section somewhat longer times can be used. Because mechanical shutters are not fast enough, the short exposure times are obtained by an electrical discharge of a capacitance as a spark or an arc. The energy in the discharge, $CV^2/2$, must be sufficient to give a good exposure on the photographic negative, but the capacitance, C, must not be too large since the time duration will be too great, nor must the voltage, V, be too large since multiple ionization will occur and the light will not be sufficiently close to being monochromatic.

One combination that is frequently used is a capacitance of about 2 microfarads charged to 2000 volts and discharged through a General Electric High Pressure Mercury-Vapor Capillary Arc BH-6. The light can be made sufficiently monochromatic to give about 200 usable fringes by insertion of a simple filter (e.g., Kodak Wratten No. 77A, or Corning Nos. 5120 and 3484).

Another satisfactory light source uses a high-voltage capacitance of 2 microfarads charged to about 16,000 volts and discharged in air between magnesium electrodes. With such a light source the writer obtains effective time durations of about 3 microseconds. Because of the high voltage, the light is far from monochromatic and a simple filter is not sufficient. A monochromator, which can be constructed from a low-cost prism spectrometer, can be used to isolate the region of the green triplet of magnesium or the blue line at 4481 angstroms.

The width of the exit slit of the monochromator should be set to pass a band of about 30 angstroms and the height of the slit should be so adjusted that it subtends an angle of about 9 minutes at a distance equal to the focal length of the concave mirror or the lens on which the light next falls. These adjustments result in a beam of light that is sufficiently monochromatic and parallel to give about 200 usable fringes. When the BH-6 mercury-vapor lamp is used, a mask containing a small hole should be used to reduce the size of the light source. The BH-6 lamp has the advantage that in addition to giving a flash of short duration it can also be burned continuously and is thus useful for adjusting the interferometer.

With either of the above light sources, it will generally be found that the photographic negative must be rather small (about 20 square cm) in order to obtain sufficient exposure.

(f) Adjustment of the Interferometer

When the interferometer is first set up, a number of adjustments must be made in order to obtain fringes and to orient them properly.

The first step in the initial adjustment is to make the reflecting surfaces of the two splitter plates and the two mirrors nearly parallel. This is done by making

the two mirrors as nearly parallel as possible by eye, and then leaving them there, because it is possible to produce all fringe orientations by adjustment of the splitter plates alone (except for adjustment for white-light fringes, which is made by rotating a compensating plate or by translating a mirror). Then the plates are set nearly parallel to the mirrors by simple inspection.

A small light source is placed 15 feet or more away from the interferometer, and the light is directed at plate S_1. Two sets of cross hairs are set up, one near the light source and the other near plate S_1. Two screens are set up on the opposite side of the interferometer in such positions that a lens placed after plate S_2 focuses one set of cross hairs on one screen and the other set on the other screen. Each set of cross hairs produces two images on one screen. One image is produced by the light traversing one path of the interferometer and the other image by the light that goes through the other path.

The splitter plates are then so adjusted that the two images of one set of cross hairs coincide, or merge into a single image. This procedure is repeated for the other set of cross hairs. As the adjustments for the two sets of images are not independent, they must be continued until the images of both sets of cross hairs appear to be single.

The light source is now replaced by a monochromatic light source. This light source should be sufficiently close to being monochromatic that many hundreds of fringes can be produced. The reason for this is that at this stage of the adjustment the two optical paths through the interferometer are likely to be considerably different. If such is the case, and a light source that would give relatively few fringes is used, then the fringes cannot be found because their apparent location would be above or below the test section and out of the light beam.

A satisfactory monochromatic light source is a sodium-arc lamp, or a General Electric BH-6 mercury lamp operated at an under-voltage of about 60 volts. The lens in the beam emerging from the interferometer is replaced by a telescope placed some 15 feet beyond the interferometer. Interference fringes generally can then be brought into focus by adjusting the telescope. If they cannot be found, either the elimination of double cross hair images has not been sufficiently achieved or the difference in optical-path length is too great. Inspection of each cross hair image (on the screens) with a magnifying glass will usually reveal that the elimination of doubling has not been completely effected.

Once the fringes have been located, a monochromatic light source is set up to give a parallel beam. If the BH-6 lamp has been chosen as the permanent source, it is set up with lens (or mirror) and filter. If the magnesium spark-monochromator light source has been chosen as the permanent source, the spark is temporarily replaced by a BH-6 lamp placed at the entrance to the monochromator, the slits are narrowed to about 0.3 millimeter and the monochromator is set to pass the 5460-angstrom line.

The first adjustment is to tilt the fringes into the desired orientation, say a horizontal position, by rotating a splitter plate. The next two adjustments are to move the fringes into the test section and to adjust them to the desired width, or spacing. (For the sake of clarity, these adjustments are described here as though the test section were located between the mirror, M_2, and the splitter plate, S_2. The test section can, of course,

be located anywhere in either of the two beams.) These two adjustments are made simultaneously by alternate rotation of the two splitter plates and by observation through the telescope of the location and the spacing of the fringes.

This adjustment is not difficult. For example, suppose that the fringes are located between S_2 and the telescope and are too narrow. The first step is to determine which of the two beams goes through which path in the interferometer. This is determined by focusing the telescope on the light source and blocking off one of the paths. It is desired to have the beams cross in the test section, midway between M_2 and S_2. If the slope of the beam that passes through the test section is positive with respect to the slope of the other beam, as shown in Fig. III-1, then plate S_2 is rotated counterclockwise to bring the fringes back almost to the test section. If this adjustment makes the fringes too broad, then S_1 is rotated clockwise to move the fringes the rest of the way to the test section and at the same time to narrow them.

The next adjustment is to make the two optical-path lengths through the interferometer equal. With the fringes in focus in or near the test section, the slits are opened until the fringes visible in the telescope become faint. By translating a mirror, the fringes are caused to appear to pass vertically through the test section until they disappear. The position of the mirror is noted, and the mirror is moved in the opposite direction until the fringes with the greatest contrast have passed through the test section and the fringes again disappear. The mirror is then positioned halfway between the two positions where the fringes disappeared.

The interferometer is then nearly in adjustment for white-light fringes. A source of white light is placed just ahead of the first splitter plate. (A convenient point source is the Western Union Laboratories Concentrated-Arc Lamp.) Then a slight rotation of a compensating plate or a slight translation of a mirror will bring the white-light fringes into view. If the disturbance of which an interferogram is to be taken contains a region in which there is a density gradient of considerable magnitude, such as a boundary layer, the fringes will be crowded together in that region, and distinguishing individual fringes may be difficult. It is advisable to place the white-light fringes in such a position that they will move, when the disturbance is produced, into the region of density gradient and thereby provide the fringes of greatest contrast in that region.

The final adjustment is to remove what might be called "twist" from the two beams. For horizontal fringes the two splitter plates have been rotated with respect to each other about horizontal axes and the two images of the light source, as seen in the telescope, lie one above the other. It may be, however, that the two beams do not lie in the same vertical plane. If they do not, sharp fringes can be observed only when the source is a line of zero width (and is also vertical, for horizontal fringes).

Because it is necessary that the light source have a finite width in order to give enough light, the fringes will appear considerably blurred unless the rotation of the plates is corrected in order that the two beams lie in the same vertical plane. To check this, the telescope is removed and the eye placed in the emergent beam some distance away from the interferometer. The fringes may then appear to be cocked at an angle to the horizontal. If so, then as one walks toward the interferometer the fringes will slowly rotate back to the horizontal

position which they had when viewed with the telescope focused on the test section. By alternately rotating the two plates about their nonhorizontal axes, the two beams can be swung until they both lie in the same vertical plane and the fringes appear horizontal when viewed from both a close and a far position.

When all these adjustments have been made, the following conditions prevail:

(1) The fringes are centered in the test section.

(2) The fringes have the desired orientation.

(3) The fringes have the desired spacing.

(4) The white-light fringes are in correct location in a cross section through the test section.

(5) The two beams lie in the same vertical plane.

Another adjustment of the interferometer that is useful for observing two-dimensional flow fields is the single-fringe adjustment. To obtain this adjustment, the above-described adjustments are made, and then the splitter plates are further adjusted to make the fringes broader and broader until only a single fringe covers the entire field of view. Then, when a disturbance is introduced into the test section, more fringes appear, each one of which is a contour of constant fringe shift.

This adjustment of the interferometer has the advantage that evaluation of the interferogram (determination of air density throughout the field of view) is very easy. But it has two disadvantages. First, because the sensitivity of the interferometer is greater the broader the fringes, the adjustment is difficult to achieve unless the interferometer is especially well designed and constructed. Second, the adjustment is difficult to maintain, consequently one cannot always be sure that the interferometer was not vibrated out of the single-fringe adjustment at the instant at which the interferogram was taken.

(g) Evaluation of Interferograms

The evaluation of an interferogram to obtain from it the variation of density in the flow is a process that requires some care and labor. The methods are different for the three kinds of interferograms: interferograms of two-dimensional flow, interferograms of two-dimensional flow taken with the single-fringe adjustment, and interferograms of axially symmetric flow. The three methods are discussed here.

The production of fringe shifts is illustrated in Fig. III-4. Consider that when no disturbance is present both beams of light travel in air of density, ρ, and refractive index, n. The value of the refractive index is a function of the density of the air, for a given wavelength of light, according to the Lorentz-Lorenz relation

$$\frac{n^2 - 1}{n^2 + 2} \alpha \rho$$

or

$$\frac{n + 1}{n^2 + 2} (n - 1) \alpha \rho .$$

Because n is very nearly equal to unity, the equation can be written

$$n - 1 = k\rho \tag{32}$$

where the constant of proportionality, k, is the Gladstone-Dale constant.

Then

$$\frac{n-1}{\rho} = \frac{n'-1}{\rho'}$$

or

$$n' - n = (n-1)\left(\frac{\rho'}{\rho} - 1\right). \tag{33}$$

Now let a portion of one of the two beams pass, for the distance L, through air of a different density, ρ', and index, n', and let values of density and index be constant along the length, L, but let them be functions of the vertical coordinate, y. Then the wavefronts will be distorted, as in Fig. III-4.

The amount of retardation, X, at any point is a function of the velocity of light at that point. The time for passage of light of velocity, V', through a distance, L, is L/V'. In that same time, light of velocity, V, will pass through a distance L+X. Therefore,

$$\frac{L}{V'} = \frac{L+X}{V}.$$

But since

$$\frac{V}{V'} = \frac{\lambda}{\lambda'}$$

where λ's are wavelengths, then

$$\frac{L}{\lambda'} = \frac{L+X}{\lambda}$$

or

$$X = \frac{L}{\lambda'}(\lambda - \lambda').$$

But, since

$$n = \frac{V_0}{V} = \frac{\lambda_0}{\lambda}$$

where the subscript, o, refers to vacuum, and since

$$n' = \frac{\lambda_0}{\lambda'}$$

therefore

$$X = \frac{L}{n}(n' - n)$$

$$= L\frac{\lambda}{\lambda_0}(n' - n).$$

By similar triangles in Fig. III-4 it follows that

$$\frac{Y}{b} = \frac{X}{\lambda} = \frac{L}{\lambda_0}(n' - n)$$

where b is the fringe spacing.

Then by use of Eq. (33),

$$\frac{Y}{b} = \frac{L}{\lambda_0}(n-1)\left(\frac{\rho'}{\rho} - 1\right)$$

or

$$\frac{\rho'}{\rho} = \frac{Y}{b}\left(\frac{\lambda_0}{L}\frac{1}{n-1}\right) + 1$$

or, by use of Eq. (32),

$$\frac{\rho'}{\rho} = \frac{Y}{b}\left(\frac{\lambda_0}{Lk\rho}\right) + 1.$$

If Y/b, the fringe shift in terms of fringe width, is designated by S(y) and the quantity in parentheses is designated by C, then

$$\frac{\rho'}{\rho} = CS(y) + 1. \tag{34}$$

In this equation ρ'/ρ is the density ratio between some position in the disturbance and the undisturbed air.

The easiest method of finding the fringe shifts, S(y) of Eq. (34), at various points throughout the field for two-dimensional flow is to superpose on the interferogram an interferogram (on transparent film) taken with no disturbance or no flow in the test section. This superposition results in the appearance of lines throughout the field, as illustrated in Fig. III-5. These lines are contours of constant fringe shift, S(y), and the value of S(y) varies by unity on adjacent contours. Therefore, the density variation over the flow field can easily be obtained if the density can be determined for one of the contours. This determination can be made by a judiciously placed static orifice in the model or in the glass window of the test section.

On interferograms of two-dimensional flow taken with the single-fringe adjustment, the fringes themselves are contours of constant fringe shift and the value of the shift varies by unity on adjacent fringes. Here again it is necessary that the fringe shift or the density be determined for one of the contours. The usual method is to calculate the fringe shift at a static orifice from the pressure measured there.

For axially symmetric flow an entirely different method of evaluation of interferograms must be used. In two-dimensional flow a ray of light that traverses the flow experiences constant air density along its path. In axially symmetric flow, however, the density is a function of the radial distance from the axis of symmetry. Consequently, a ray of light through the test section experiences a constantly changing density. The fringe shift at any point on an interferogram is therefore the summation of the shifts produced in each element of path of the ray of light.

The method of analysis is, in simple terms, to divide a cross section of the flow into zones of equal width that are concentric about the axis of symmetry, to find the fringe shift for a ray that traversed only the outermost zone, and from that and the known path length through the zone, to find the density in that zone. Then, for the ray that traversed the outermost zone and the next adjacent zone, the fringe shift must be measured and the density in the next to the outermost zone must be calculated. And so on for all of the zones. The same procedure must be repeated at all cross sections for which results are desired. The process is rather tedious and requires considerable computation, but it has been systematized and tables of numerical coefficients for use in the computations are available (Ref. 164).

(h) The Diffraction-Grating Interferometer

There is a new interferometer that is less complicated, less costly, and less difficult to adjust than the Mach-Zehnder arrangement. This is the diffraction-grating interferometer that was developed in 1950 (Refs. 167 and 168).

This new interferometer is somewhat similar in arrangement to the grid-screen, or Ronchi, schlieren system, but works on an entirely different principle. The light is divided into two beams by a diffraction grating and then recombined by another diffraction grating to produce interference (Fig. III-6). Light from the source, S, is focussed by the lens, L_1, onto the plane diffraction grating, G_1. One-half of the beam, however, is eliminated by a stop. Only the zero-order and the first-order spectra are used, and the angle, β, and the spacing of the lines on the grating should be so chosen that the light in each of these

two orders will essentially fill half of the lens (or concave mirror), L_2. Each of the two beams is focussed by L_2 into an essentially parallel beam and then is brought to a focus at the second grating, G_2, by the lens (or mirror) L_3. After diffraction at the second grating, the first order of the incident zero order beam is used and the zero order of the incident first order beam is used. These two beams are superposed, and other orders are eliminated by a stop. These two beams have received essentially identical optical treatment and are therefore able to interfere with each other. Fringes therefore can be formed.

The apparent source for the two final beams is the image of the first grating. When the second grating is placed at the image of the first grating, there is in effect a single source for the two final beams, and the single-fringe adjustment is obtained. When, however, the second grating is moved slightly away from the image of the first grating, the first-zero order beam still appears to originate from the same source, but the zero-first order beam appears to come from a virtual source that is displaced from the real source, as shown in Fig. III-7. The two beams therefore cross at a small angle and form fringes whose spacing depends on the angle and thus on the displacement of the second grating from the image of the first.

This kind of interferometer is relatively uncomplicated in construction. A conventional twin-mirror schlieren system can be rather easily converted into an interferometer. The adjustment is relatively easy because both beams are handled by the same optical elements. In contrast to the Mach-Zehnder arrangement, however, the two beams are not widely separated. The disturbance to be studied must occur in only one of the beams, and the other beam, because of the proximity of the two, must generally also go through the test section, but through a region in which the density is uniform.

(i) Examples of Application of Interferometry to Specific Problems

We consider a vertical cross section through a horizontal flow. If the density of the air at that cross section is a function of only one coordinate, then it is possible to obtain values of air density from an interferogram. For the flows that have been called "two-dimensional" in this paper, the density at any cross section depends only on the vertical location and not on the depth into the flow. In other words, a horizontal ray of light through the flow experiences the same density all along its path.

For axially-symmetric flows, the density at a given cross section again depends on only one coordinate, the radial distance from the axis of symmetry. In this case a ray of light experiences a variable density along its path but, because of the axial symmetry, it is possible to obtain the value of the density at any point.

For other flows, for which the density at any point of a cross section depends on two coordinates, interferograms can not be quantitatively interpreted. The application of the interferometer is therefore limited to study of the flow about two-dimensional models and axially-symmetric models and the latter must be at zero incidence with respect to the free stream.

Another limitation of the interferometer is due to the refraction of light. In a region of large density gradient a ray of light is

refracted, or bent, and its path is not close enough to being a straight line for it to experience constant density along its path. Consequently, interferograms do not give correct density variations near stagnation regions nor the correct density profiles through boundary layers. Some work has been done to calculate the corrections for the refraction that occurs in boundary layers, but the corrections are rather large and the results are not as accurate as is desirable.

Despite its various limitations, the interferometer is a useful instrument for quantitative measurement in aerodynamic research. The following examples illustrate the kinds of problems for which the interferometer is suited.

When an airfoil with a sharp or a thin leading edge is at an angle of attack and the subsonic Mach number of the free stream is increased, a change takes place in the kind of flow pattern that occurs in the vicinity of the leading edge. The two kinds of flow pattern are shown in Figs. III-8 and III-9, which show interferograms of the flow and Mach number distributions in the flow field obtained from analysis of the interferograms. These results, taken from Ref. 166, illustrate the applicability of the interferometer in the quantitative determination and examination of the flow field around a two-dimensional body at transonic speeds.

Another example, taken from Ref. 165, is shown in Fig. III-10. The model here is half of a circular-arc airfoil mounted on a flat plate (to increase the Reynolds number). In this example the interferogram permits the determination of the detailed structure of the imbedded supersonic zone on the airfoil, of the conditions along and near the base of the shock wave where it interacts with the boundary layer, and of the pressure distribution on the surface of the airfoil. This example also illustrates the fact that the interferometer enables the pressure distribution to be measured on a model that is too small to be instrumented with many pressure orifices.

The use of an interferometer to study axially symmetric flows is illustrated by Figs. III-11 and III-12, which were taken from Ref. 164 and which show an interferogram of the flow about a sphere and the contours of constant density obtained by evaluation of the interferogram.

There are other examples of the application of the interferometer method, such as Refs. 153 and 160, which describe investigations of the flow around various axially-symmetric models; Ref. 154, which is a study of a supersonic jet; and Ref. 163, a study of the mixing zone of a supersonic jet. Boundary layers are investigated in Refs. 155 and 162. Studies of various kinds in shock tubes are reported in Refs. 156 and 157. Wind tunnel flows around two-dimensional models are discussed in Refs. 158 and 168. Application of an interferometer to the study of projectiles in free flight is described in Ref. 161.

REFERENCES

152. Zobel, Th., "Entwicklung und Bau eines Interferenzgerätes zur optischen Messung von Dichtefeldern," Deutsche Luftfahrtforschung, Forschungsbericht Nr. 1008. (Translation available as NACA TM 1184, 1947.)

153. Ladenburg, R., Winckler, J., and Van Voorhis, C. C., "Interferometric Studies of Faster than Sound Phenomena, Part I, The Gas Flow around Various Objects in a Free, Homogeneous, Supersonic Air Stream," Physical Review, Vol. 73, No. 11, pp. 1359-1377, 1 June 1948.

154. Ladenburg, R., Van Voorhis, C. C., and Winckler, J., "Interferometric Studies of Faster than Sound Phenomena, Part II, Analysis of Supersonic Air Jets," Physical Review, Vo. 76, No. 5, pp. 662-677, 1 September 1949.

155. Bershader, Daniel, "An Interferometric Study of Supersonic Channel Flow," Review of Scientific Instruments, Vol. 20, No. 4, pp. 260-275, April, 1949.

156. Bleakney, W., and Taub, A. H., "Interaction of Shock Waves," Reviews of Modern Physics, Vol. 21, No. 4, pp. 584-605, October 1949.

157. Griffith, Wayland, "Shock-Tube Studies of Transonic Flow over Wedge Profiles," Journal of the Aeronautical Sciences, Vol. 19, No. 4, pp. 249-257, April 1952.

158. Bryson, Arthur Earl, Jr., "An Experimental Investigation of Transonic Flow Past Two-Dimensional Wedge and Circular-Arc Sections Using a Mach-Zehnder Interferometer," NACA TN 2560, 1951.

159. Ashkenas, Harry I., and Bryson, Arthur E., "Design and Performance of a Simple Interferometer for Wind-Tunnel Measurements," Journal of the Aeronautical Sciences, Vol. 18, No. 2, pp. 82-90, February 1951.

160. Cole, J. D., Solomon, G. E., and Willmarth, W. W., "Transonic Flow Past Simple Bodies," Journal of the Aeronautical Sciences, Vol. 20, No. 9, pp. 627-634, September 1953.

161. Bennett, F. D., Carter, W. C., and Bergdolt, V. E., "Interferometric Analysis of Airflow about Projectiles in Free Flight," Journal of Applied Physics, Vol. 23, No. 4, pp. 453-469, April 1952.

162. Blue, Robert E., "Interferometer Corrections and Measurements of Laminar Boundary Layers in Supersonic Stream," NACA TN 2110, 1950.

163. Gooderum, Paul B., Wood, George P., and Brevoort, Maurice J., "Investigation with an Interferometer of the Turbulent Mixing of a Free Supersonic Jet," NACA Report 963, 1950.

164. Gooderum, Paul B., and Wood, George P., "Density Fields around a Sphere at Mach Numbers 1.30 and 1.62," NACA TN 2173, August 1950.

165. Wood, George P., and Gooderum, Paul B., "Investigation with an Interferometer of the Flow around a Circular-Arc Airfoil at Mach Numbers between 0.6 and 0.9," NACA TN 2801, October 1952.

166. Wood, George P., "Experiments on Transonic Flow Around Wedges," NACA TN 2829, November 1952.

167. Kraushaar, R., "Diffraction Grating Interferometer," Journal of the Optical Society of America, Vol. 40, No. 7, pp. 480-481, July 1950.

168. Sterrett, James R., and Erwin, John R., "Investigation of a Diffraction-Grating Interferometer for use in Aerodynamic Research," NACA TN 2827, November 1952.

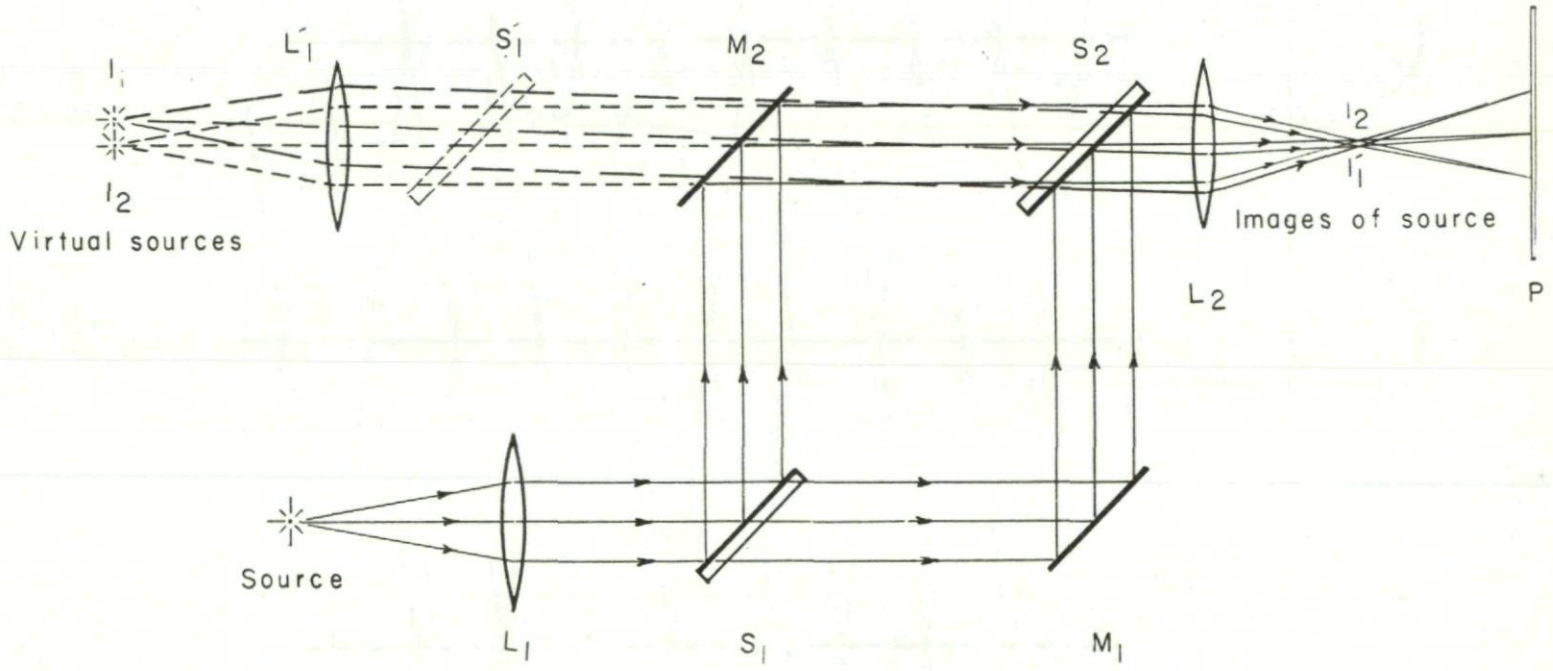

Fig. III-1. Basic arrangement of Mach-Zehnder interferometer.

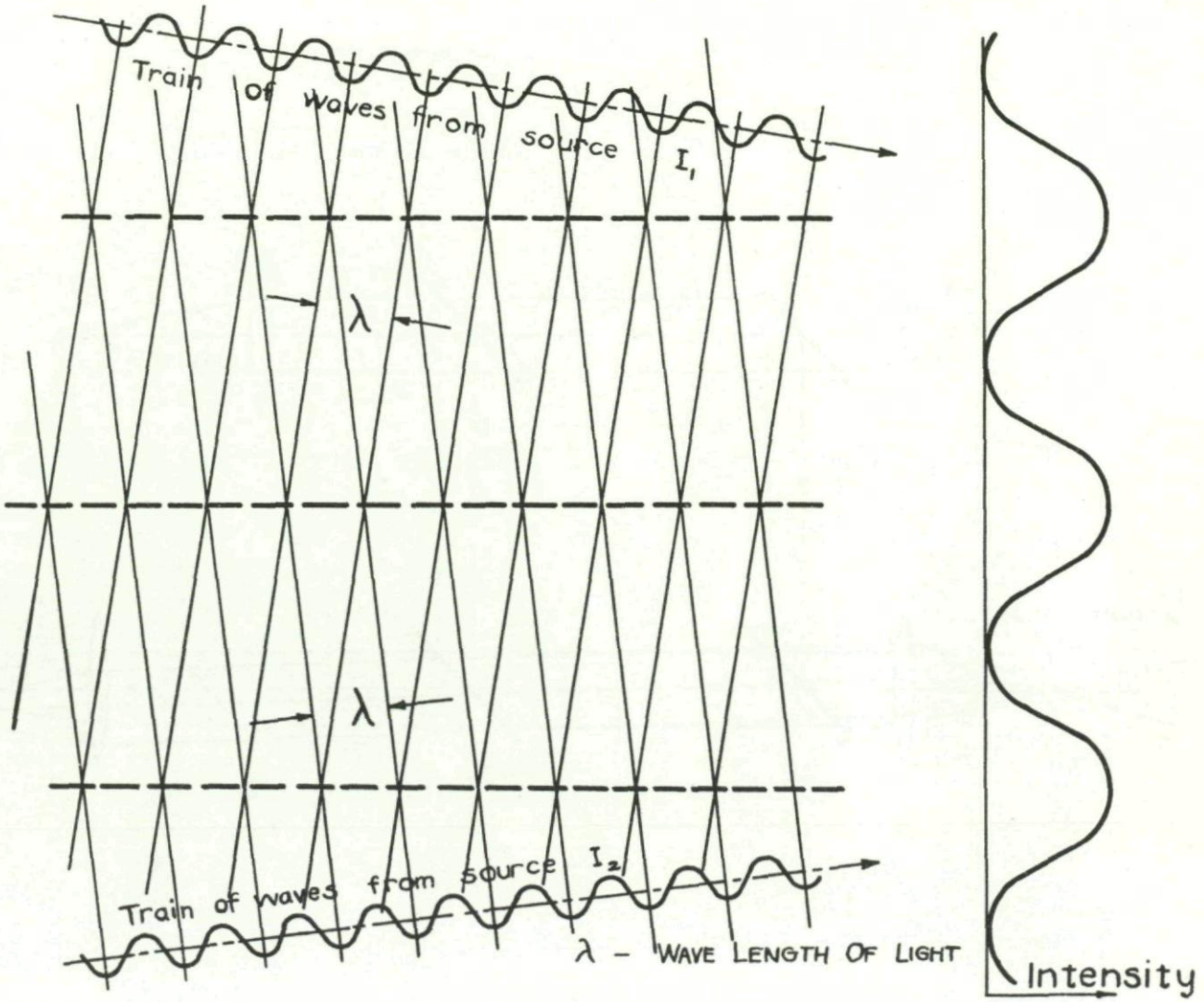

Fig. III-2. Production of fringes by crossed beams.

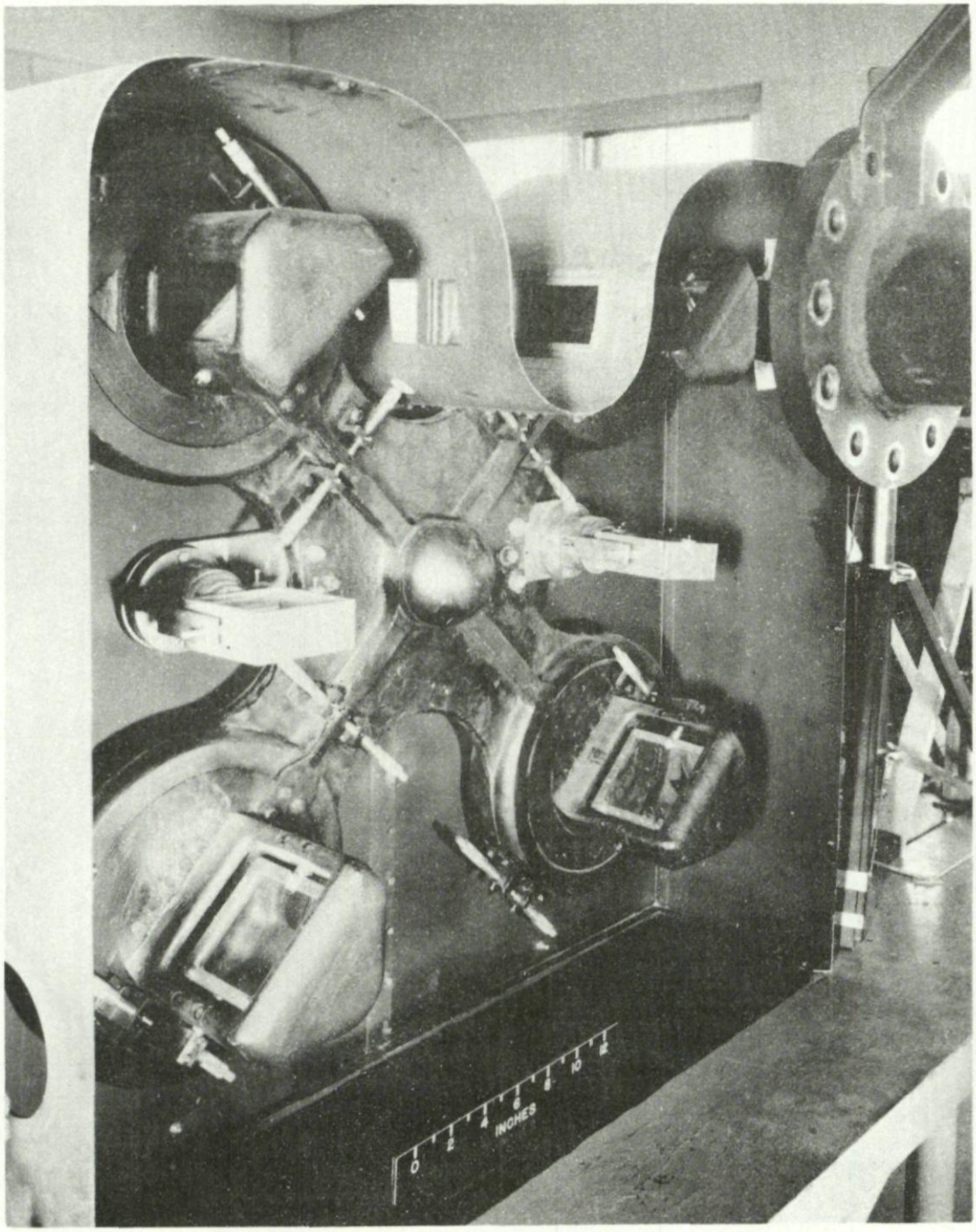

Fig. III-3. Interferometer. (Splitter plates, lower left and upper right; mirrors, upper left and lower right.)

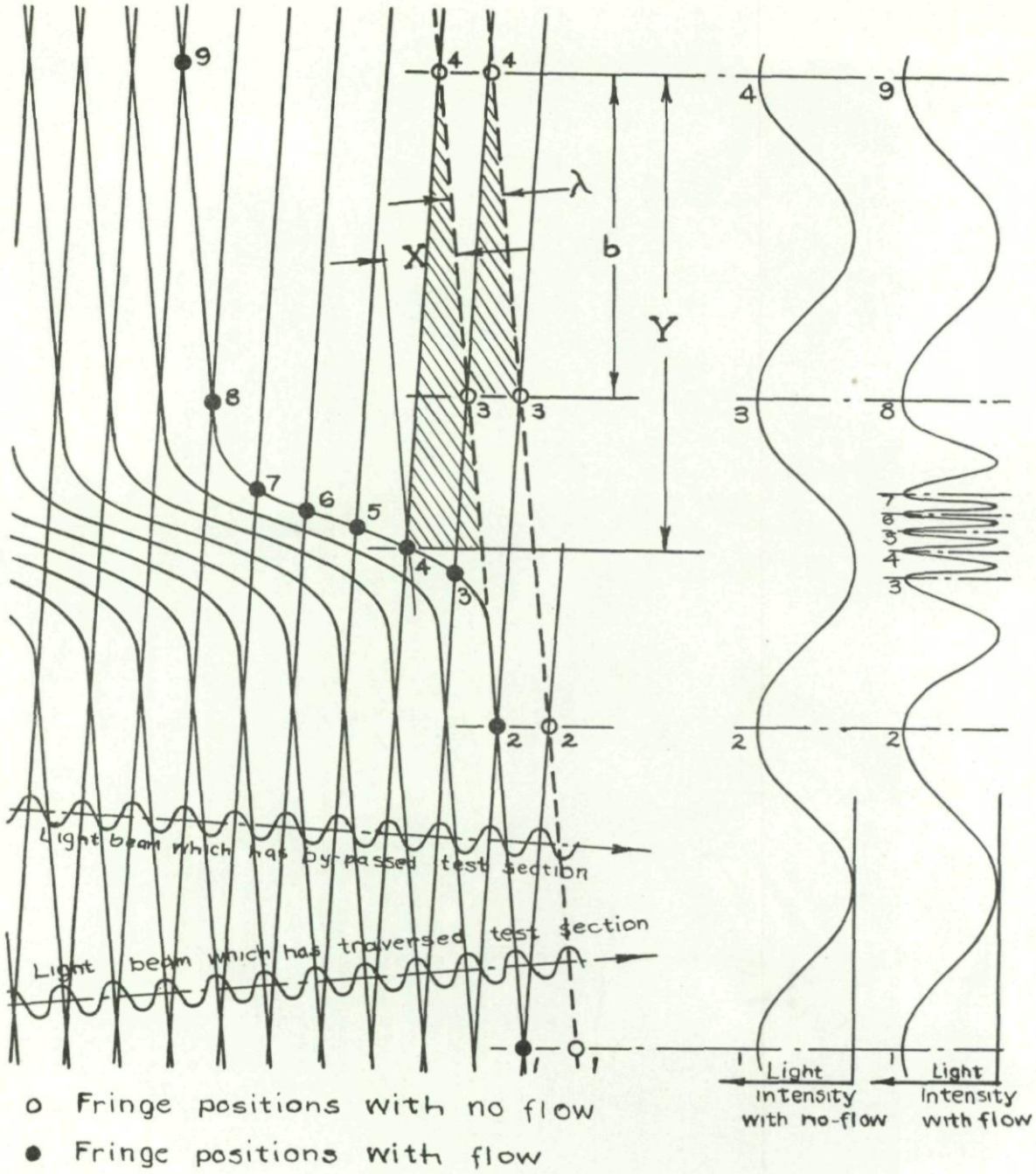

Fig. III-4. Production of fringe shifts.

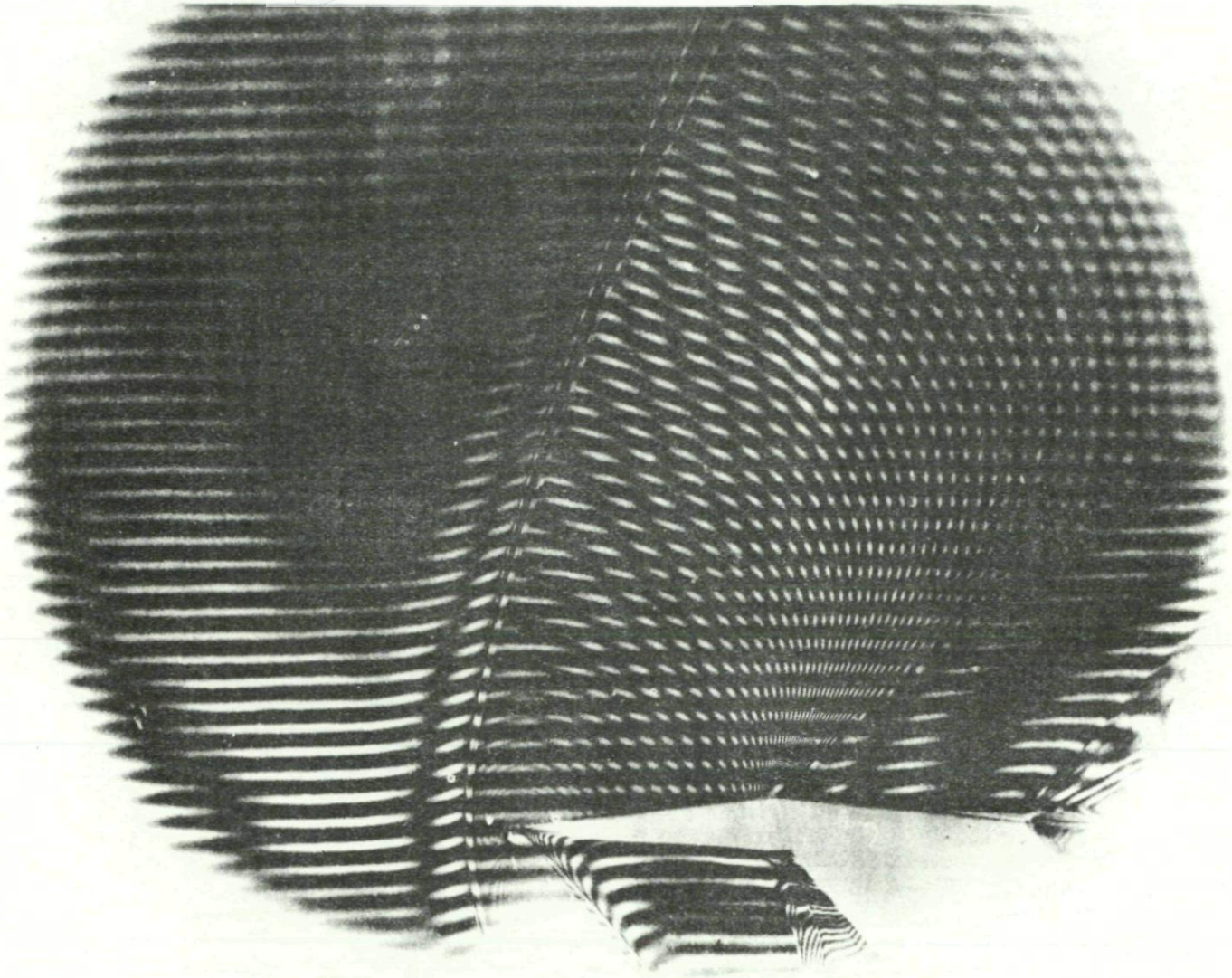

Fig. III-5. Contours of constant fringe shift made visible by superposition of interferograms with and without flow.

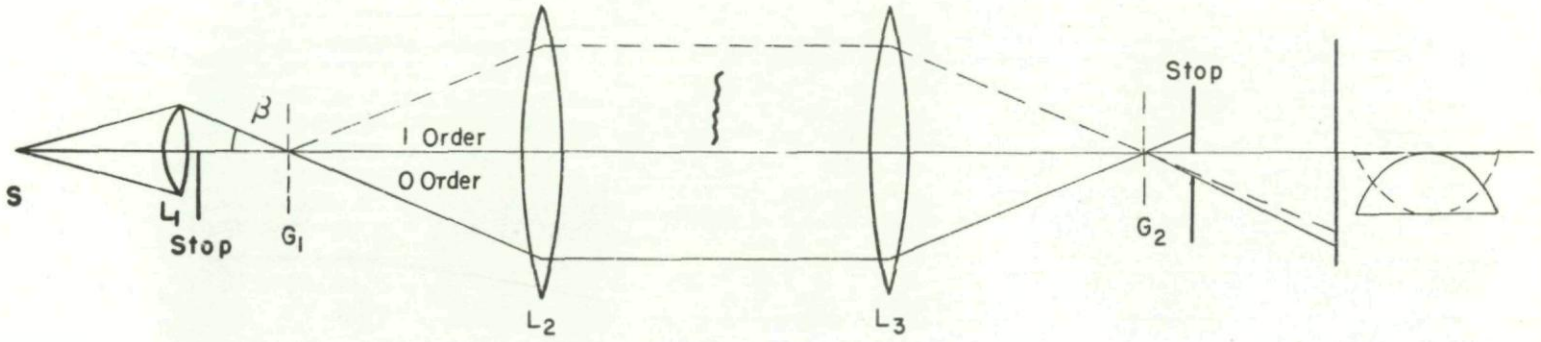

Fig. III-6. Basic arrangement of diffraction-grating interferometer.

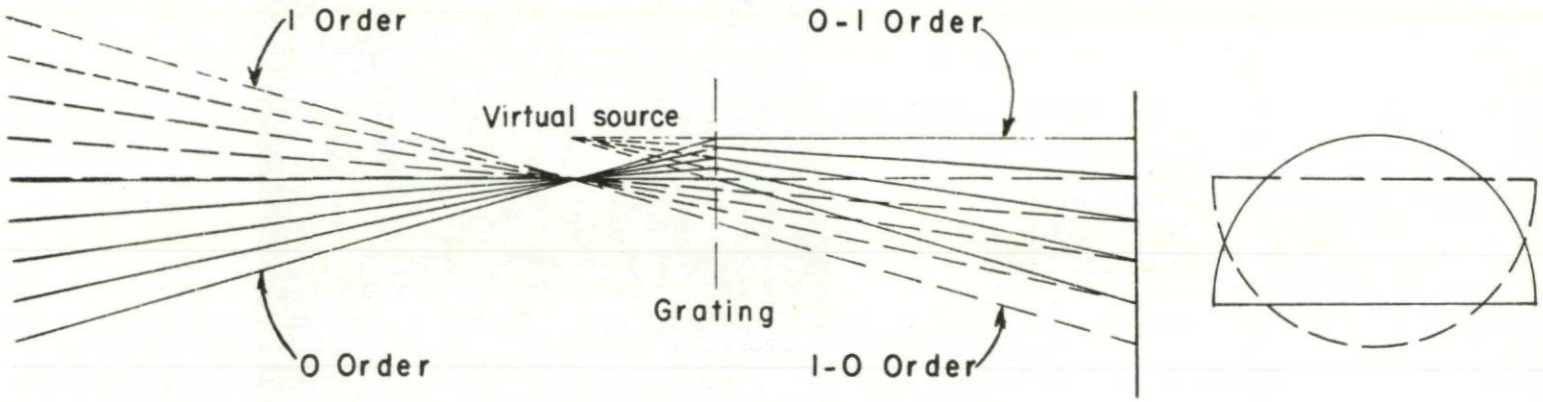

Fig. III-7. Crossed beams resulting from displacement of second grating.

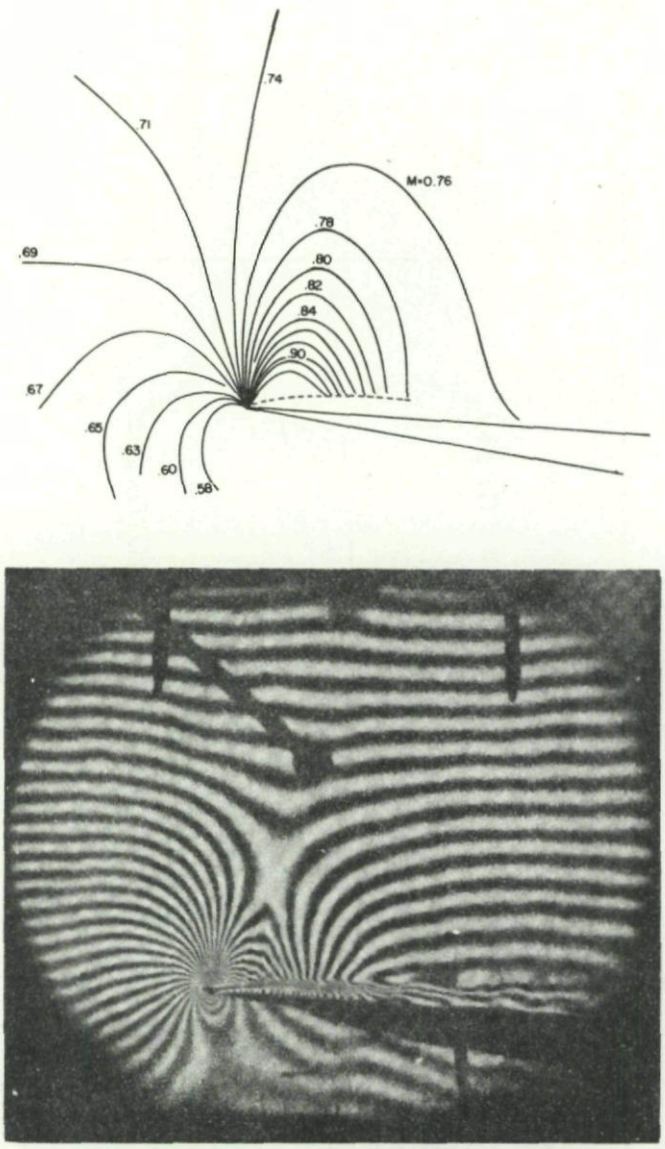

Fig. III-8. Interferogram and Mach number distribution of the flow about the leading edge of a wedge. $M_o = 0.72$.

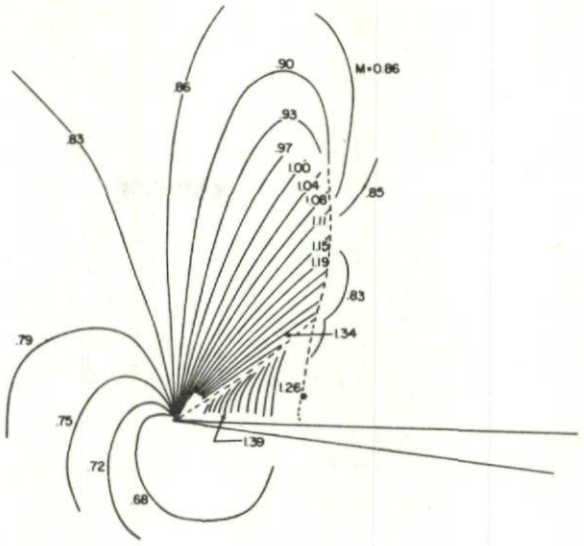

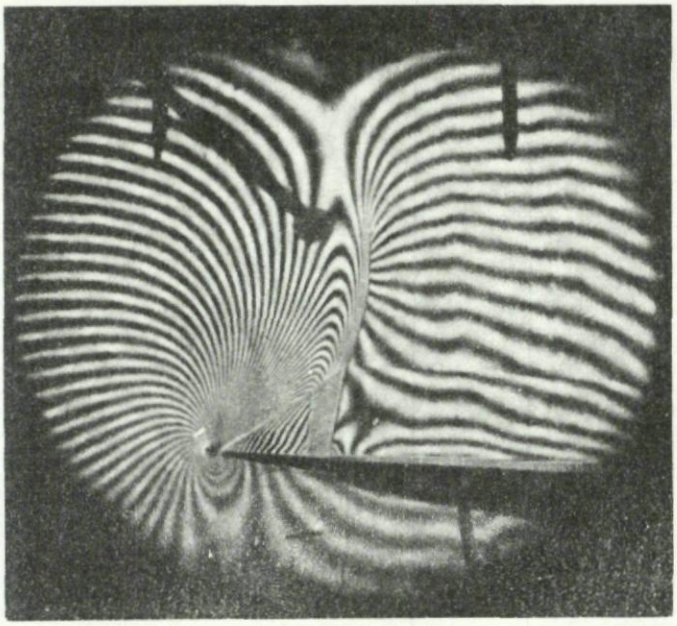

Fig. III-9. Interferogram and Mach number distribution of the flow about the leading edge of a wedge. $M_o = 0.85$.

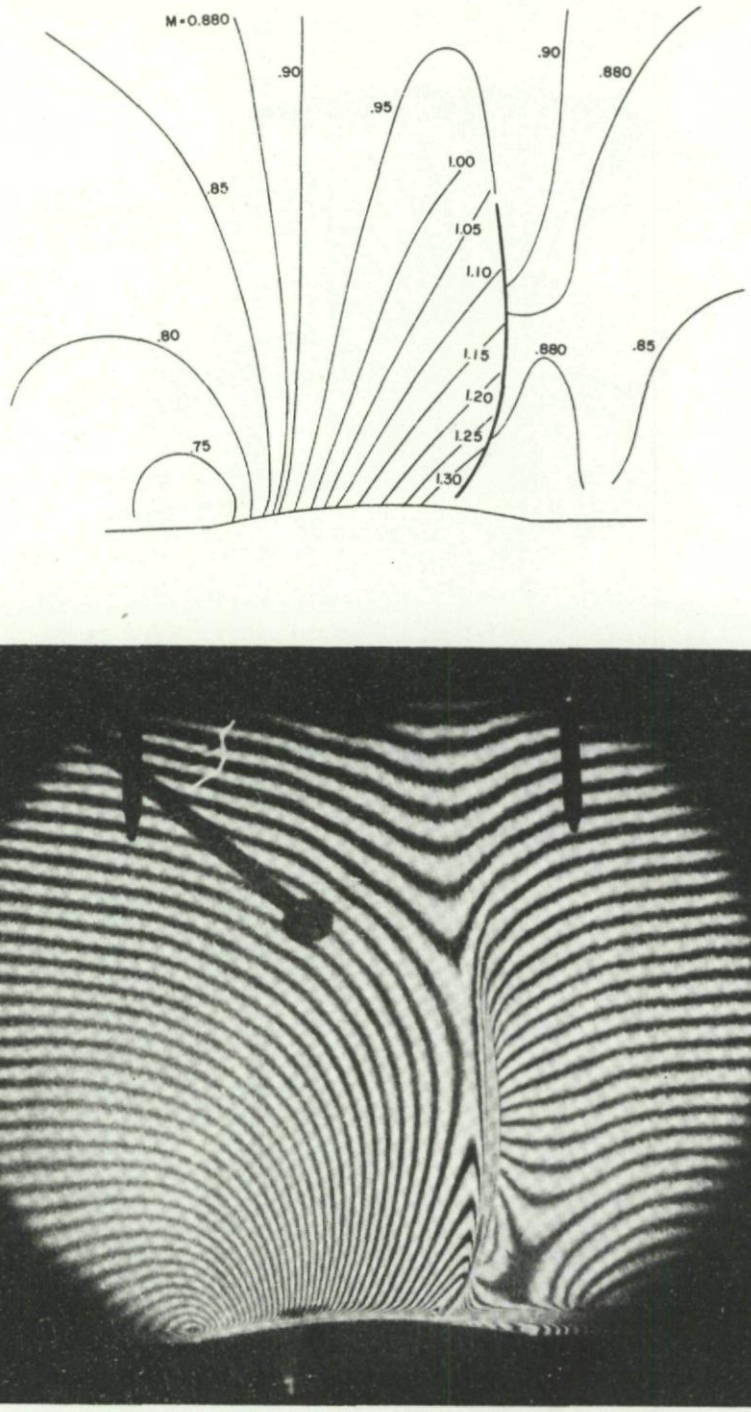

Fig. III-10. Interferogram and Mach number distribution of the flow about a circular-arc airfoil with turbulent boundary layer. $M_o = 0.88$.

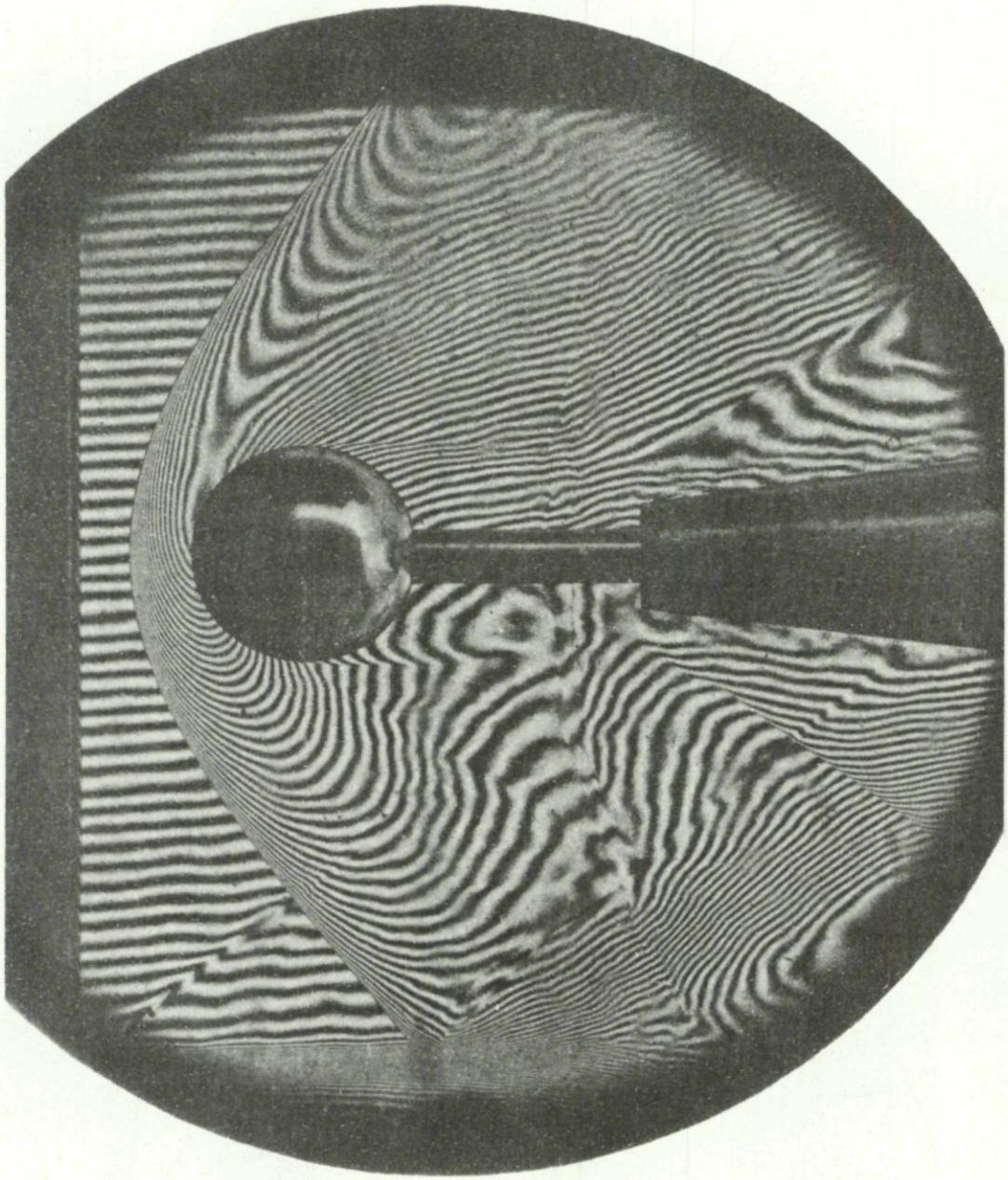

Fig. III-11. Interferogram of flow around sphere. $M_o = 1.62$.

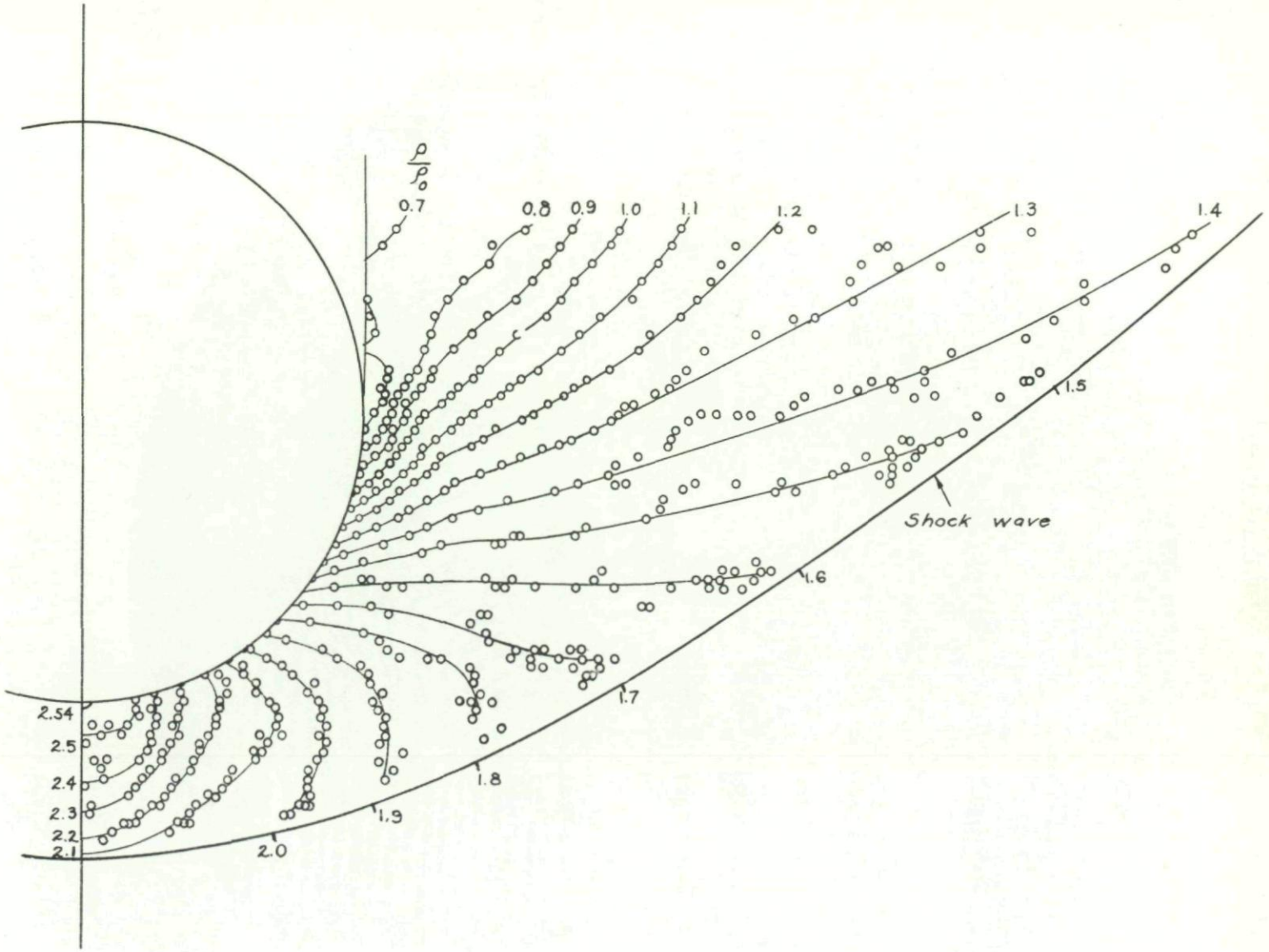

Fig. III-12. Contours of constant ratio of density to free stream density in flow-around sphere. $M_0 = 1.62$.

DISTRIBUTION

Copies of AGARD Publications May be Obtained in the Various Countries at the Addresses Given Herewith

BELGIUM
Centre National d'Etudes et de
Recherches Aéronautiques
11, rue d'Egmont
Bruxelles, Belgique

CANADA
Director of Scientific Information Service
Defence Research Board
Department of National Defence
"A" Building
Ottawa, Ontario, Canada

DENMARK
Military Research Board
Defence Staff
Kastellet, Copenhagen Ø, Denmark

FRANCE
ONERA (Direction)
25, avenue de la Division-Leclerc
Châtillon-sous-Bagneux, Seine, France

GERMANY
Wissenschaftliche Gesselschaft für
Luftfahrt
Zentralstelle der Luftfahrtdokumentation
München 64, Flughafen, Germany
Attn: Dr. Ing. H. J. Rautenberg

GREECE
Greek Nat. Def. Gen. Staff
B. MEO
Athens, Greece

ICELAND
Iceland Delegation to NATO
Palais de Chaillot
Paris 16, France

ITALY
Centro Consultivo Studi e Ricerche
Ministero Difesa Aeronautica
Via Salaria 336, Roma, Italy

LUXEMBOURG

NETHERLANDS
Netherlands Delegation to AGARD
Kanaalstraat 10
Delft, Holland

NORWAY
Chief Engineering Division
Royal Norwegian Air Force
Deputy Chief of Staff/Materiel
Myntgaten 2, Oslo, Norway
Attn: Lt. Col. S. Heglund

PORTUGAL
Subsecretariado da Estado da Aeronautica
Av. da Liberdade 252
Lisbon, Portugal
Attn: Lt. Col. Jose Pereira do Nascimento

TURKEY
M. M. Vekaleti
Erkaniharbiyei Umumiye Riyaseti
Ilmi Istisare Kurulu Mudurlugu
Ankara, Turkey
Attn: Colonel Fuat Ulug

UNITED KINGDOM
Ministry of Supply
T.I.L., Room 009A
First Avenue House
High Holborn
London W.C.1, England

UNITED STATES
National Advisory Committee for
Aeronautics
1512 H Street, N.W.
Washington 25, D.C., U.S.A.

AGL (1) 4-57-2M-57925